LOW SENSITIVITY DISTRIBUTED RC ACTIVE REALIZATION OF RATIONAL TRANSFER FUNCTIONS

Mohamed Said Abougabal

A THESIS

in

The Faculty

of

Engineering

Presented in Partial Fulfillment of the Requirements
for the Degree of Doctor of Engineering at
Sir George Williams University
Montreal, Canada

May, 1974

ABSTRACT

LOW SENSITIVITY DISTRIBUTED RC ACTIVE REALIZATION
OF RATIONAL TRANSFER FUNCTIONS

Mohamed Said Abougabal

The thesis presents an exact distributed RC-active synthesis procedure for realizing any open circuit rational voltage transfer function. For this purpose, a novel transformation of the complex frequency variable s, using the one port impedance of a short circuited RC tapered line and that of an ideal gyrator terminated by the open circuited dual of the RC line, is first developed. The synthesis procedure is then effected by utilizing this transformation and in general, finite gain amplifiers, which in turn can be realized using operational amplifiers.

It is found that there exists a band of frequencies over which the transformation is adversely affected if the lines are not duals of each other, while it remains relatively unaffected above or below the above frequency band. It is further found that not much is gained by using tapered RC lines instead of commensurate uniform RC lines. The rest of the thesis is, therefore, devoted to realizations using uniform lines.

A simple step by step method is given for realizing rational transfer functions using commensurate uniform RC lines. The effect of the lines not being commensurate is also established to be negligible on the transformation, provided that the total RC product of the lines is such that ωRC is less than 0.01 or greater than 30.

It is shown that in order to implement efficiently the synthesis procedure, a low sensitivity lumped RC-active network with

all of its capacitors grounded, is required in the transformed plane. One such second order configuration is proposed along with an optimum design for it. A modification of this configuration then allows the development of a significantly improved design. The modified network is shown to be stable during activation. The effect on the design of the finite d.c gains of the operational amplifiers has been found to be low. The finite bandwidth of the amplifiers has a negligible effect on pole frequency while it gives rise to an enhancement of the pole Q. A simple scheme is described to compensate for the Q-enhancement without affecting the pole frequency. A tuning procedure for the compensated network is given which involves the trimming of only three resistors. The theoretical results for the network have been verified by extensive experimental tests.

The synthesis procedure is illustrated by designing, in detail, second order band pass filters. It is verified that the effect of the lines being non commensurate, on the response, is negligible provided that the main part of the response lies in a frequency region such that the RC product of the lines satisfies any one of the conditions derived before. Guidelines are developed, for choosing the gyration resistance as well as the parameters of the lines, such that the gyrator imperfections have little influence on the responses. The effect of the finite bandwidth of the amplifiers is shown to result in a de-enhancement of the pole Q of the distributed realization. Finally, a design is presented for a second order low pass Butterworth filter with a cut off frequency of 10 radians per sec and it is shown that the entire filter is hybrid integrable.

ACKNOWLEDGEMENTS

The author is deeply indebted to Dr. B.B. Bhattacharyya for his supervision and suggestions throughout the preparation of this thesis.

Appreciation is extended to Dr. M.N.S. Swamy for many useful discussions and to Dr. B. Lombos for providing information on the fabrication of thin film components. Thanks are due to Dr. V. Ramachandran for going through the manuscript and to Miss Lilian Mikhail for her excellent job in typing the thesis.

The author also gratefully acknowledges the patience and sacrifices offered by his wife during the entire period of the study.

This work was supported under the National Research Council of Canada, Grant No. A-7740 awarded to Dr. B.B. Bhattacharrya and by a study leave from the University of Alexandria, Egypt.

TABLE OF CONTENTS

LIST OF TABLES

LIST OF FIGURES

LIST OF IMPORTANT ABBREVIATIONS AND SYMBOLS

		Page
$\hat{Q}_{ZB}$	Zero Q-Factor Realized by the Compensated Network when both the Finite d.c. Gain and Corner Frequency of OA are Taken into Account	97
Q_{ZN}	Zero Q-Factor with Perturbed Passive Elements	70
r_o	Scaling Constant for r(x)	17
r(x)	Per Unit Length Resistance at Distance x from the Input of a $\overline{TRC}$ = $r_o f(x)$	17
R_c	Compensating Resistor	92
R_T	$r_o \ell$ = Total Resistance of a $\overline{URC}$	21
r_g	Gyration Resistance	130
s	Complex Frequency Variable	17
S	$R_T C_T s$	21
S_e^x	Sensitivity of x With Respect to e	27
T(s)	Open Circuit Voltage Transfer Function in the s-Plane	56
$\overline{TRC}$	Tapered RC Line	9
u(s)	Transformed Frequency Variable = 1/S	21
$\hat{u}(s)$	Transformed Frequency Variable Taking into Account Gyrator Imperfections	130
$\overline{URC}$	Uniform RC Line	9
x	Distance Along Transmission Line	16
y(s,x)	Per Unit Length Admittance of a $\overline{TRC}$	16
y_o	Admittance Scaling Constant	17
z(s,x)	Per Unit Length Impedance of a $\overline{TRC}$ = $z_o(s)f(x)$	16
z_o	Impedance Scaling Constant	17

		Page
β_i	Gains of the Finite Gain Amplifiers.....	56
γ_i	Gain of the Output Summer at Its i^{th} Input.....	56
δ_i	Gain of the Input Summer at Its i^{th} Input.....	56
μ	OA Gain.....	4
μ_o	OA d.c. Gain.....	4
ω_c	Corner Frequency of OA.....	4
ω_N	Notch Frequency.....	57
$\hat{\omega}_{NB}$	Notch Frequency of the Compensated Network When Both the Finite d.c. Gain and Corner Frequency of OA are Taken into Account.....	97
ω_p	Pole-Frequency in Radians.....	57
ω_{PB}	Pole-Frequency Realized by Lumped Network when Both the Finite d.c. Gain and Corner Frequency are taken Into Account.....	87
$\hat{\omega}_{PB}$	Pole-Frequency in Radians Realized by the Compensated Network when Both the Finite d.c. Gain and Corner Frequency of the OA are Taken Into Account.....	92
$\hat{\omega}_{pd}$	Pole-Frequency in Radians Realized by the Distributed Structure When Both the Finite d.c. Gain and Corner Frequency of the OA are Taken into Account.....	139
$\omega_{p\mu}$	Pole-Frequency in Radians Realized by the Lumped Network when Finite d.c. Gain of the OA is Taken Into Account.....	65
ω_z	Zero-Frequency in Radians.....	57

CHAPTER I

INTRODUCTION

1.1 GENERAL

A considerable amount of literature exists on the theory and design of passive RLC filters [1] - [3]. However, there are several problems encountered in the design of such filters. One of them is the magnetic coupling between elements which may introduce errors in instruments such as those carried by satellites for measuring very weak signals. Further, the nonlinear frequency dependence of the quality factor Q of the inductors, coupled with the variation of Q from one inductor to another makes an accurate design of passive RLC filters fairly complicated. Another serious difficulty arises in the case of low frequency applications (less than 1 kHZ), such as control systems and analog computers, where practical inductors of reasonable Q tend to become unrealistically bulky and expensive.

Recently there is a surge of activity in the rapidly developing area of integrated circuit technology. In this technology, a complex network, with all its elements are fabricated on a single chip. The main attractions of integrated circuit fabrication are the following [4] - [5]:

(i) Increased system reliability

(ii) Reduction of size and weight

(iii) Reduction in power consumption

It is perhaps in the above area that one is confronted with the major drawback in the use of inductors. This is due to the fact that it has not yet been possible to fabricate inductors with reasonable value of inductances and quality factors by integrated circuit techniques. On the other hand, conventional inductors, when miniaturized to be consistent in size with other integrated circuit components, are extremely poor in quality to be of any use for many applications [4].

A promising way of overcoming these problems is to design filter networks without inductors, using active elements, resistors and capacitors which are integrable. In addition active RC filters can be designed to have the following advantages over RLC filters [6]:

(i) The filter output impedance can be made very low, thereby making the filter response independent of the load impedance. Consequently, the filters can be cascaded without additional buffer stages.

(ii) Frequently, the input impedance of the filter is high compared with the source impedance. Hence, very little power may be drawn from the signal.

(iii) The filters often provide insertion gain, thereby eliminating the need for additional amplifiers.

The active RC networks, however, may have two problems associated with them. These are:

(i) the circuit may become unstable if improperly designed, while passive RLC networks are absolutely stable.

(ii) active filters, if proper attention is not given to their design, may become highly sensitive to the variation of network parameters. For most resistively terminated LC filters the sensitivity problem is not serious.

Hence, special care should be exercised in the design of active RC filters. In addition, the filter designer should be aware of the limitations of practical passive and active components in order to be able to develop methods of circuit design which account for and minimize the effects of these limitations.

1.2 ACTIVE DEVICES

Many active devices have appeared in the literature such as controlled sources, negative immittance converters (NIC), gyrators, generalized immittance converters and operational amplifiers (OA) [4, 6]. Most of these devices can be realized using the operational amplifier. Since in this thesis OA's and gyrators are used, it is worthwhile to discuss their properties.

1.2.1 The Operational Amplifier

Presently, inexpensive and reliable commercial OA's are available in monolithic integrated form as off-the-shelf components (e.g.,

the Fairchild μA 741, which is internally compensated and input over-voltage and output short circuit protected). It has an input resistance of 2MΩ, output resistance of 75Ω and gain bandwith product of 1 MHZ (15 MHZ for LM 318). Its price is less than $1.00, compared with $70.00 for μA 709 in 1965, and there is every indication of OA prices going down even further.

The most commonly used OA is a d.c. voltage amplifier with differential input and single output and is represented as shown in Figure 1.1. Differential output OA's are also available but they are not widely used at present. The OA is a non-reciprocal two-port, ideally characterized by an infinite gain, infinite input impedance and zero output impedance. In practice, however, the OA has a frequency dependent finite gain μ, a finite differential input impedance and finite output impedance. For a frequency compensated OA, the differential open loop gain is given by

$$\mu = \mu_o\omega_c/(s + \omega_c) \qquad (1.1)$$

where μ_o, ω_c and $B = \mu_o\omega_c$ are the d.c. gain, the cut-off frequency and the gain bandwith product, respectively.

1.2.2 The Gyrator

The ideal gyrator is a two port which has a y-matrix [y] given by

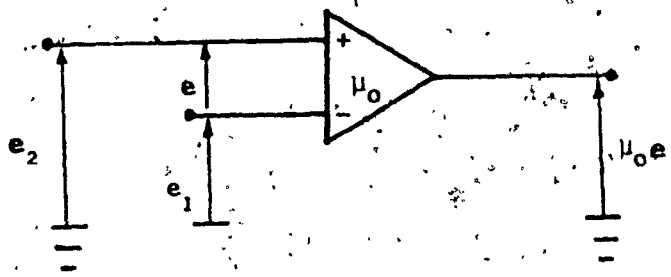

Fig. 1.1: Symbol for OA.

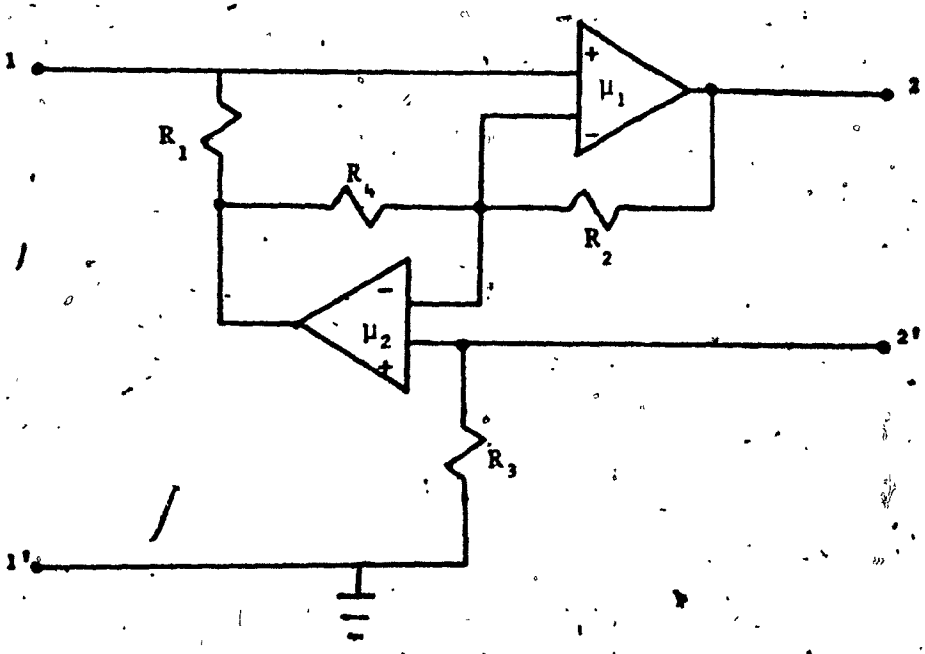

Fig. 1.2: Antoniou's Gyrator.

$$[y] = \begin{bmatrix} 0 & g \\ -g & 0 \end{bmatrix} \qquad (1.2)$$

From (1.2) it is easy to show that

$$Z_i = \frac{Y_L}{g^2} \qquad (1.3a)$$

where Z_i and Y_L are the input impedance and load admittance respectively, connected to the input and output ports.

Letting $K = 1/g^2$, equation (1.3a) becomes

$$Z_i = K\, Y_L \qquad (1.3b)$$

where K is referred to as the gyration constant. It is seen from (1.3b) that an ideal gyrator has the property of inverting an immittance.

Many gyrator realizations using OA's have appeared in the literature [6]. One of the better realizations of gyrators is the one proposed by Antoniou [7]. This is shown in Figure 1.2. Presently they are being mass produced and are available at low price [8, 9].

1.3 RC-ACTIVE SYNTHESIS METHODS

There are basically two approaches to the RC - active filter design [10]:

1) The direct realization approach

2) The cascade realization approach

In the first approach [11, 12, 13], the filter transfer function is synthesized directly as a two port network. On the other hand, in the cascade realization approach [14-20], the filter is synthesized as a cascade connection of second order, and possibly several first order, filter sections.

The cascade method of synthesis offers two practical advantages over the direct method as follows:

(i) The tuning of the network is simplified.

(ii) A small number of universal building blocks can be designed which can realize a multitude of network specifications [21].

1.4 IMPLEMENTATION OF LUMPED RC ACTIVE FILTERS USING HYBRID INTEGRATED TECHNOLOGY

It has been pointed out [22], that cost considerations may make it difficult to justify the manufacture, in large quantities, of RC active filters using discrete components. However, utilizing the batch processing methods of integrated circuit technology, active filters can be made to compete economically with their passive LC counterparts. A realistic design, then, shall assume integrated circuit (particularly hybrid-integrated) implementation. In this implementation, a complex filter is built by cascading second order building blocks. The second order hybrid-integrated sections consist of thin-film RC networks and monolithic integrated OA's.

The processing and properties of thin film resistors and capacitors are well documented [5], [21-25]. One of the main limitations of this technology is the stable range of these components. Typical thin film resistor values range from 1Ω to 0.5 megohm. A practical range for thin film capacitors is from 100 pf to 0.01 μf [23, 26]. Thus attention should be given to the following design considerations if the realizations are to be suitable for the available hybrid integrated technology:

(i) As low an element spread as possible. This is because element values have to lie within a certain range as mentioned above. A lower element spread also results in better fabrication tolerances [4, 10, 19].

(ii) Minimization of the total capacitance, as capacitors occupy, by far, the largest substrate area.

(iii) To have as few capacitors as possible. It is also desirable for the capacitors to have a common ground [5]. These result in a reduction of the number of gold contacts and in the elimination of the etching process, thereby leading to a greater circuit reliability [26, 28].

1.5 DISTRIBUTED RC-ACTIVE FILTERS

The fabrication process of resistors and capacitors in thin film technology is such that a resistor has a distributed capacitance invariably associated with it, while the capacitor is inherently distributed in

practice with a series parasitic resistor. Therefore, the nature of thin film components itself suggests that it may be desirable to employ distributed RC components as unit elements instead of resistors and capacitors [26, 29]. The RC tapered line ($\overline{TRC}$) is one such unit element. The use of $\overline{TRC}$'s eliminates the parasitics associated with resistors and capacitors and, consequently should lead to improved performance. The shunting capacitance of resistors and the series resistance of capacitors should no longer be limiting factors in the design. Further, what may be more significant is that, the use of $\overline{TRC}$'s may result in reduction of the chip area [5, 30] and hence in reduced cost and weight.

This, along with the continuous advance of thin film technology, suggests that it may be profitable to investigate the possibilities of using $\overline{TRC}$'s, particularly uniform RC-lines ($\overline{URC}$), as unit elements in filter design [29]. It is possible to fabricate a $\overline{TRC}$ or a $\overline{URC}$ in thin film technology by suitably varying the geometry of the fabricated structure [29]. However, uniform RC lines are the simplest to design and construct, since in a $\overline{URC}$ the per unit length resistance and the per unit length capacitance are constant over the entire length of the line. Many different materials and methods may be used in the fabrication of $\overline{URC}$'s [27]. One method is to sputter a resistive layer of tantalum on a glass substrate. The tantalum is then anodized to form a dielectric layer of tantalum oxide upon which a conductive layer

of tantalum is next deposited. Finally, contact electrodes are obtained by evaporating gold on the resistive and conductive layers. Figure 1.3a shows a typical thin film URC and Figure 1.3b shows its electrical symbol, where R_T and C_T are, respectively, the total resistance and capacitance of the line. Practical values of R_T's and C_T's lie in the ranges 10Ω - 100KΩ and 600 pf - 0.03 μf, respectively [27].

1.5.1 Methods of Synthesis Using Distributed Elements

Many synthesis procedures for realizing network functions using distributed elements, particularly uniform RC transmission lines and active elements, have appeared in the literature [31] - [43]. One approach which has received considerable attention is to transform the distributed RC-synthesis problem in the s-plane (complex frequency plane) into an equivalent lumped one in some transformed plane and then to use the known methods of lumped synthesis [31] - [33]. However, these methods require approximation of network functions in terms of irrational functions of the complex frequency variable s. This approximation, in practice, is rather difficult to obtain and hence, these methods seem to offer a very limited scope of application at the present time.

Another approach that has been used to realize approximately a second order rational transfer function is the dominant pole technique [34] - [38]. A higher order transfer function may be realized, using this technique, by cascading second order sections. One of the important limitations of this method is that it is necessary for the higher order

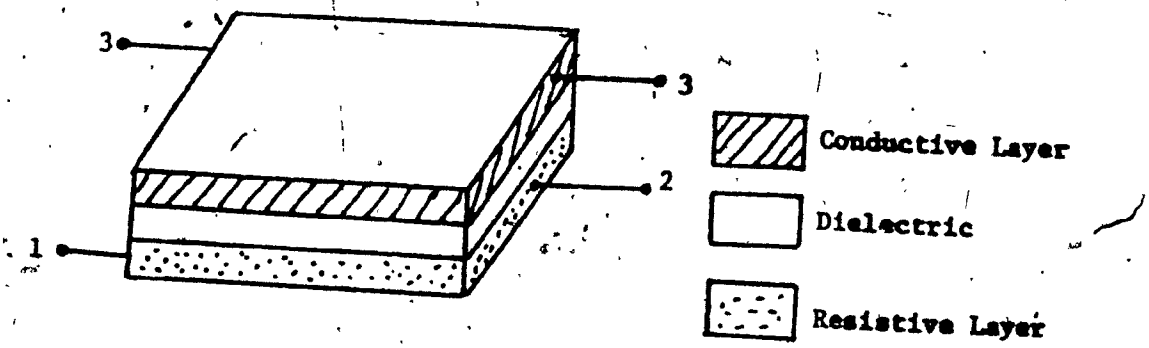

(a)

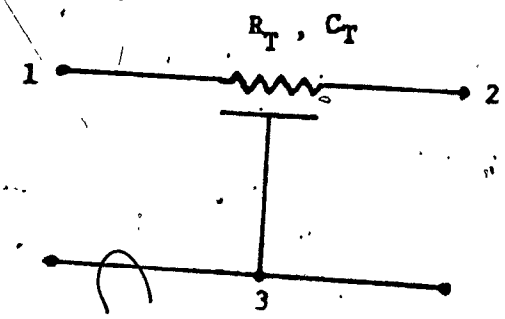

(b)

Fig. 1.3: a) Thin-Film Realization of $\overline{URC}$.
b) Symbol of $\overline{URC}$

poles of the transfer function not to be in the vicinity of the non-dominant poles of the different distributed second order sections. Also in these realizations, the sensitivity of Q with respect to the amplifier gain is of the order of Q. Another feature of this design is that the product ωRC is much greater than unity. Therefore, assuming thin film technology where the maximum RC product presently available is 10^{-3} secs, it is seen that this approach [34 - 38] only covers adequately frequencies above several kilohertz. However, the low frequency range, particularly the range $0.1 < f < 100$ is of great importance in many applications such as biomedical sciences [44 - 50], oceanography [51], stress analysis [52], measurement of surface roughness and machine tool control [53], vibration analysis [53] etc. As yet no distributed realization exists to cover adequately the above frequency range.

Several attempts have also been made to realize exactly a rational transfer function using distributed elements. This is because rational functions of s are easier to work with and many useful results are already available in the area. Further, approximation problems are more readily solvable in the s domain; as a result, a considerable amount of research has been devoted to developing distributed RC networks with rational transfer functions. Existing techniques for exactly realizing a rational transfer function using distributed elements are all based on the idea of incorporating

suitable cuts in the conducting layer of an RC line [39] - [43]. However, all these methods seem to suffer some drawbacks. In general, the cuts in the conducting layer have to be such that the sum of two (or three) distributed capacitances at every point of the RC line is held constant. Thus, one may be confronted with a difficult tuning problem. In addition, the cuts themselves depend on the transfer functions being realized and may be quite complex. Also, these methods may require lumped (active or passive) terminations. Further, since some of these methods use negative impedance converters and difference decompositions of the polynomials, the Q-sensitivity of these realizations will be high.

Thus, it appears to be of interest to have a synthesis procedure for exactly realizing a rational transfer function. It will be desirable for this procedure not to be limited to above or below any particular frequency range. To be useful, the procedure should be simple and yield realizations which are insensitive to the variations of various passive and active parameters in the resulting networks.

1.6 SCOPE OF THE THESIS

In this thesis, a simple method is first developed for exactly realizing any rational transfer function using a tapered RC line, its dual and an ideal gyrator as basic building blocks. The method is then employed to obtain and study in detail low sensitivity realizations of second order open circuit voltage transfer functions

using commensurate $\overline{\text{URC's}}$.

For this purpose, the thesis is divided into four main chapters. In Chapter II, a frequency transformation u, which is proportional to 1/s, where s is the complex frequency variable, is introduced. This transformation enables any rational transfer function to be realized exactly using any tapered RC line, its dual, a gyrator and in general finite gain amplifiers. It is then shown that little is gained by using tapered lines instead of commensurate $\overline{\text{URC's}}$ in the realization. Further, it is established that, even if any one of the RC products deviates from its nominal value, there is negligible effect on the realized response provided the RC product is chosen properly. It is also shown in this chapter that, in order to implement efficiently the proposed synthesis procedure it is desirable to have a low sensitivity grounded capacitor lumped RC active configuration in the u-plane.

In Chapter III, a grounded capacitor RC active structure which realizes any rational voltage transfer function is first developed. The attention is then concentrated on the second order section and an insensitive design of this section is derived.

The second order section discussed in Chapter III is modified in Chapter IV resulting in a configuration whose properties are superior to those of the one in Chapter III. This second order section is by itself attractive from the point of view of thin film implementation.

Hence, the properties of this structure are then studied extensively both theoretically and experimentally.

In Chapter V, the proposed synthesis procedure of Chapter II is illustrated by designing a band pass section using commensurate $\overline{\text{URC's}}$. The validity of the conclusions derived in Chapter II, namely that the non commensurate behaviour of the $\overline{\text{URC's}}$ is negligible on the realized response if the RC product is properly chosen, is also verified for the band pass filter. The gyrator of Figure 1.2 is then considered and the effect of its imperfections on the frequency transformation u is studied. Some important conclusions are reached and verified for a band pass filter. The chapter is concluded with the design of a very low frequency low pass section and it is shown that the entire filter can be fabricated using hybrid IC technology.

The last chapter summarizes the results obtained in the thesis and indicates possible extensions of the work.

CHAPTER II

EXACT REALIZATION OF RATIONAL TRANSFER FUNCTIONS USING TAPERED RC LINES AND THEIR DUALS

2.1 INTRODUCTION

A novel transformation of the complex frequency variable s is introduced in this chapter. The transformed variable is then utilized to obtain a method for an exact synthesis of rational transfer functions in s using, as unit elements, any tapered RC line, its dual, an ideal gyrator and, in general, active elements with real gain parameters. The effect on the realization of the lines not being dual is then examined. Further, it is shown that not much is gained by using a tapered line in the synthesis procedure instead of commensurate URC's. Finally, a detailed study of realizations using URC's is made.

2.2 SOME RESULTS ON TAPERED LINES

This section discusses some necessary results on the analysis of tapered lines as well as synthesis of distributed networks using such lines.

2.2.1 Analysis

A tapered RC transmission line (L) may be characterized by the distributions

$$\left.\begin{aligned} z(s,x) &= z_0(s)\, f(x) \\ y(s,x) &= y_0(s)\, g(x) \end{aligned}\right\} \quad (0 \le x \le \ell) \qquad (2.1)$$

where $z(s,x)$, $y(s,x)$ are the per unit length impedance and admittance, respectively, s is the complex frequency, $z_o(s)$ and $y_o(s)$ are immittance scaling constants and the functions $f(x)$ and $g(x)$ describe the taper of the line as a function of x, the distance along the line. For RC lines $z(s,x) = r(x) = r_o f(x)$ and $y(s,x) = sc(x) = sc_o g(x)$. The schematic symbol for the RC line is shown in Figure 2.1.

The dual line (L_D) of the line characterized by 2.1 is defined to have the distributions [54]

$$\begin{aligned} z(s,x) &= z_o(s)\, g(x) \\ y(s,x) &= y_o(s)\, f(x) \end{aligned} \qquad 0 \le x \le \ell \qquad (2.2)$$

A set of ψ-functions [55] has been found useful in analyzing tapered lines. These functions are defined as follows:

$$\begin{aligned} \psi_1 &= \Theta'_\ell\, \phi_o - \phi'_\ell\, \Theta_o \\ \psi_2 &= \Theta'_o\, \phi_\ell - \phi'_o\, \Theta_\ell \\ \psi_3 &= \Theta'_o\, \phi_o - \phi'_o\, \Theta_o \\ \psi_4 &= \Theta'_\ell\, \phi_\ell - \phi'_\ell\, \Theta_\ell \\ \psi_5 &= \Theta'_o\, \phi'_\ell - \phi'_o\, \Theta'_\ell \\ \psi_6 &= \Theta_\ell\, \phi_o - \phi_\ell\, \Theta_o \end{aligned} \qquad (2.3)$$

where Θ_x and ϕ_x are the two independent voltage solutions at a distance x along the line given by (2.1) and the prime denotes differentiation with respect to x. It is also known [54] that

$$\psi_3 Z_L = \psi_4 Z_o \qquad (2.4)$$

and

$$\psi_1 \psi_2 = \psi_3 \psi_4 + \psi_5 \psi_6 \qquad (2.5)$$

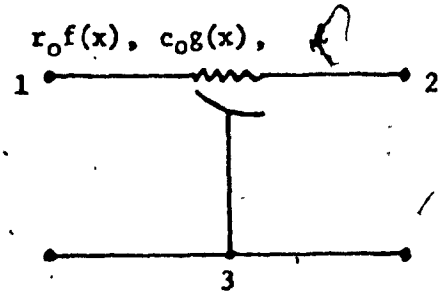

Fig. 2.1: Tapered RC Line.

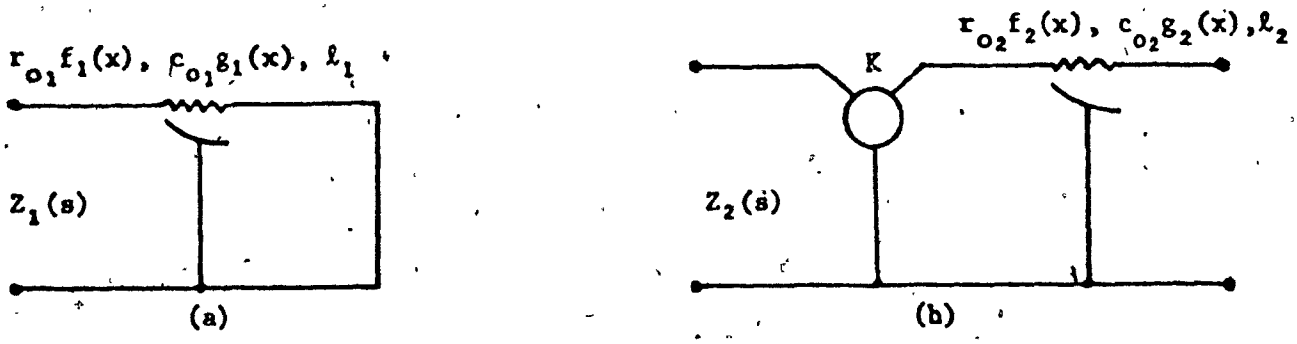

Fig. 2.2: (a) Input Impedance of a Short Circuited TRC

(b) Input Impedance of a Gyrator, of Gyration Constant K, Terminated by an Open Circuited TRC.

Further, the ψ-functions contain z_o and y_o as products only [56].

The y-matrix of L and the z-matrix of L_D may be obtained in terms of the ψ-functions as [54]:

$$[Y] = \frac{1}{\psi_6}\begin{bmatrix} \psi_2/z(s,o) & -\psi_3/z(s,o) \\ -\psi_4/z(s,\ell) & \psi_1/z(s,\ell) \end{bmatrix} \tag{2.6}$$

and

$$[Z]_D = \frac{1}{\psi_6}\begin{bmatrix} \psi_2/y(s,o) & \psi_3/y(s,o) \\ \psi_4/y(s,\ell) & \psi_1/y(s,\ell) \end{bmatrix} \tag{2.7}$$

2.2.2 Synthesis Using Tapered Lines

It may be shown [33] that, for a passive network consisting of an arbitrary interconnection of one port impedance (OPI) $a_1 p(s)$ and $a_2 q(s)$ of tapered lines where a_1 and a_2 are scaling factors, any driving point impedance function $Z(s)$ can always be expressed as:

$$Z(s) = p(s)\ [\text{RC impedance function in } f = p(s)/q(s)]$$

Further, if such a network is used as a two-port, its open circuit voltage transfer functions in the f-plane, namely T(f), is of the form of an RC transfer function in f [33].

In addition, if the network contains active elements such as finite gain amplifiers, then T is of the form

$$T(f) = \frac{P(f)}{Q(f)} \tag{2.8}$$

where P and Q are arbitrary polynomials in f with real coefficients.

It is also known that [56], if a transfer function of the form (2.8) is given, it can always be realized first in the appropriate plane (f) by any known lumped RC passive or active technique, after which the different resistors R_{fi}'s and capacitors C_{fi}'s are replaced by RC lines having OPI's given by $R_{1f}p$ and $(\frac{1}{C_{if}})q$ respectively.

2.3 THE NEW TRANSFORMATION

The synthesis procedure discussed in the previous section is accomplished by using the transformed variable f(s). The main difficulty in this technique is that it requires approximation of network specifications in terms of the transformed variable f. This approximation is relatively difficult to obtain and hence the method appears to be of limited use at the present time.

However, this problem may be overcome by introducing a frequency transformation which is rational in s.

For this purpose, let us consider the short circuited RC line L_1, shown in Figure 2.2a, with the per unit length distributions

$$z_1(s,x) = r_{o_1} f_1(x) , \quad y_1(s,x) = s\, c_{o1}\, g_1(x) \quad (0 \le x \le \ell_1) \qquad (2.9a)$$

Let us also consider the network of Figure 2.2b which represents an ideal gyrator, of gyration constant K, terminated by an open circuited line L_2 having per unit length distributions

$$z_2(s,x) = r_{o2} f_2(x) , \quad y_2(s,x) = s\, c_{o2}\, g_2(x) \quad (0 \le x \le \ell_2) \qquad (2.9b)$$

The OPI's of the networks as shown in Figure 2.2 can be written in the form

$$Z_1(s) = f_1(0)R_{1T}p(s) \quad , \quad Z_2(s) = g_2(0)\left(\frac{K}{R_{2T}}\right)q(s) \tag{2.10a}$$

where

$$R_{1T} = r_{01}\ell_1 \quad , \quad R_{2T} = r_{02}\ell_2 \tag{2.10b}$$

Let L_2 be L_{1D}, the dual of L_1. Hence, from (2.1) and (2.2) we have

$$r_{01} = r_{02} = r_0 \quad , \quad c_{01} = c_{02} = c_0 \quad , \quad \ell_1 = \ell_2 = \ell \tag{2.11a}$$

Therefore

$$R_{1T} = R_{2T} = R_T \quad , \quad C_{1T} = C_{2T} = C_T \tag{2.11b}$$

and

$$r_{01}c_{01}\ell_1^2 = r_{02}c_{02}\ell_2^2 = r_0c_0\ell^2 = R_TC_T \tag{2.11c}$$

where

$$C_{1T} = c_{01}\ell_1 \quad , \quad C_{2T} = c_{02}\ell_2 \tag{2.11d}$$

Also from (2.6) and (2.7), we obtain

$$Sp(s) = q(s) = \frac{S\,\psi_6(s)}{\ell\,\psi_2(s)} \tag{2.12a}$$

and from (2.1) and (2.2)

$$g_2(0) = f_1(0) \tag{2.12b}$$

where

$$S = R_TC_Ts \tag{2.12c}$$

Defining now u(s) to be

$$u(s) = p(s)/q(s) \tag{2.13a}$$

we observe from (2.12a) that

$$u(s) = \frac{1}{S} = \frac{1}{R_TC_Ts} \tag{2.13b}$$

that is, u is rational in s.

From (2.10) to (2.12), we observe that

$$Z_1(s)/p(s) = f_1(0)R_T \qquad (2.14a)$$

and

$$Z_2(s)/q(s) = \left(\frac{f_1(0)K}{R_T}\right)\cdot\frac{1}{u} \qquad (2.14b)$$

These expressions show that the OPI's corresponding to Figure 2.2a and Figure 2.2b can be regarded as a resistor and a capacitor respectively in the u-plane.

In view of equation (2.13) which shows that the transformed variable u is rational in s, the synthesis procedure in section 2.2.2 now would yield an exact realization of any rational transfer function, provided the various resistors R_{ui}'s and capacitors C_{ui}'s in the u-plane are replaced by the one ports corresponding to Figure 2.2a and Figure 2.2b respectively.

In this procedure, the resistors R_{ui}'s are replaced by short circuited lines L_1's, and the capacitors C_{ui}'s are replaced by gyrators terminated by open circuited lines L_{1D}'s. Thus, it is desirable to have in the u-plane a network that requires minimum number of resistors and capacitors. Further, the capacitors should be grounded. In that case, the number of the RC lines and gyrators used will be minimum and, in addition, all the gyrators will be grounded, an attractive feature from the point of view of power supply considerations.

2.4 THE EFFECT ON THE TRANSFORMATION OF THE LINES NOT BEING DUAL

The proposed synthesis procedure described is based on the assumption that the RC-lines L_1 and L_2 in Figure 2.2 are the duals of one another. Indeed, it is this very property which ensures that u is rational in s thus, allowing the exact realization of rational transfer functions. Therefore, it is essential to study the effect of the non-dual behaviour of the lines. The non-dual behaviour arises out of one or both of the following factors:

i) The variation of the tapers of the lines

ii) The violation of condition (2.11a) due to variations of the distributed parameters.

It is not possible to study the effect of these two factors on the transformation u(s) for any arbitrary distributions of the tapered lines, since solutions of the telegrapher's equations are not available for any such line. Even for all solvable lines, it may neither be desirable nor practical to study this effect. However, it has been shown that a tapered RC line is equivalent to an infinite cascade of commensurate $\overline{\text{URC's}}$ [57]. Thus, first a study of the effect of non-duality between a cascade of two $\overline{\text{URC's}}$ and its dual on u(s) is made. The two $\overline{\text{URC's}}$ while being commensurate may have different total resistances and capacitances. From this study, some general conclusions will be drawn, in the following section, regarding the effect of the non-duality between any tapered line and its dual.

2.4.1 Effect on the Transformation u of Non Duality Between a Cascade of two URC's and Its Dual

Consider the RC line L_{1c} consisting of a cascade of two commensurate URC's as shown in Figure 2.3a. Let the per unit distributions of L_1 be:

$$z_1(s,x) = r_{o_1} \quad (0 \le x < \ell_1) \qquad (2.15)$$
$$= r_{o_2} \quad (\ell_1 < x \le \ell_2)$$

and

$$y_1(s,x) = sc_{o_1} \quad (0 \le x < \ell_1) \qquad (2.16)$$
$$= sc_{o_2} \quad (\ell_1 < x \le \ell_2)$$

where $\ell_1 = \ell_2$.

Since the lines are commensurate,

$$R_{1T}C_{1T} = R_{2T}C_{2T} \qquad (2.17a)$$

where

$$R_{1T} = r_{o_1}\ell_1 \ , \quad R_{2T} = r_{o_2}\ell_2 \qquad (2.17b)$$

$$C_{1T} = c_{o_1}\ell_1 \ , \quad C_{2T} = c_{o_2}\ell_2 \qquad (2.17c)$$

Let

$$\frac{R_{2T}}{R_{1T}} = \frac{C_{1T}}{C_{2T}} = m_1 \qquad (2.17d)$$

Consider also the line L_{2c}, which is a cascade of two commensurate URC's, as shown in Figure 2.3b, with the per unit length distributions

$$z_2(s,x) = r_{o_3} \quad (0 \le x < \ell_3) \qquad (2.18a)$$
$$= r_{o_4} \quad (\ell_3 < x \le \ell_4)$$

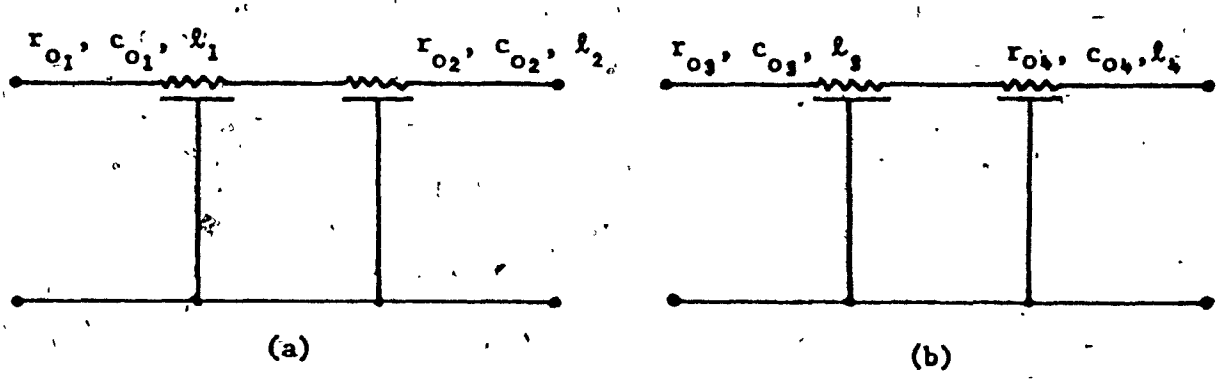

Fig. 2.3 (a) L_{1C}, Cascade of Two Commensurate $\overline{\text{URC}}$'s $(r_{o_1}, c_{o_1}, \ell_1)$ and $(r_{o_2}, c_{o_2}, \ell_2)$

(b) L_{2C}, Cascade of Two Commensurate $\overline{\text{URC}}$'s $(r_{o_3}, c_{o_3}, \ell_3)$ and $(r_{o_4}, c_{o_4}, \ell_4)$

$$y_2(s,x) = sco_3 \qquad (0 < x < \ell_3) \qquad (2.18b)$$
$$= sco_4 \qquad (\ell_3 < x < \ell_4)$$

Let now L_{2C} be L_{1CD}, the dual of L_{1C}. It may be shown [58] that the dual of a cascade of RC lines is equal to the cascade of the dual of the corresponding RC lines. Further, from (2.1) and (2.2) it is easy to show that the dual of a $\overline{URC}$, of length ℓ and with distributions $z(s,x) = m\, r_o$, $y(s,x) = s(co/m)$ is another $\overline{URC}$, with the same length and distributions $z_d(s,x) = r_o/m$, $y_d(s,x) = s(mc_o)$. Hence, we have:

$$\ell_1 = \ell_3\,, \quad \ell_2 = \ell_4\,, \quad R_{3T} = R_{1T}\,, \quad C_{3T} = C_{1T} \qquad (2.18c)$$

and

$$\frac{R_{4T}}{R_{3T}} = \frac{C_{3T}}{C_{4T}} = m_2 = 1/m_1 \qquad (2.18d)$$

where

$$R_{3T} = r_{o_3}\ell_3\,, \quad R_{4T} = r_{o_4}\ell_4\,, \quad C_{3T} = c_{o_3}\ell_3\,, \quad C_{4T} = c_{o_4}\ell_4 \qquad (2.18e)$$

Using, in the two OPI's of Figure 2.2, lines L_{1C} and L_{1CD} instead of lines L_1 and L_{1D} respectively and also using (2.9) to (2.12), it may be shown that

$$u = \frac{1}{R_T C_T s} = \frac{1}{S} \qquad (2.19a)$$

provided that

$$R_{jT}C_{jT} = R_{(j+1)T}C_{(j+1)T} = R_TC_T \quad (j = 1,2,3) \qquad (2.19b)$$

However, if the lines are not duals of each other then u becomes

$$u = \frac{1}{S} \frac{\sqrt{\alpha_1} R_{2T}/R_{1T} \cosh \sqrt{\alpha_1 S} \sinh \sqrt{\alpha_2 S} + \sqrt{\alpha_2} \sinh \sqrt{\alpha_1 S} \cosh \sqrt{\alpha_2 S}}{R_{2T}/R_{1T}\alpha_1 \sinh \sqrt{\alpha_1 S} \sinh \sqrt{\alpha_2 S} + \sqrt{\alpha_1 \alpha_2} \cosh \sqrt{\alpha_2 S} \cosh \sqrt{\alpha_1 S}} \times$$

$$\frac{\sqrt{\alpha_3} \cosh \sqrt{\alpha_3 S} \cosh \sqrt{\alpha_4 S} + R_{3T}/R_{4T} \sqrt{\alpha_4} \sinh \sqrt{\alpha_3 S} \sinh \sqrt{\alpha_4 S}}{\alpha_3 \sinh \sqrt{\alpha_3 S} \cosh \sqrt{\alpha_4 S} + R_{3T}/R_{4T} \sqrt{\alpha_3 \alpha_4} \cosh \sqrt{\alpha_3 S} \sinh \sqrt{\alpha_4 S}} \qquad (2.20)$$

where

$$R_{jT} C_{jT} = \alpha_j R_T C_T \quad (j = 1,2,3,4) \qquad (2.21)$$

In order now to study the effect of the deviation of the RC products from their nominal values and the effect of taper (m) on u, $S_{x_i}^u$, the classical sensitivity of u with respect to any of the distributed parameters x_i, is considered. The classical sensitivity $S_{x_i}^u$ is defined as [6]

$$S_{x_i}^u = \frac{d(\ell n\, u)}{d(\ell n\, x_i)} = S_{x_i}^{|u(j\omega)|} + j\, S_{x_i}^{\angle u(j\omega)} \qquad (2.22a)$$

where

$$S_{x_i}^{|u(j\omega)|} = \frac{d\, \ell n\, |u(j\omega)|}{d\, \ell n\, x_i}, \quad S_{x_i}^{\angle u(j\omega)} = d\angle u(j\omega)/d\, \ell n\, x_i \qquad (2.22b)$$

In investigating this effect of non-dual behaviour, the frequency range over which $S_{x_i}^{\angle u(j\omega)}$ and $S_{x_i}^{|u(j\omega)|}$ are both zero is of interest. In this case, even if the distributed parameters deviate from their nominal values, u remains rational in s over this range. However, the frequency range over which $S_{x_i}^{|u(j\omega)|}$ is constant and small is also of interest provided $S_{x_i}^{\angle u(j\omega)}$ is very small over the same range. Over such a range u(jω) instead of being equal to 1/jω will be equal to $\frac{1+\epsilon}{j\omega}$ where ε is a real but small number. Hence, it is seen that u(jω) will also remain rational over this range.

Thus, if the main part of the frequency response is designed to be within any one of the above ranges, it is expected that the sensitivity of the response will be low with respect to the variations of the distributed parameters. Using (2.17d), (2.18d), (2.20), (2.22) a computer program and

$$S^u_{C_{jT}} = S^u_{\alpha_j} \qquad (j = 1,2,3,4)$$

$$S^u_{R_{jT}} = (-1)^j S^u_{m_1} + S^u_{\alpha_j} \qquad (j = 1,2) \qquad (2.23)$$

$$= (-1)^j S^u_{m_2} + S^u_{\alpha_j} \qquad (j = 3,4)$$

and

$$S^u_{m_1} = S^u_{m_2}$$

the various $S^{|u(j\omega)|}_{x_i}$ and $S^{\angle u(j\omega)}_{x_i}$ were calculated and plotted for different values of the tapers m. Figure 2.4 shows these sensitivity plots versus $\omega R_T C_T$ for various m's. The sensitivities are seen to decrease with decreasing values of m. Further, it is observed that there are two regions over which $S^{\angle u(j\omega)}_{x_i}$ is very small and $S^{|u(j\omega)|}_{x_i}$ is constant and small. There is also a region over which both $S^{|u(j\omega)|}_{x_i}$ and $S^{\angle u(j\omega)}_{x_i}$ are varying rapidly. Hence, u cannot remain rational over this range. It may also be observed that the lower range is improved with decreasing taper.

From various plots of Figure 2.4 and the subsequent discussion, one is strongly led to a conjecture about the effect of the non-dual behaviour between any line and its dual on u. The conjecture consists of two parts:

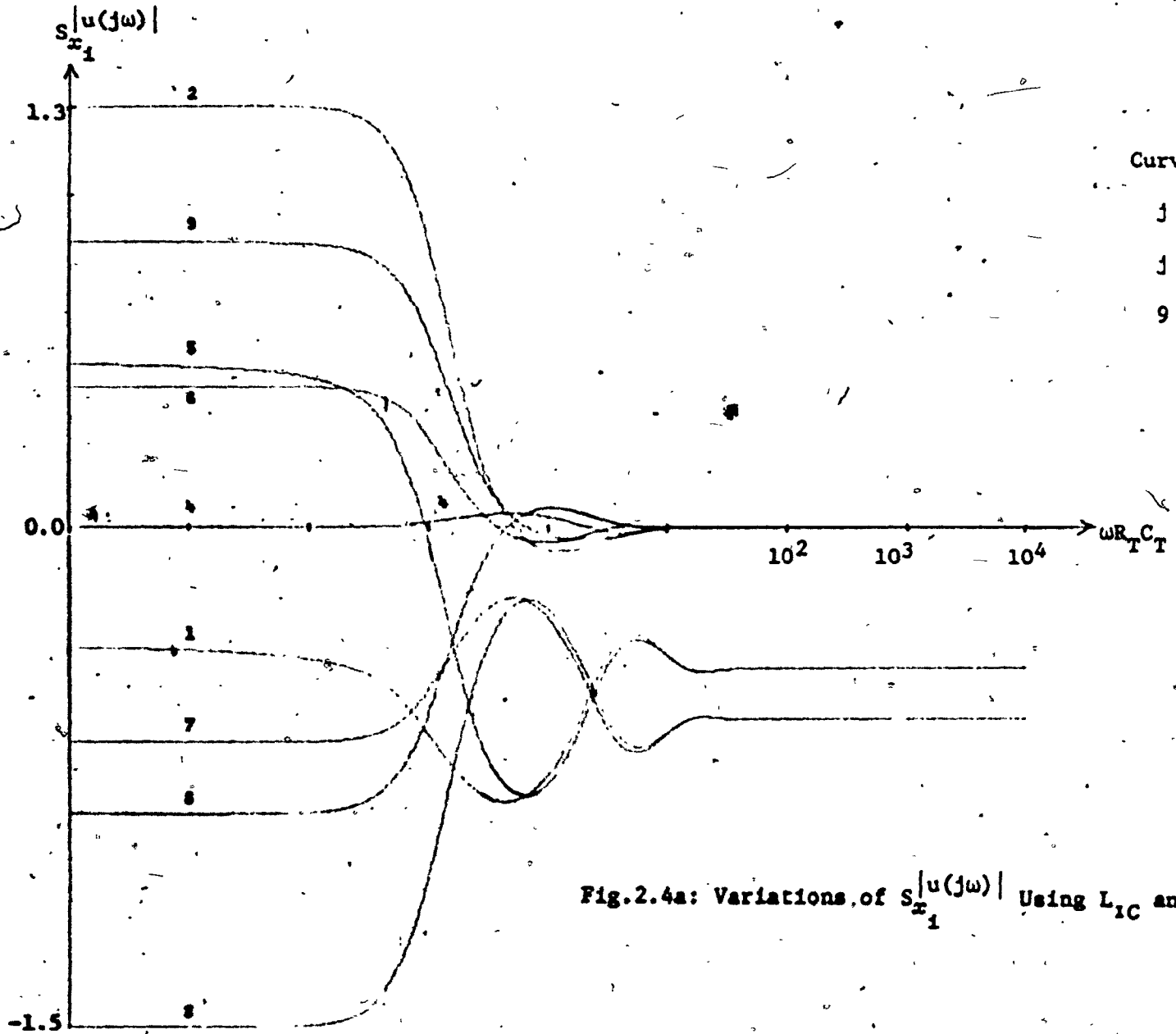

Curve	x_i	
j	R_{jT}	j = 1,2,3,4
j	C_{jT}	j = 5,6,7,8
9	m_1	

Fig.2.4a: Variations of $S^{|u(j\omega)|}_{x_i}$ Using L_{1C} and L_{2C}, $m_1 = 6$

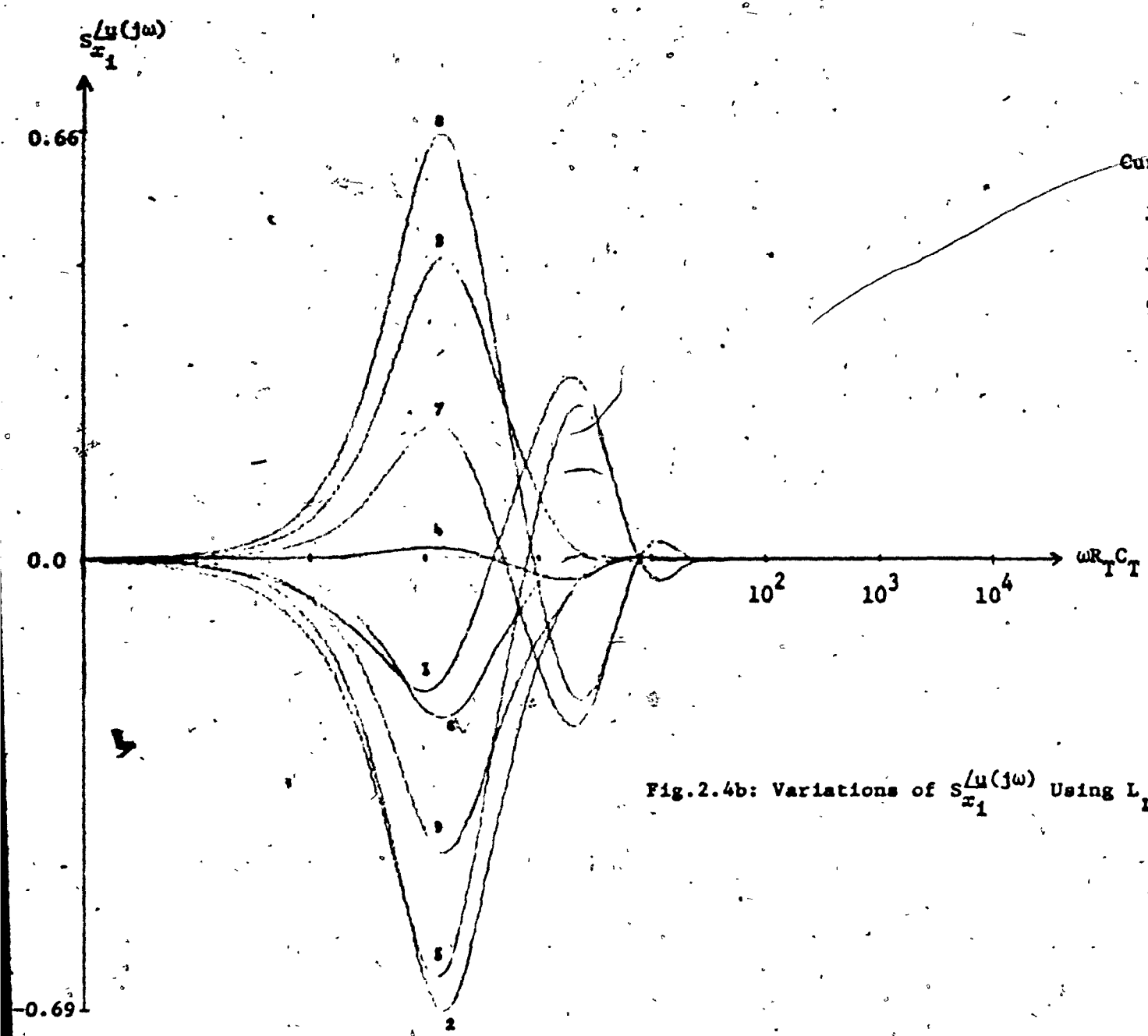

Fig.2.4b: Variations of $S_{x_1}^{/u(j\omega)}$ Using L_{1C} and L_{2C}, $m_1 = 6$

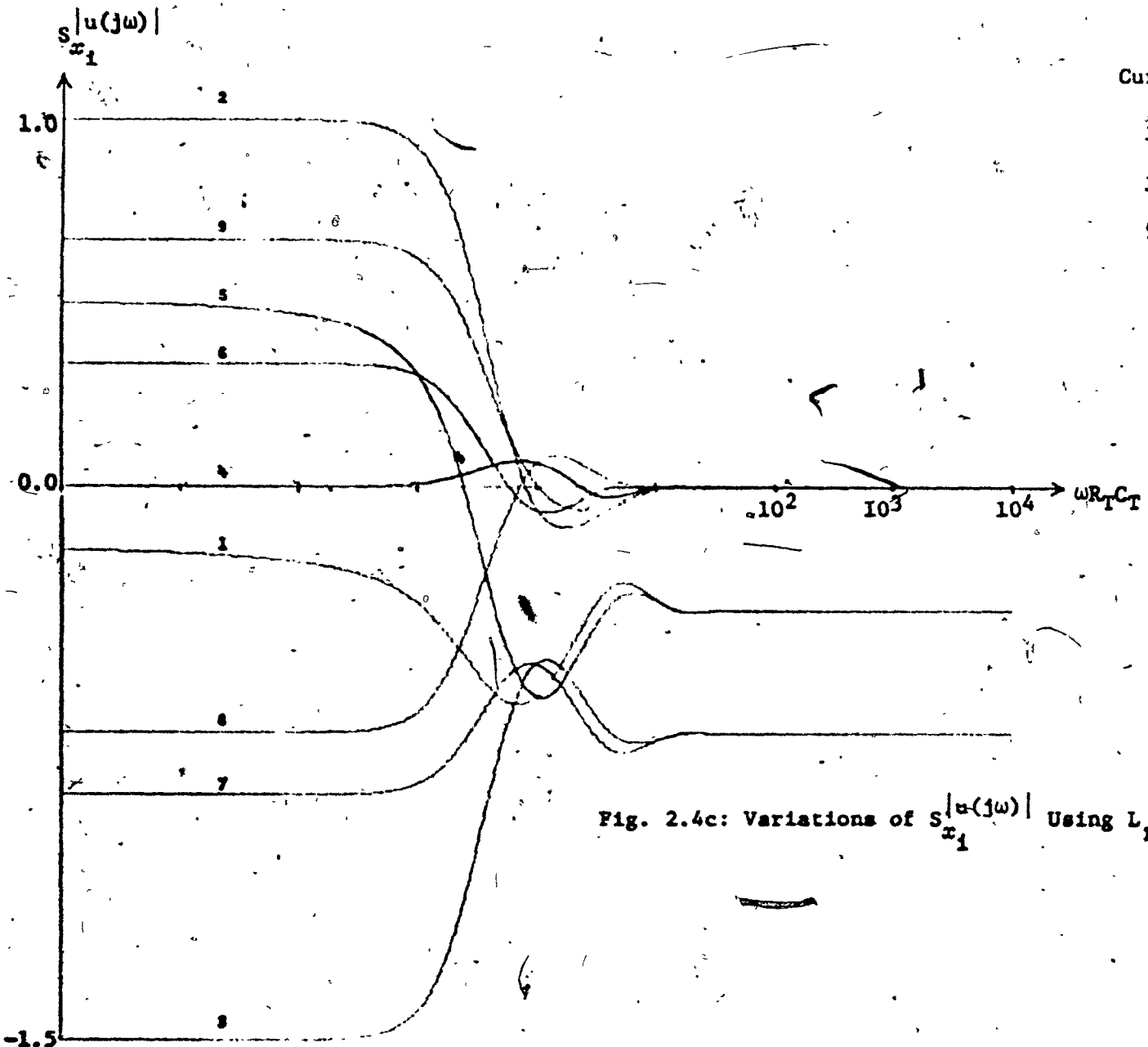

Curve	x_i	
j	R_{jT}	j = 1,2,3,4
j	C_{jT}	j = 5,6,7,8
9	m_i	

Fig. 2.4c: Variations of $S^{|u(j\omega)|}_{x_i}$ Using L_{1C} and L_{2C}, $m_i = 2$

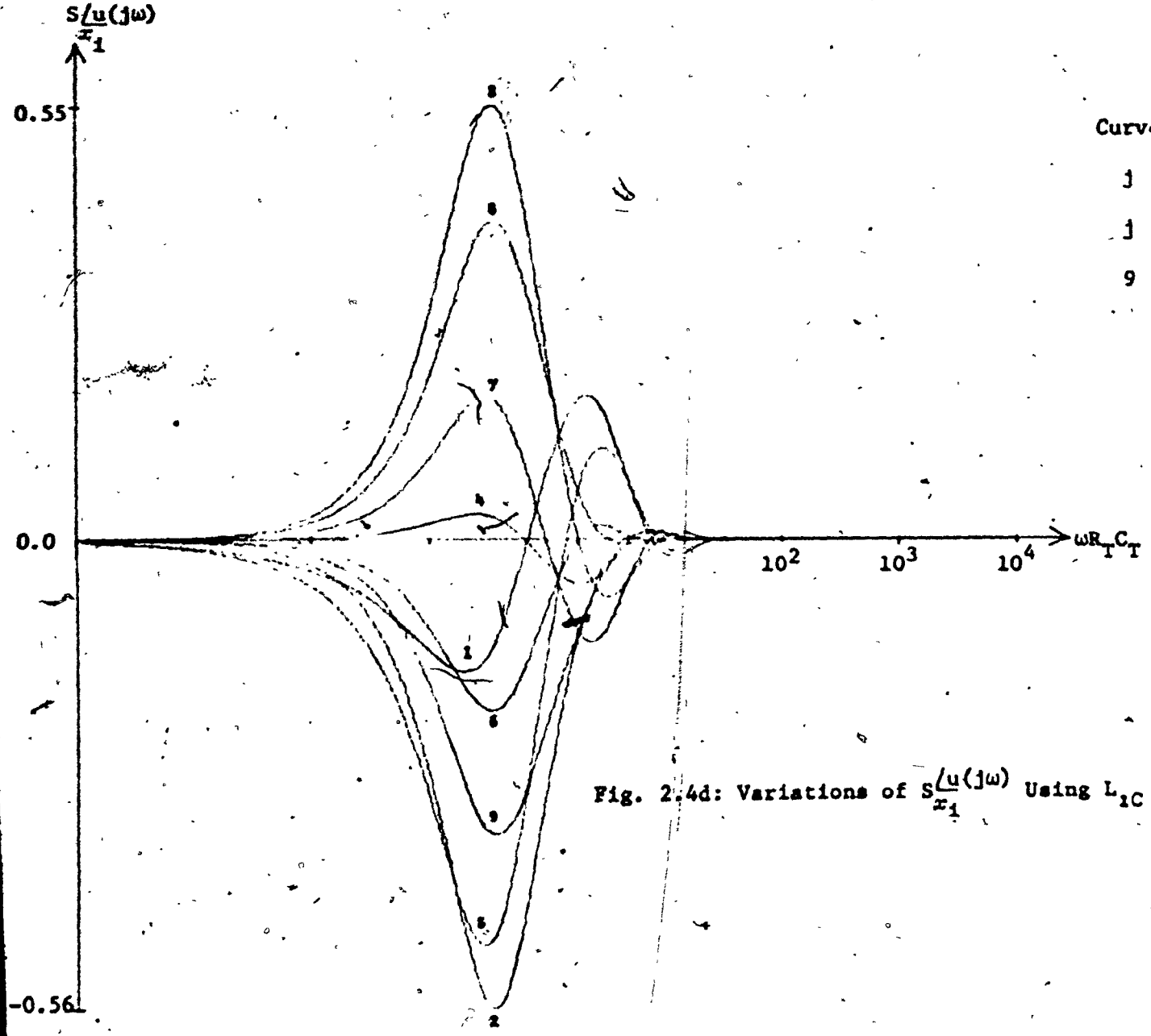

Curve	x_i	
j	R_{jT}	j = 1,2,3,4
j	C_{jT}	j = 5,6,7,8
9	m_1	

Fig. 2.4d: Variations of $S^{\angle u(j\omega)}_{x_i}$ Using L_{1C} and L_{2C}, $m_1 = 2$

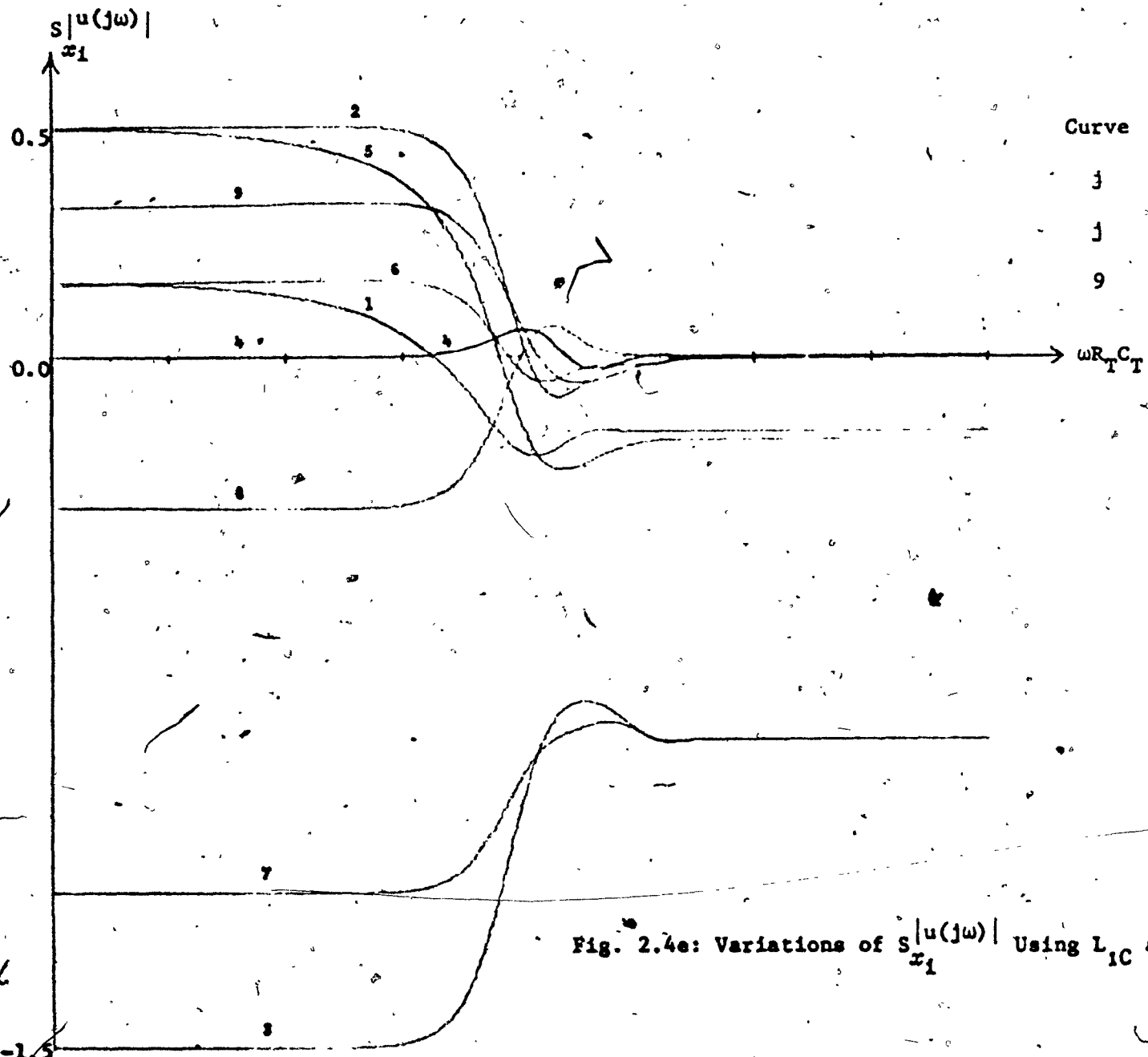

Fig. 2.4e: Variations of $S^{|u(j\omega)|}_{x_i}$ Using L_{1C} and L_{2C}, $m_1 = 0.5$

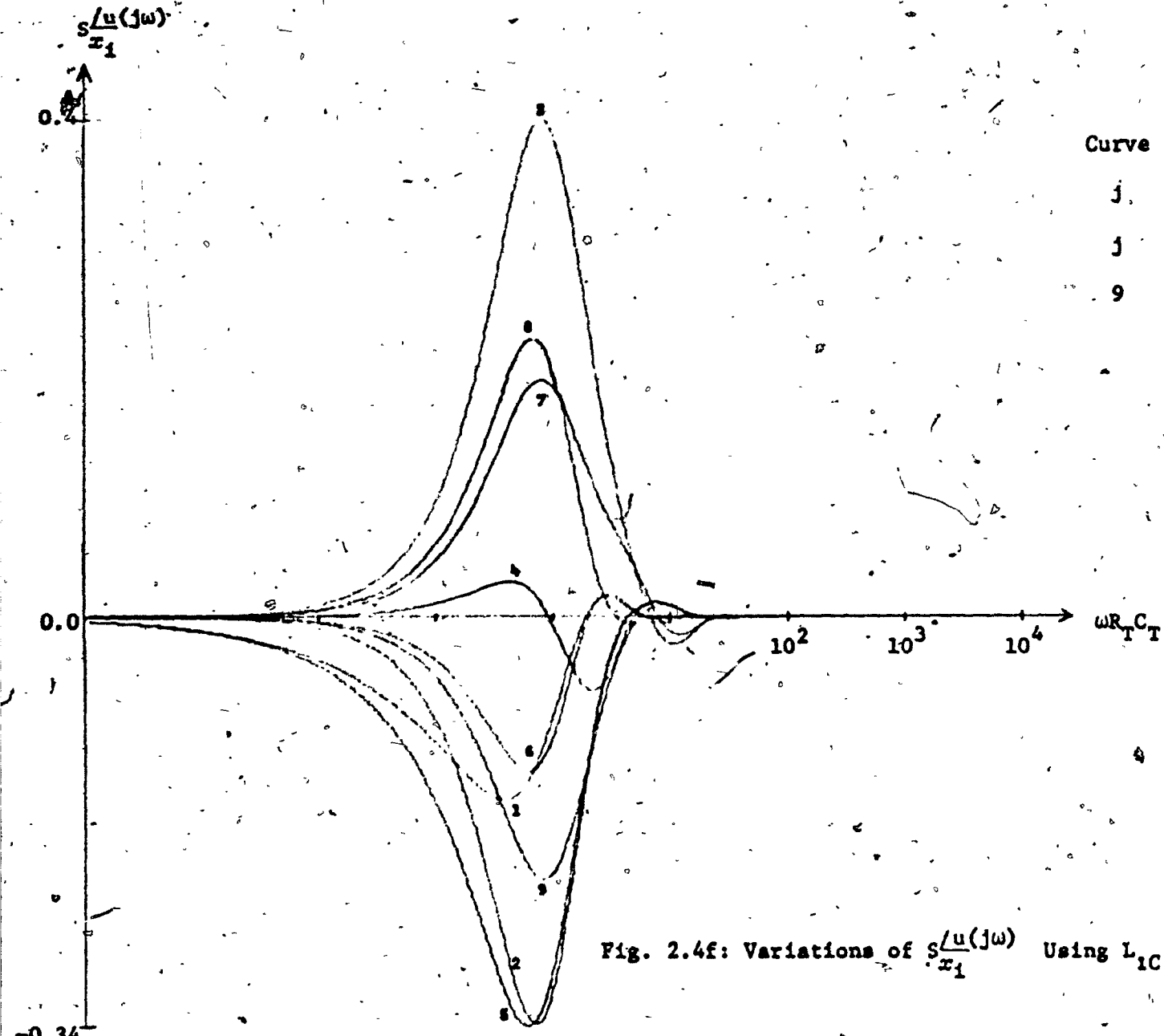

Fig. 2.4f: Variations of $S^{/u(j\omega)}_{x_1}$ Using L_{1C} and L_{2C}, m_1 = 0.5

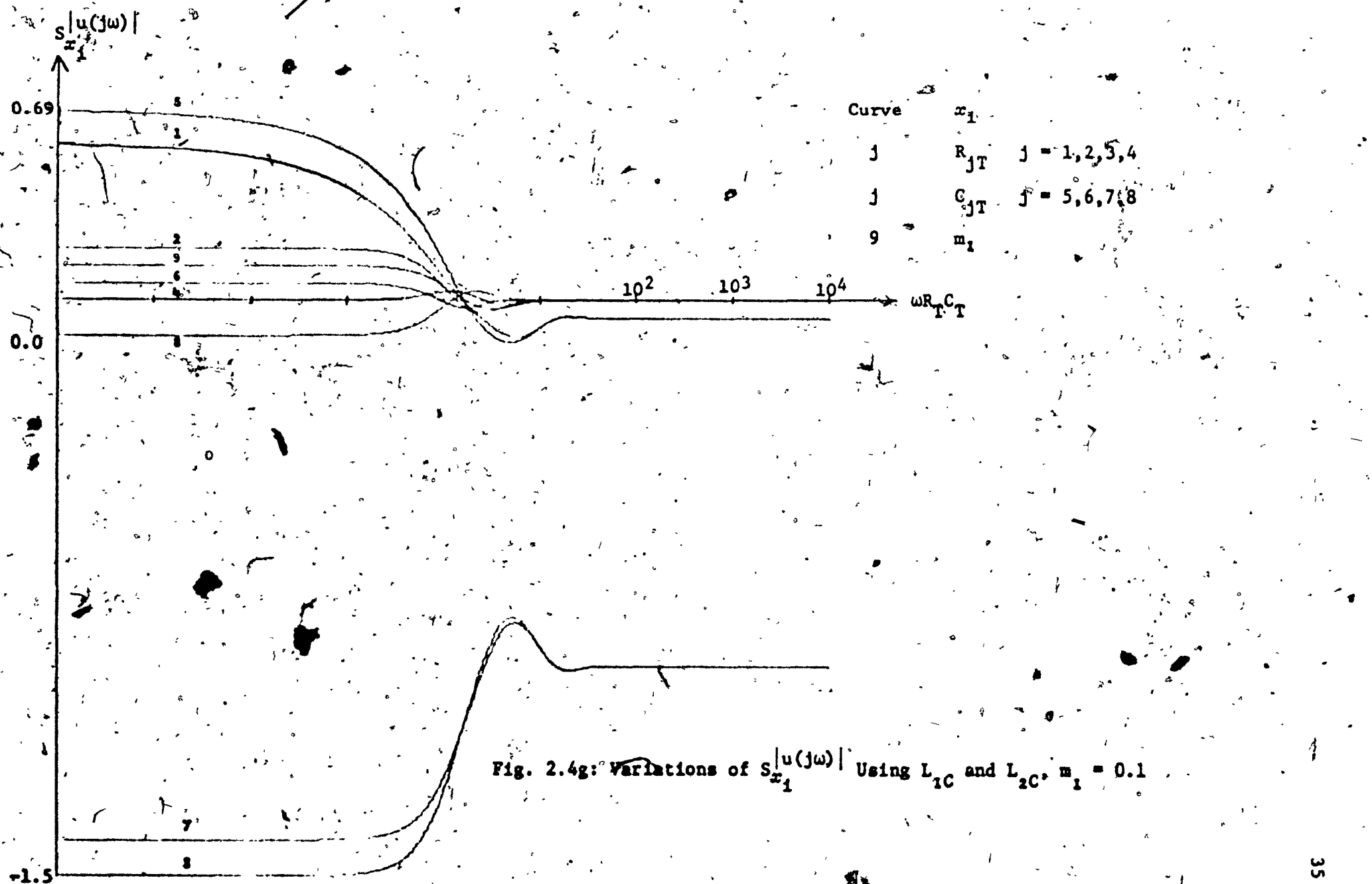

Fig. 2.4g: Variations of $S_{x_1}^{|u(j\omega)|}$ Using L_{1C} and L_{2C}, $m_1 = 0.1$

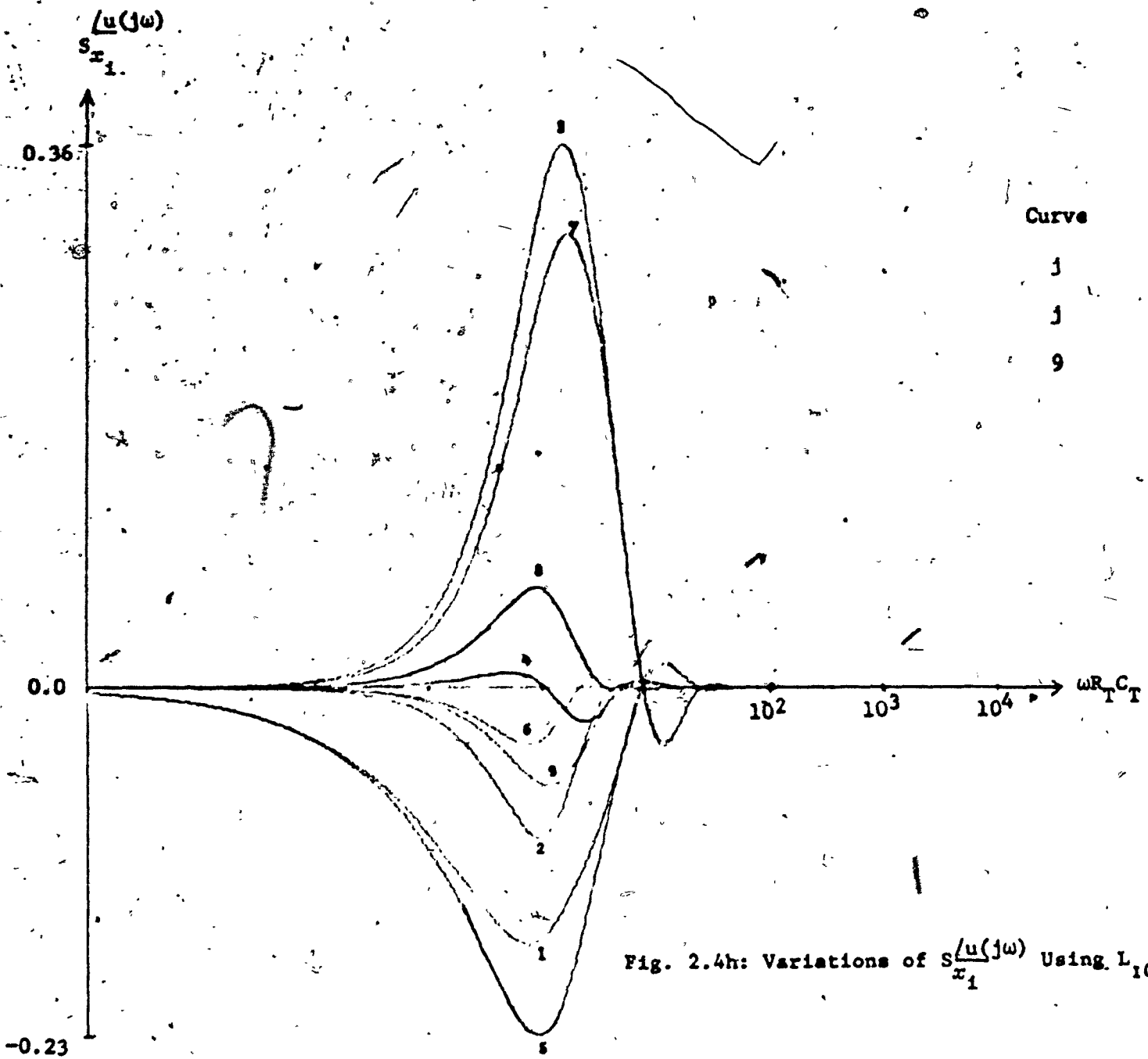

Curve	x_i	
j	R_{jT}	j = 1,2,3,4
j	C_{jT}	j = 5,6,7,8
9	m_i	

Fig. 2.4h: Variations of $S^{\angle u(j\omega)}_{x_i}$ Using L_{1C} and L_{2C}, $m_i = 0.1$

i) if the lines L and L_D are not exactly dual of each other, there are two regions of ω, namely, a lower and an upper region, over which u will remain rational in ω. In between these two region, u cannot remain rational.

ii) The range of the lower region will increase with decreasing value of the taper.

In what follows, this conjecture is verified for the case of an exponential line.

2.4.2 Verification of the Conjecture

Consider the two exponential lines L_{1E} and L_{2E} with per unit length distributions, respectively.

$$z_1(s,x) = r_{o1}\, e^{2k_1 x}\,,\quad y_1(s,x) = sc_{o1}e^{-2k_1 x}\ (0 < x < \ell_1) \qquad (2.24a)$$

and

$$z_2(s,x) = r_{o2}\, e^{2k_2 x}\,,\quad y_2(s,x) = sc_{o2}e^{-2k_2 x}\ (0 < x < \ell_2) \qquad (2.24b)$$

as shown in Figures 2.5a and 2.5b, respectively. Let these two lines be duals of each other, that is

$$r_{o1} = r_{o2} = r_o,\ c_{o1} = c_{o2} = c_o\,,\ \ell_1 = \ell_2 = \ell,\ k_1 = -k_2 = k \qquad (2.24c)$$

Therefore, using these two lines it can be readily shown that

$$u = \frac{1}{R_T C_T s} = \frac{1}{S} \qquad (2.25)$$

where

$$R_T C_T = (r_o\, \ell)(c_o\, \ell) \qquad (2.26)$$

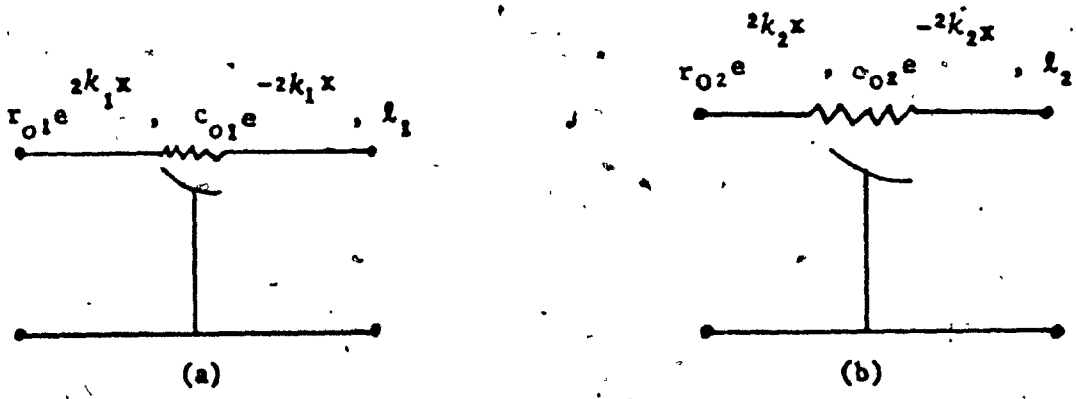

Fig. 2.5: (a) L_{1E}, Exponential Line (r_{o_1}, c_{o_1}, k_1).

(b) L_{2E}, Exponential Line (r_{o_2}, c_{o_2}, k_2).

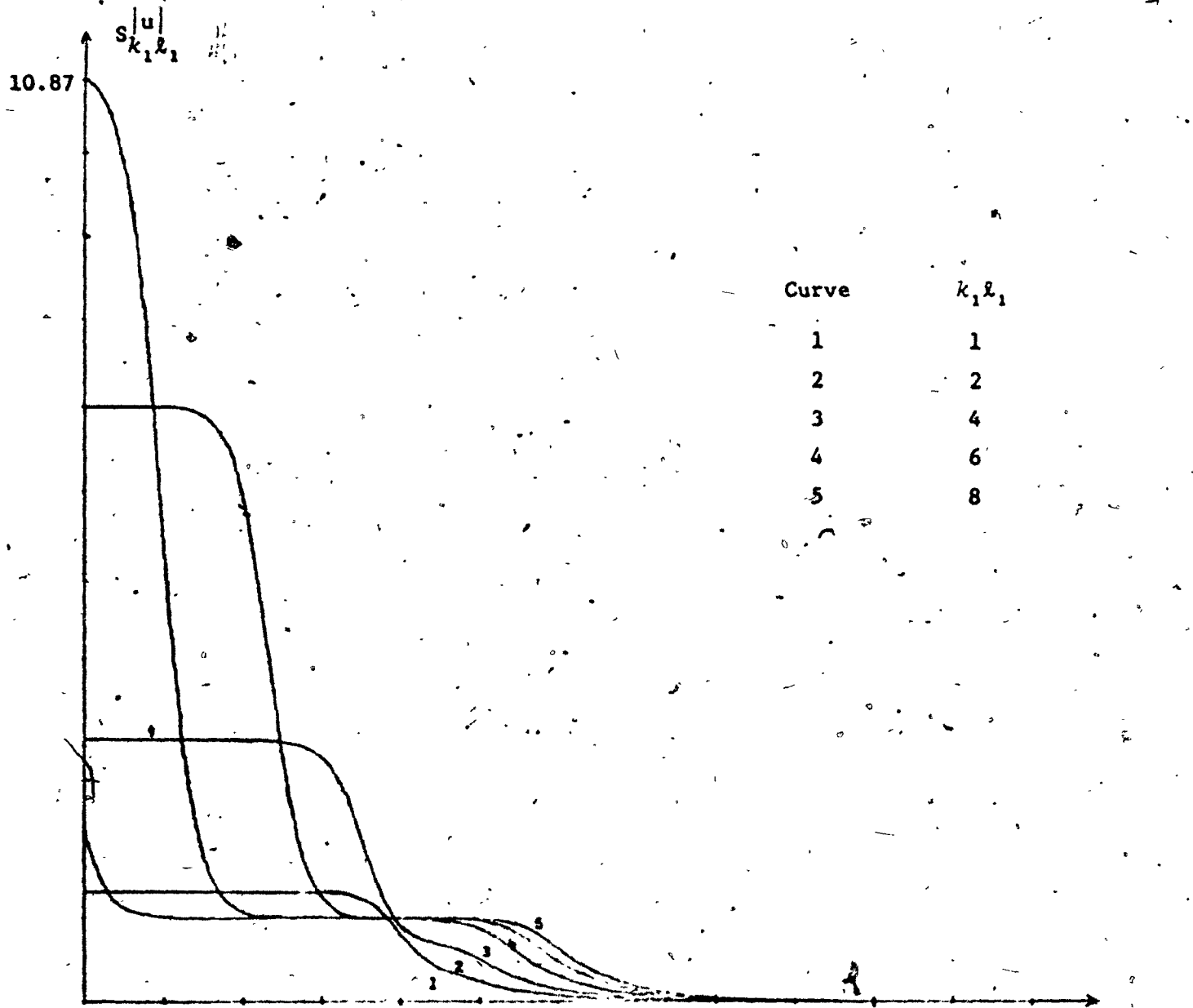

Fig. 2.6a: Variations of $S^{|u|}_{k_1\ell_1}$

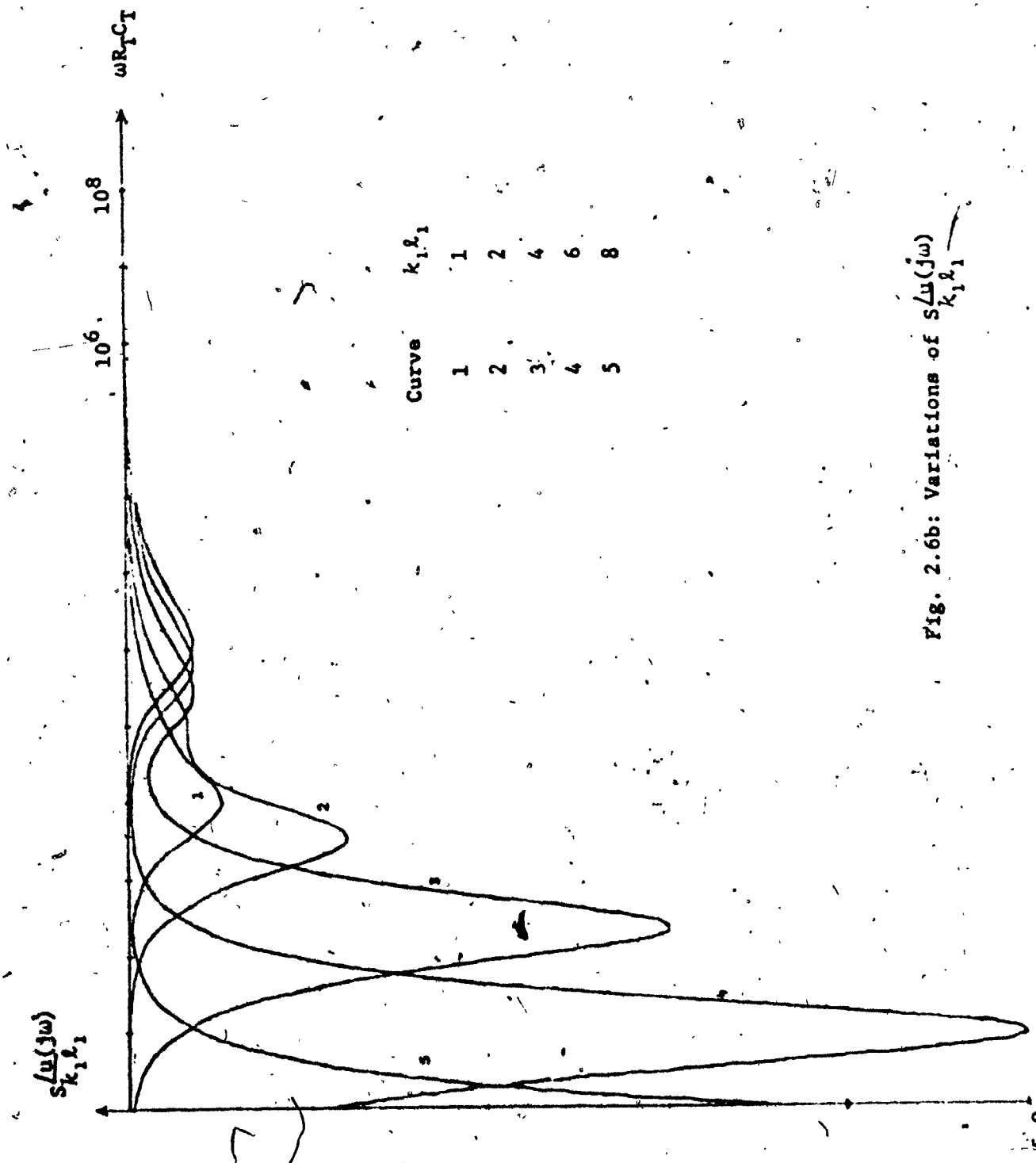

Fig. 2.6b: Variations of $s\angle\mu(j\omega)$ $k_1\ell_1$

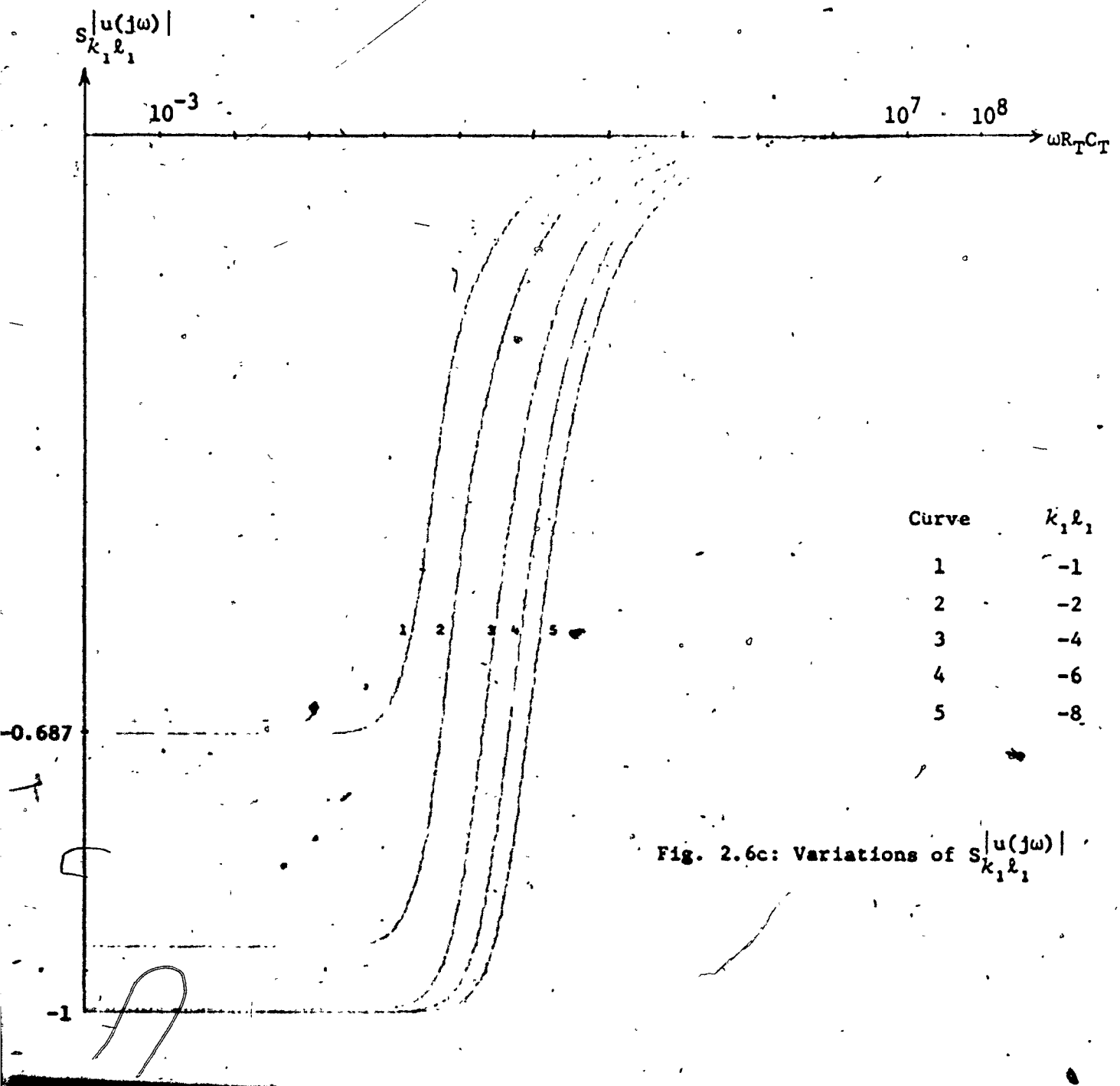

Curve	$k_1 \ell_1$
1	-1
2	-2
3	-4
4	-6
5	-8

Fig. 2.6c: Variations of $S^{|u(j\omega)|}_{k_1 \ell_1}$

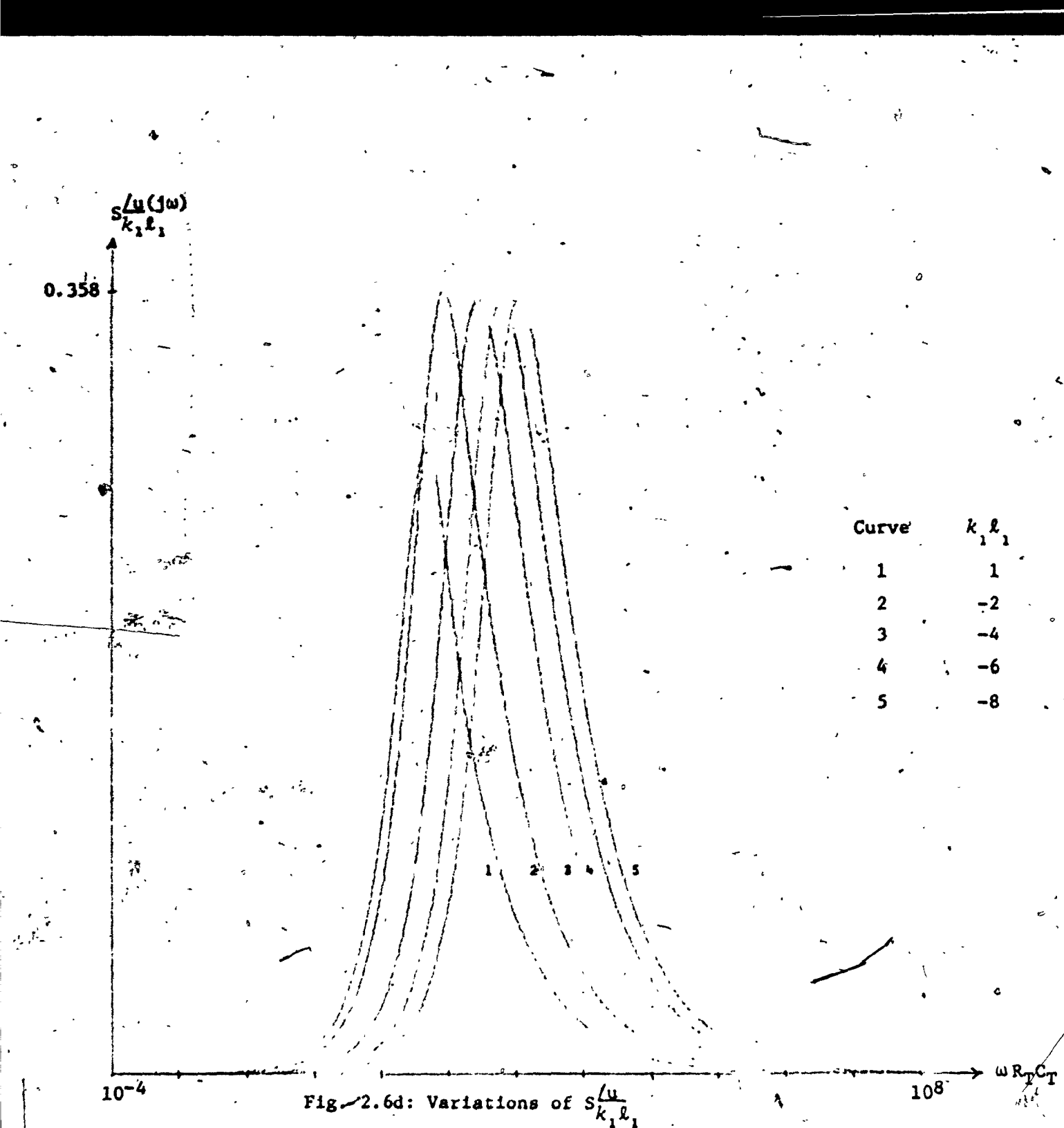

Curve	$k_1 \ell_1$
1	1
2	-2
3	-4
4	-6
5	-8

Fig 2.6d: Variations of $S^{\angle u}_{k_1 \ell_1}$

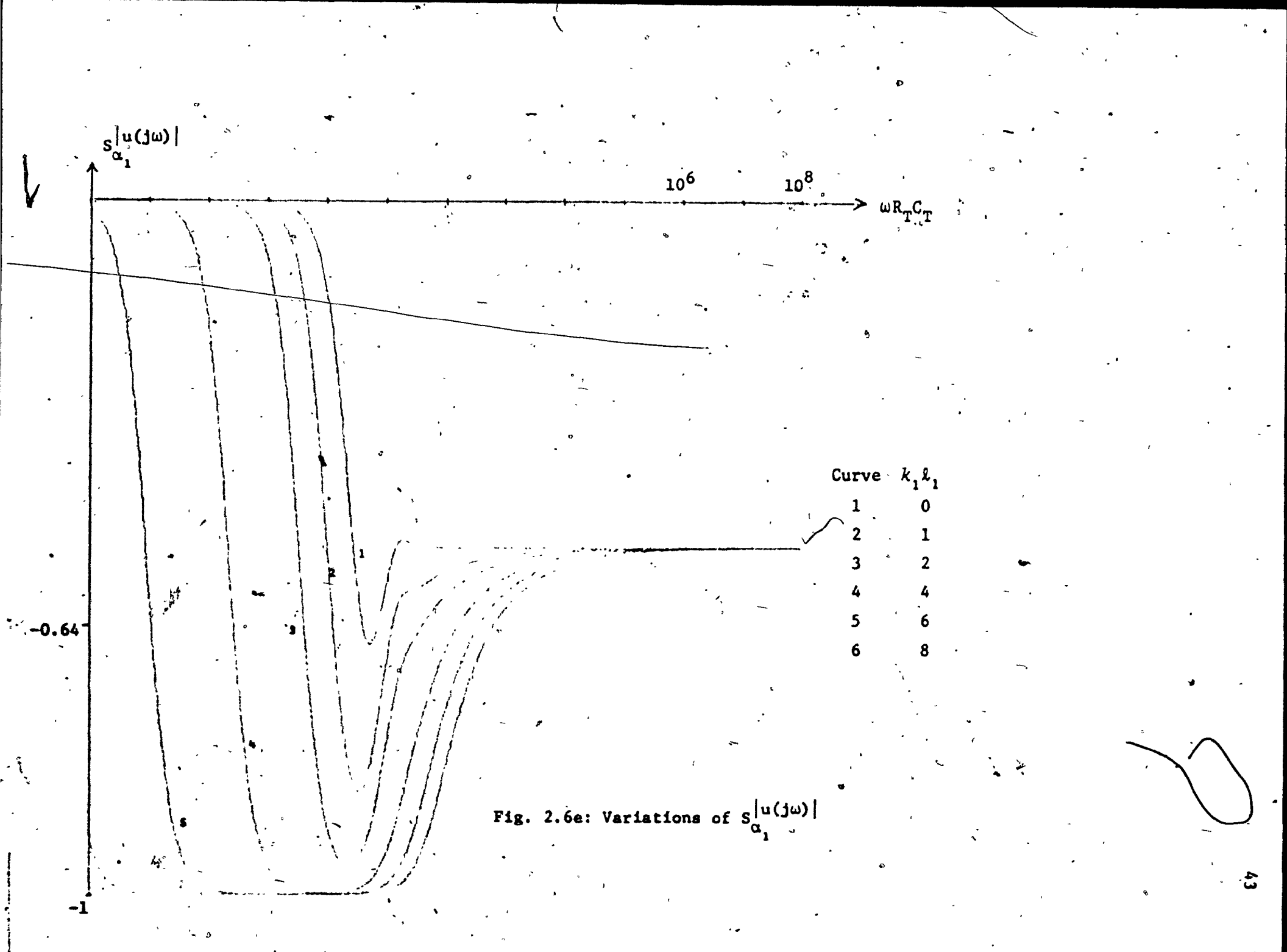

Curve	$k_1 \ell_1$
1	0
2	1
3	2
4	4
5	6
6	8

Fig. 2.6e: Variations of $S_{\alpha_1}^{|u(j\omega)|}$

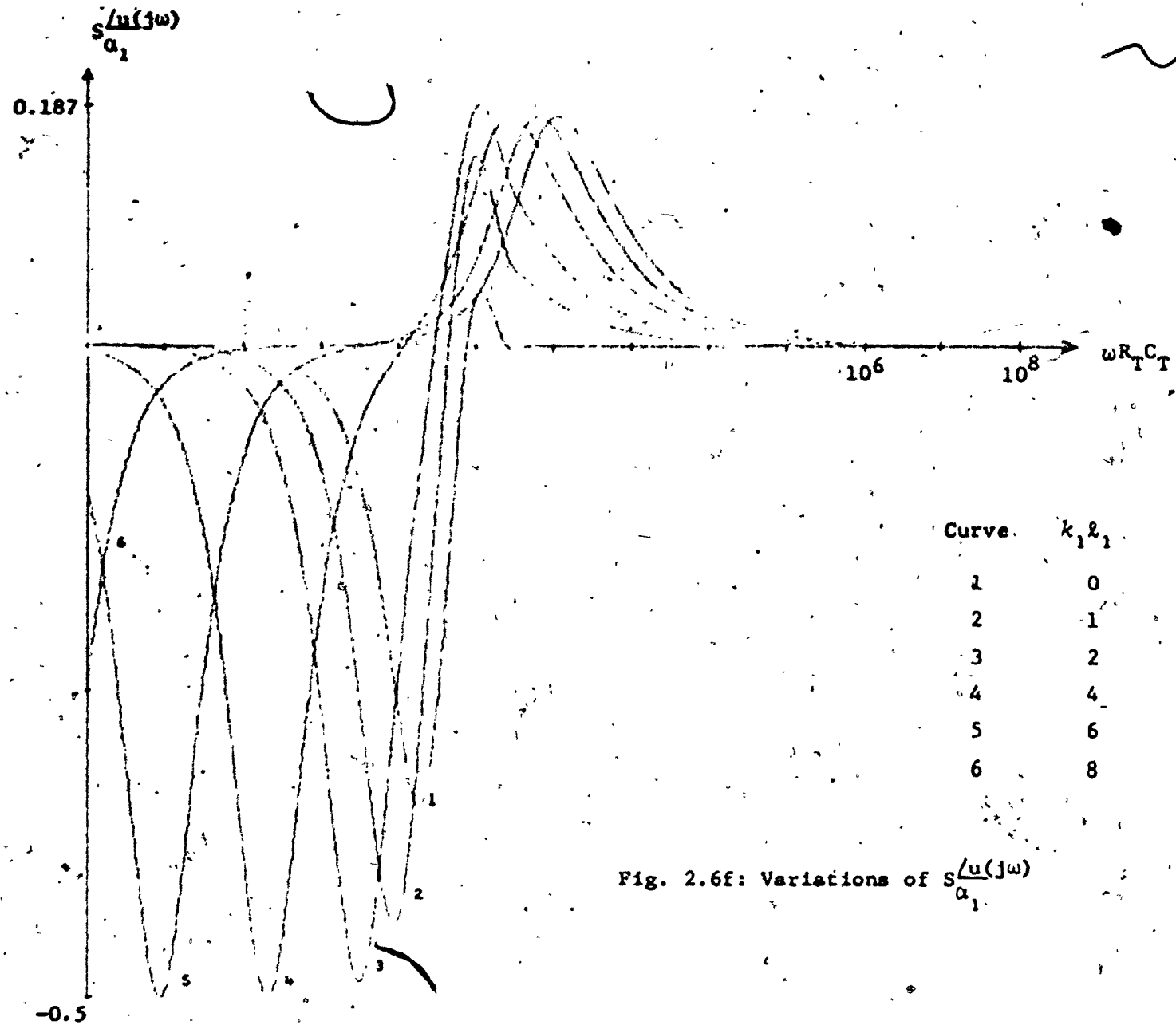

Curve	$k_1 \ell_1$
1	0
2	1
3	2
4	4
5	6
6	8

Fig. 2.6f: Variations of $S^{/u(j\omega)}_{\alpha_1}$

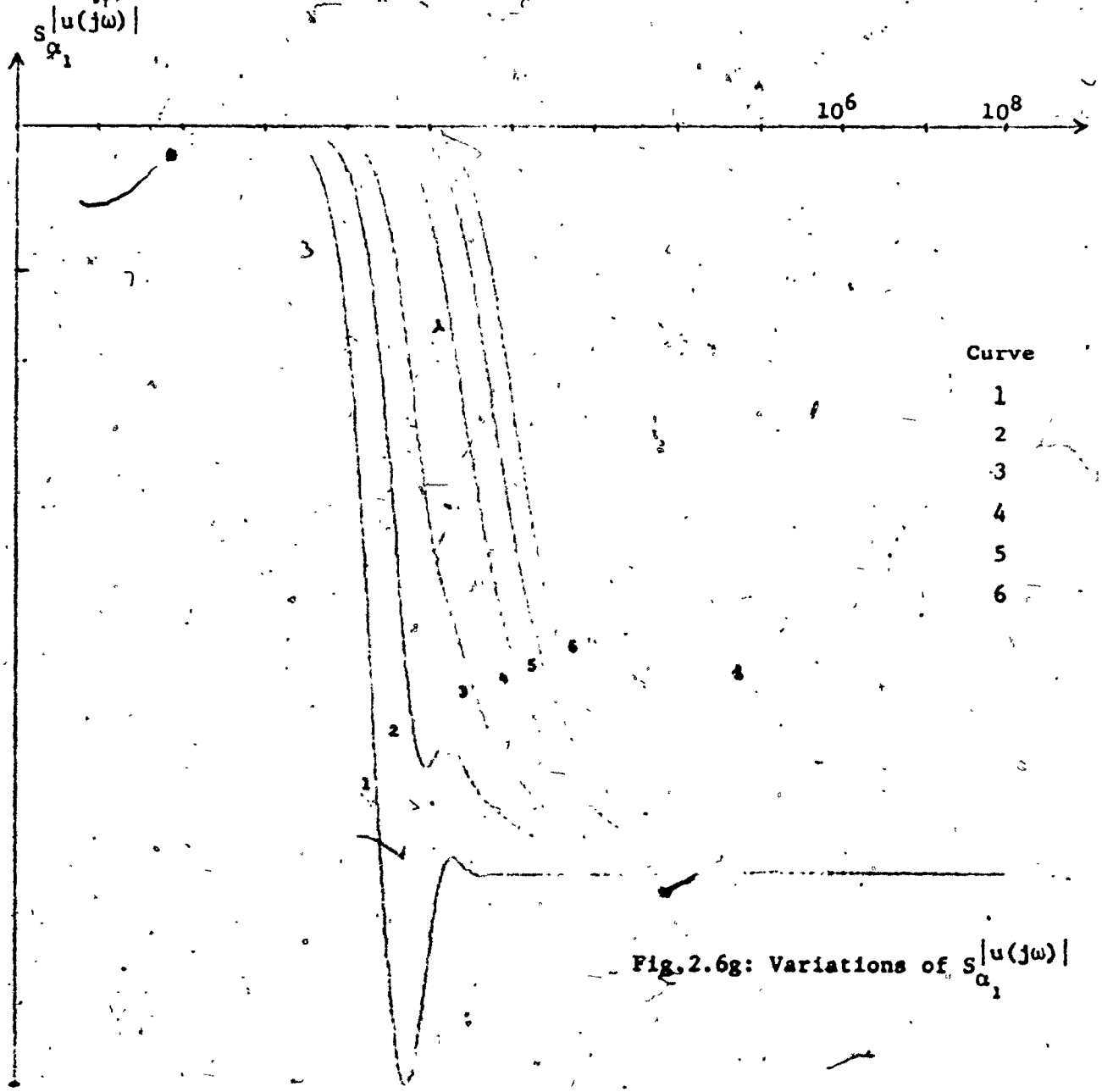

Curve	$k_1 \ell_1$
1	0
2	-1
3	-2
4	-4
5	-6
6	-8

Fig.2.6g: Variations of $S^{|u(j\omega)|}_{\alpha_1}$

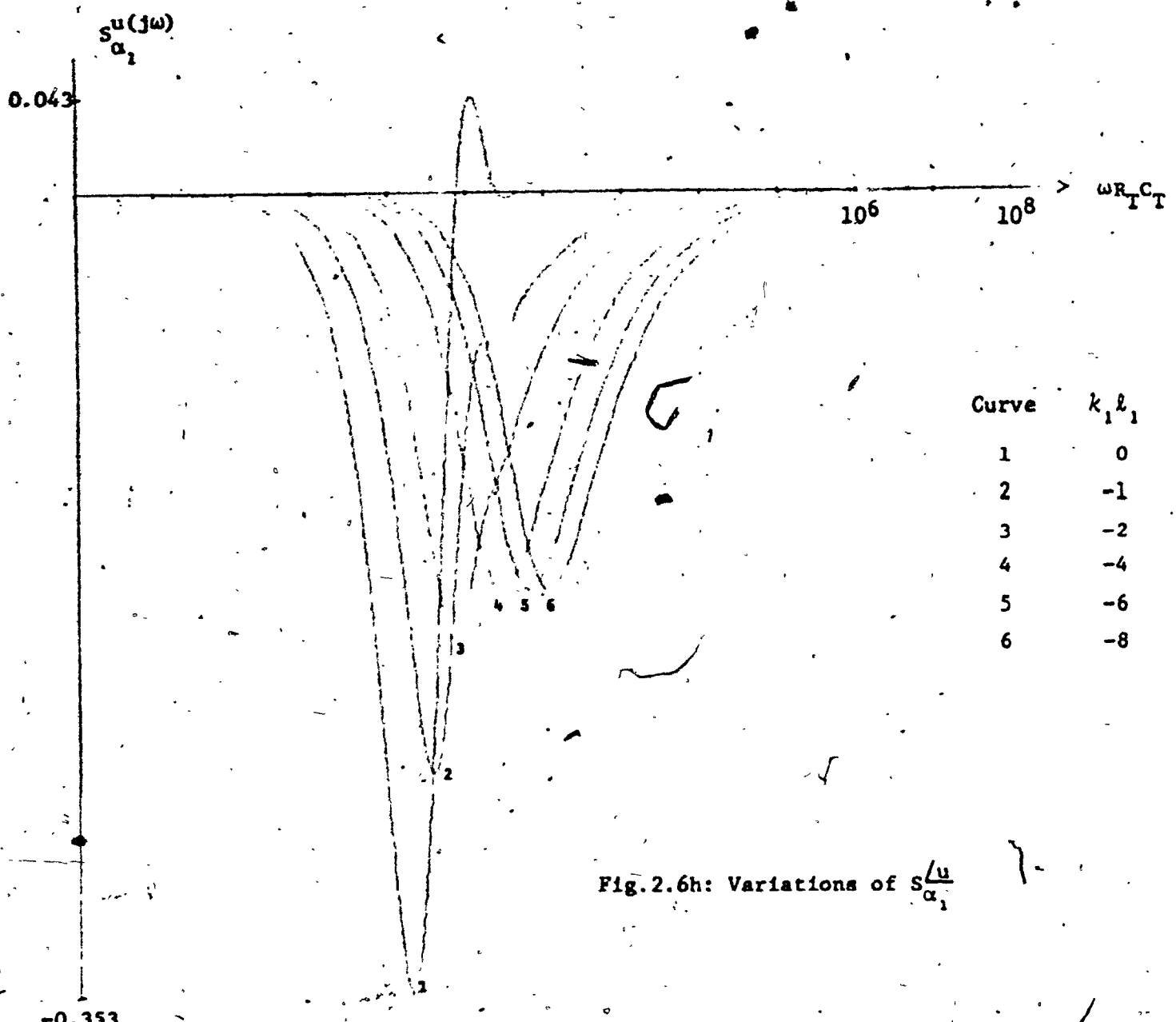

Curve	$k_1 \ell_1$
1	0
2	-1
3	-2
4	-4
5	-6
6	-8

Fig. 2.6h: Variations of $S^{u}_{\alpha_1}$

However, if the lines are not duals, then the expression for u becomes

$$u = \frac{1}{\alpha_2 S} \frac{\sinh \sqrt{(k_1 \ell_1)^2 + \alpha_1 S}}{(\cosh \sqrt{(k_1 \ell_1)^2 + \alpha_1 S}) \cdot \sqrt{(k_1 \ell_1)^2 + \alpha_1 S} - (k_1 \ell_1) \sinh \sqrt{(k_1 \ell_1)^2 + \alpha_1 S}} \times$$

$$\frac{(\cosh \sqrt{(k_2 \ell_2)^2 + \alpha_2 S}) \cdot \sqrt{(k_2 \ell_2)^2 + \alpha_2 S} - (k_2 \ell_2) \sinh \sqrt{(k_2 \ell_2)^2 + \alpha_2 S}}{\sinh \sqrt{(k_2 \ell_2)^2 + \alpha_2 S}} \qquad (2.27)$$

where

$$(r_{oj}\, \ell_j) \cdot (c_{oj}\, \ell_j) = R_{jT} C_{jT} = \alpha_j\, R_T C_T \quad (j = 1,2)$$

The various plots for $S^u_{x_i}$ (where x_i is any one of the parameters of the lines) are shown in Figure 2.6. Note that $S^u_{k_1 \ell_1} = - S^u_{k_2 \ell_2}$ and $S^u_{\alpha_2} = - 1 - S^u_{\alpha_1}$. It is easily observed from these plots, that the results are in agreement with the conjecture of the previous section.

2.5 EXACT SYNTHESIS OF RATIONAL TRANSFER FUNCTIONS USING COMMENSURATE UNIFORM RC LINES

It has been pointed out earlier that an important case of the tapered RC line is the $\overline{\text{URC}}$. Geometrically, it is the simplest line to design and also to construct using thin film technology. In this section, we shall consider realizations using commensurate $\overline{\text{URC}}$'s [59]. For this purpose, it is necessary that the two OPI's corresponding to Figure 2.2 use a short circuited $\overline{\text{URC}}$ and an open circuited $\overline{\text{URC}}$ instead of L_1 and L_{1D}, respectively. These two OPI's are shown in Figure 2.7 and are

$$Z_1(s) = R_{1T} p(s) \;, \quad Z_2(s) = (K/R_{2T}) q(s) \qquad (2.28)$$

where

$$p(s) = \frac{\tanh\Theta_1}{\Theta_1} \quad , \quad q(s) = \frac{\Theta_2}{\coth\Theta_2} \tag{2.29a}$$

$$\Theta_1 = \sqrt{sR_{1T}C_{1T}} \quad , \quad \Theta_2 = \sqrt{sR_{2T}C_{2T}} \tag{2.29b}$$

$$R_{jT} = r_{oj}\ell_j \quad , \quad C_{jT} = c_{oj}\ell_j \quad (j = 1,2) \tag{2.29c}$$

Therefore, from (2.13a)

$$u(s) = \frac{1}{s\sqrt{R_{1T}C_{1T}R_{2T}C_{2T}}} \; \frac{\tanh\sqrt{R_{1T}C_{1T}s}}{\tanh\sqrt{R_{2T}C_{2T}s}} \tag{2.30}$$

It may be noted that (2.30) could be obtained from (2.27) by setting $k_1 = k_2 = 0$. Note that $\lim_{s\to\infty} su(s) = \frac{1}{R_{2T}C_{2T}}$ and $\lim_{s\to\infty} su(s) = \frac{1}{\sqrt{R_{1T}C_{1T}R_{2T}C_{2T}}}$.

It is interesting to note that for $\overline{URC}$'s the only condition for u to be rational in S is that the lines be commensurate, that is,

$$R_{1T}C_{1T} = R_{2T}C_{2T} = R_TC_T \tag{2.31a}$$

In that case

$$u = \frac{1}{R_TC_Ts} = \frac{1}{S} \tag{2.31b}$$

To study the effect of the lines not being commensurate, eq. (2.30) was used and the sensitivities of u with respect to the different RC products were obtained. Figures 2.8a and 2.8b show plots for $S^{\angle u(j\omega)}_{R_{1T}C_{1T}}$ and $S^{|u(j\omega)|}_{R_{1T}C_{1T}}$ respectively. From (2.30) it may be shown that $S^{\angle u(j\omega)}_{R_{2T}C_{2T}} = -S^{\angle u(j\omega)}_{R_{1T}C_{1T}}$ and $S^{|u|}_{R_{2T}C_{2T}} = -1 - S^{|u|}_{R_{1T}C_{1T}}$. Therefore, it is seen from these plots that if the RC product is chosen to lie in either of the two regions, namely $\omega R_TC_T < 0.01$ or $\omega R_TC_T > 30$, where $S^{\angle u(j\omega)}_{R_{jT}C_{jT}} = 0$ $(j = 1,2)$ and $S^{|u(j\omega)|}_{R_{jT}C_{jT}}$ $(j = 1,2)$ are constant and small,

Fig. 2.7: (a) Input Impedance of a Short Circuited $\overline{URC}$

(b) Input Impedance of a Gyrator of Gyration Constant K, Terminated by an Open Circuited URC.

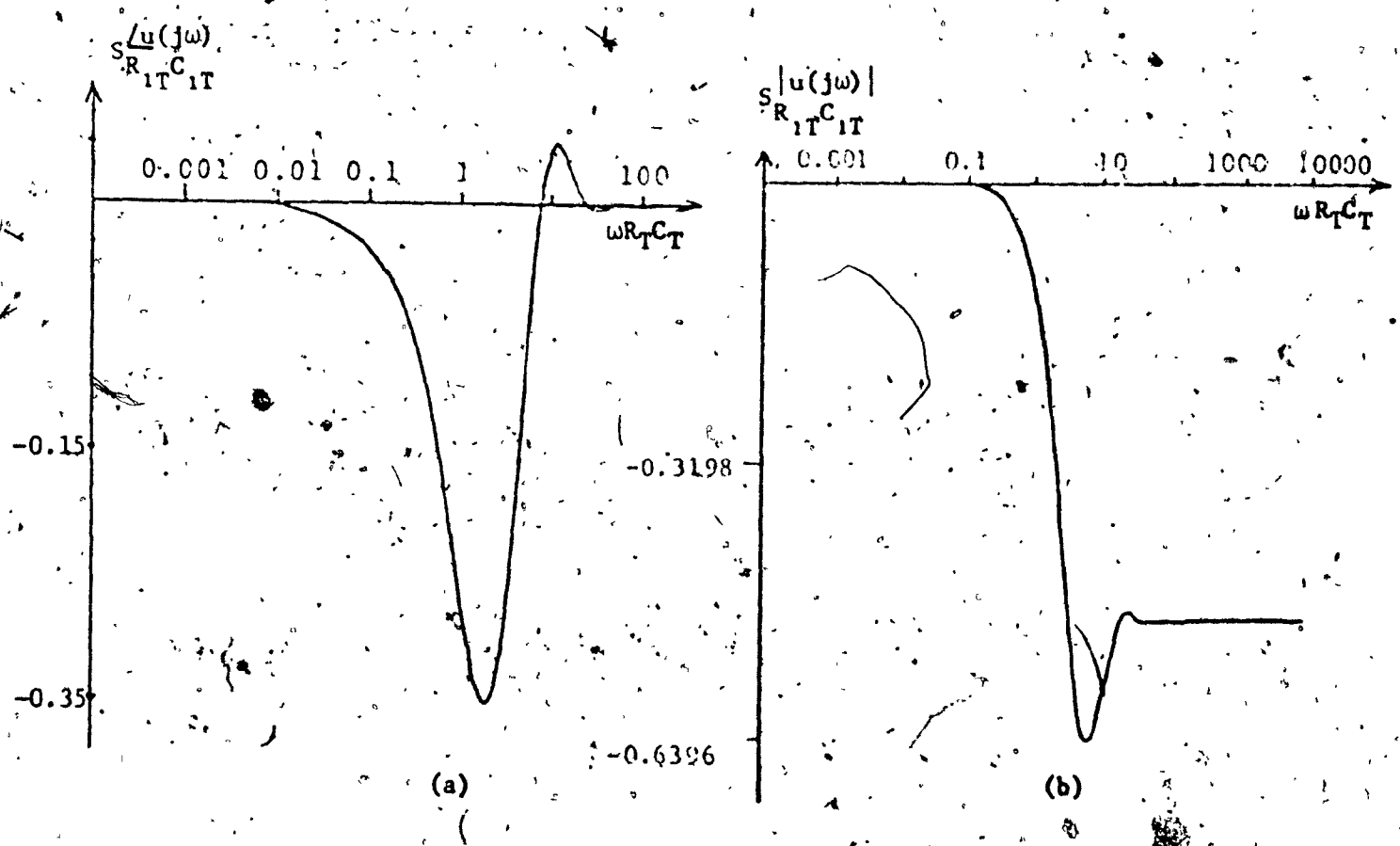

Fig. 2.8: (a) Variations of $S^{\angle u}_{R_{1T}C_{1T}}$ Using URC, (b) Variations of $S^{|u|}_{R_{1T}C_{1T}}$ Using $\overline{URC}$.

then u remains rational even if the lines are not exactly commensurate. Further, since the variation in $|u(j\omega)|$ is very small with respect to the changes of the RC products over these ranges, it is expected that the sensitivity of the response with respect to the RC products of the URC's will be low, if the main part of the response is designed to lie within either of the above two regions. The choice of a particular region will depend on practical considerations such as those imposed by thin film technology and the frequency range of interest. However, the first region namely $\omega R_T C_T < 0.01$ suggests that this method could be useful for very low frequency applications ($0.1 < f < 100$) [44-53], a range which other distributed realizations cannot adequately cover.

In the range $0.01 < \omega R_T C_T < 30$, u has a magnitude as well as a phase which are varying. Thus u can not be rational in s in this range. However, it may be noted that both $S^{u}_{R_{iT}C_{iT}}$ and $S^{|u|}_{R_{iT}C_{iT}}$ are also quite low in this range. Hence, even in this frequency range the response of the designed network is not expected to deviate adversely from that of the rational one. However, the realized response may now be sensitive to the variation of the distributed parameters.

It is observed from Figures 2.4, 2.6 and 2.8 that not much of the useful frequency range, in which u(s) remains rational in s, is lost if URC's are used instead of tapered lines. Therefore, it may be concluded that not much advantage is gained by using tapered RC lines instead of URC's in the realizations.

A step by step procedure is now given for realizing a given rational transfer function T(s) using $\overline{\text{URC}}$'s:

i) Using transformation (2.31) obtain the rational transfer function

$$G(u) = T\left(\frac{1}{R_T C_T u}\right) \tag{2.32}$$

ii) Synthesize G(u) in the u-plane by any known technique as a passive or active lumped RC network. It is assumed that active elements with real gain parameters only are used.

iii) T(s) is now realized by replacing the different lumped resistors R_{ui}'s and capacitors C_{ui}'s in the u-plane by the appropriate OPI's of Figure 2.7, that is,

$$R_{1Ti} = R_{ui} \ , \ (K_i/R_{2Ti}) = 1/C_{ui} \tag{2.33}$$

iv) Choose the commensurate RC product of the lines such that the main part of the response lies in either of the regions $\omega R_T C_T \leq 0.01$ or $\omega R_T C_T \leq 30$ whichever is suitable.

2.6 GENERAL SENSITIVITY CONSIDERATIONS

An important performance criterion of any realization is its sensitivity with respect to the different network elements. When the $\overline{\text{URC}}$'s are commensurate, the sensitivities of T(s) of the distributed structure with respect to its parameters, using (2.31), (2.32) and (2.33) are:

$$S^{T}_{R_{1T1}} = S^{G}_{R_{ui}} \quad , \quad S^{T}_{R_{2T1}} = S^{G}_{C_{ui}} \quad \text{and} \quad S^{T}_{K_i} = -2S^{G}_{C_{ui}} \qquad (2.34)$$

Hence, we note from (2.34) that if the lumped structure in the u-plane has low sensitivities with respect to its elements, then the corresponding distributed realization will automatically possess these low sensitivity properties in the s-plane.

2.7 CONCLUSIONS

A new transformation u(s) of the complex frequency variable s has been developed. The variable u(s) has been employed to derive a technique for an exact realization of rational transfer functions in s, using any tapered RC line, its dual, an ideal gyrator, and in general, active elements with real gain parameters as building blocks. The effect of the non duality between the lines on the realization has been examined. It has been established that not much is gained by using tapered lines instead of commensurate $\overline{\text{URC}}$'s in the realization. Realizations using $\overline{\text{URC}}$'s have been studied. These $\overline{\text{URC}}$ realizations can easily be adapted for hybrid IC implementation and are particularly suitable for very low frequency applications, where other described is very simple compared to any of the other known distributed realizations. The effect, on the realized response, due to the $\overline{\text{URC}}$'s being not exactly commensurate has been studied in detail and found to be relatively negligible if the RC product of the $\overline{\text{URC}}$'s is chosen such that the main part of the desired response lies either in the region $\omega R_T C_T \leq 0.01$ or $\omega R_T C_T \geq 30$. It has been pointed

out that, in order to implement efficiently the synthesis procedure, a lumped RC active low sensitivity network is required as an intermediate step. In this network, it is desirable to have minimum number of resistors and capacitors and, further, all the capacitors should be grounded. The number of $\overline{\text{URC's}}$ as well as gyrators will then be minimum. In addition, all the gyrators will be able to share a common power supply. The purpose of the next Chapter is to derive one such network and investigate its properties.

CHAPTER III

GROUNDED CAPACITOR RC ACTIVE NETWORK

3.1 INTRODUCTION

It has been observed that a low sensitivity RC active network with all of its capacitors grounded is required, as an intermediate step, in implementing efficiently the synthesis procedure proposed in Chapter II. The aim of this chapter is to develop one such network. First, a network which is capable of realizing any open circuit voltage transfer function is obtained. Then, the second order case of this network is considered in detail.

3.2 ACTIVE RC REALIZATION OF AN ARBITRARY TRANSFER FUNCTION USING FINITE GAIN AMPLIFIERS AND GROUNDED CAPACITORS.

Consider the n-section RC recurrent ladder shown in Figure 3.1, whose transmission matrix is given by [a]:

$$[a] = \begin{bmatrix} b_n(\bar{S}) & R_o B_{n-1}(\bar{S}) \\ sC_o B_{n-1}(\bar{S}) & b_{n-1}(\bar{S}) \end{bmatrix} \qquad (3.1a)$$

where

$$\bar{S} = sRC \qquad (3.1b)$$

and the polynomials $B_n(s)$ and $b_n(s)$ are defined by

$$B_n(\bar{S}) = \sum_{k=0}^{n} \binom{n+k-1}{n-k} \bar{S}^k \qquad (3.2a)$$

and

$$b_n(\bar{S}) = \sum_{k=0}^{n} \binom{n+k}{n-k} \bar{S}^k \qquad (3.2b)$$

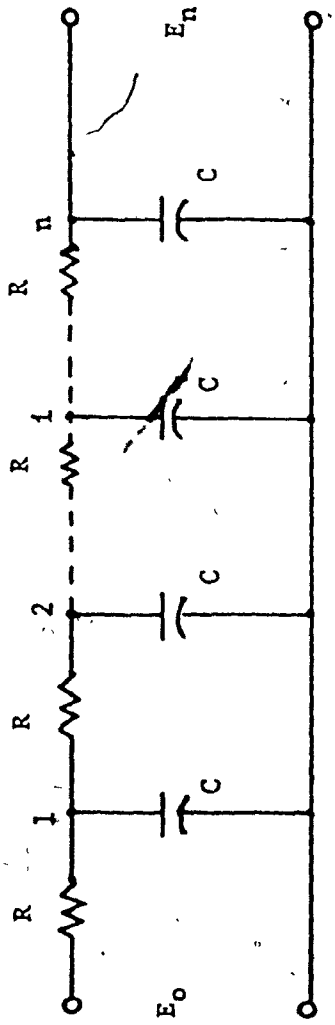

Fig. 3.1: Recurrent RC Ladder

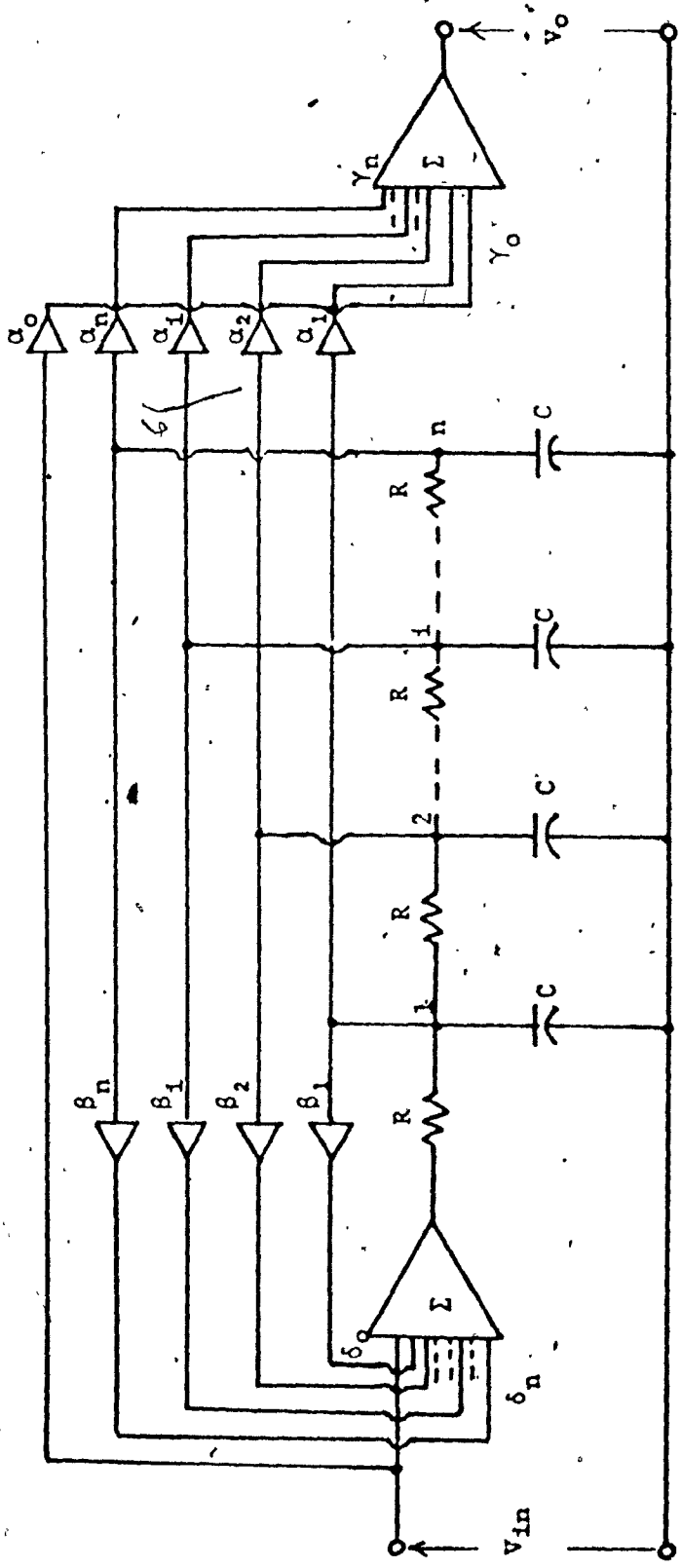

Fig. 3.2: Grounded Capacitor Filter

The open circuit voltage transfer function of the network is

$$T(s) = \frac{E_n}{E_o} = \frac{1}{b_n} \tag{3.3}$$

Also the open circuit transfer function between nodes i and n is

$$\frac{E_n}{E_i} = \frac{1}{b_{n-i}} \tag{3.4}$$

Hence from (3.3) and (3.4), we get

$$\frac{E_i}{E_o} = \frac{b_{n-i}}{b_n} \tag{3.5}$$

This transfer function has both poles and zeros on the negative real axis. However, if we modify the structure of Figure 3.1 to that of Figure 3.2, it realizes an arbitrary transfer function, where the zeros of transmission are controlled by forward feed (α_i's) and the poles by backward feed (β_i's) using finite gain amplifiers. From (3.4) and (3.5), we obtain the transfer function of Figure 3.2 as

$$T(S) = \frac{\alpha_o \gamma_o b_n + \sum_{i=1}^{n} (\delta_o \alpha_i \gamma_i - \alpha_o \gamma_o \beta_i \delta_i) b_{n-i}}{b_n - \sum_{i=1}^{n} \beta_i \delta_i b_{n-i}} \tag{3.6}$$

where δ_i and γ_i are the gains of the input and output summers, respectively at their i^{th} input. It should be noted that if it is required to realize a zero at infinity the forward feed operational amplifier with gain α_o is disconnected.

3.3 SECOND ORDER REALIZATION

As mentioned in section 1.3, filters are usually constructed as a cascade of second order sections. The commonly used second order sections are:

1) Low-pass (LP)

2) High-pass (HP)

3) Band-pass (BP)

4) All-pass (AP)

5) Notch (N)

Most practical filter specifications can be realized by a suitable cascade combination of these sections.

A general biquad may be expressed in the form

$$T(s) = \frac{a_2 s^2 + a_1 s + a_o}{b_2 s^2 + b_1 s + b_o} \qquad (3.7a)$$

Defining the following quantities

$$\omega_z = \sqrt{a_o/a_2} \quad , \quad Q_z = (\sqrt{a_o\, a_2})/a_1 \qquad (3.7b)$$

and

$$\omega_p = \sqrt{b_o/b_2} \quad , \quad Q_p = (\sqrt{b_o\, b_2})/b_1 \qquad (3.7c)$$

equation (3.7) may be written as

$$T(s) = H \frac{s^2 + \omega_z/Q_z\, s + \omega_z^2}{s^2 + \omega_p/Q_p\, s + \omega_p^2} \qquad (3.8a)$$

where

$$H = a_2/b_2 \qquad (3.8b)$$

For a notch section, $Q_z \to \infty$ and ω_z is known as the notch frequency and is usually indicated by the symbol ω_N. The quantity ω_p is called the undamped frequency of oscillation or pole frequency, while Q_p is known as the pole-Q or Q-factor. For a highly selective response, whose transmission

zeros are sufficiently far from the poles (for example LP, HP and BP responses), Q_p and ω_p adequately describe the behaviour of the filter in the frequency range of interest. However, for the N and AP sections the properties of Q_z and ω_z also have to be considered.

In this section a second order filter is first derived from the network proposed in the previous section. Then a design, which makes the sensitivities of Q_p and ω_p very low with respect to the various passive and active parameters, is presented. Thus, this design will be suitable for LP, HP and BP responses. This design is also used to obtain N and AP sections, and the sensitivity properties of ω_z and Q_z) for N(AP) sections are then examined.

3.3.1 The Second Order Section

If in (3.6) n is set equal to 2, then

$$T(s) = V_{out}/V_{in}$$

$$= \frac{\gamma_o s^2+\tau s[\gamma_o (3-\delta_1\beta_1)+\delta_o\beta_1\gamma_1]+[\gamma_o(1-\beta_1\delta_1-\beta_2\delta_2)+\delta_o(\gamma_1\beta_1+\gamma_2\beta_2)]\tau^2}{s^2+\tau(3-\beta_1\delta_1)s+\tau^2(1-\beta_1\delta_1-\beta_2\delta_2)} \qquad (3.9)$$

This transfer function may be realized by the configuration of Figure 3.3, where δ_i's, γ_i's and β_i's are the gains of the input summer, output summer and feed back amplifiers, respectively.

From equations (3.7) and (3.8) the Q_p and ω_p of the structure of Figure 3.3 are

$$Q_p = \frac{\sqrt{1-\beta_1\delta_1-\beta_2\delta_2}}{3-\beta_1\delta_1} \qquad (3.10a)$$

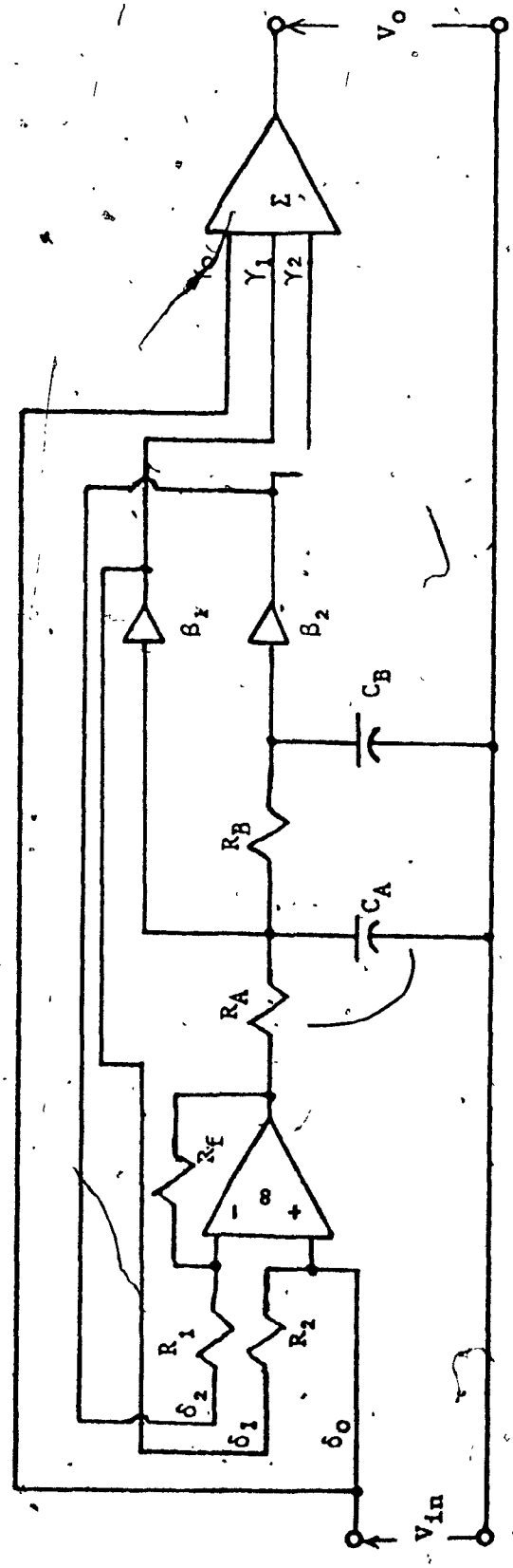

$R_A = R_B = R$

$C_A = C_B = C$

$\tau = \frac{1}{RC}$

Fig. 3.3: Second Order Grounded Capacitor Filter.

and

$$\omega_p = \frac{\sqrt{1 - \beta_1\delta_1 - \beta_2\delta_2}}{RC} \qquad (3.10b)$$

In the next subsection a design which minimizes simultaneously the worst case deviations in the pole-Q as well as in the pole frequency is presented. This design also yields a minimum spread in gains.

3.3.2 Minimum Worst Case Deviation and Gain Spread Design

If the passive elements of the recurrent ladder of the structure shown in Figure 3.3 are perturbed from their nominal values, then the resulting transfer function is

$$T(S) = \frac{\{\gamma_o s^2 + \tau_1 s[\gamma_o(\lambda_1\lambda_2+\lambda_1+1-\delta_1\beta_1)+\gamma_1\beta_1\delta_o]+[\delta_o(\gamma_1\beta_1+\gamma_2\beta_2)+\gamma_o(1-\delta_1\beta_1-\beta_2\delta_2)]\tau_1\tau_2\}}{\{s^2+\tau_1 s(\lambda_1\lambda_2+\lambda_1+1-\beta_1\delta_1) + \tau_1\tau_2\,(1-\beta_1\delta_1-\beta_2\delta_2)\}} \qquad (3.11)$$

where

$$\tau_1 = \frac{1}{R_A C_A}\,,\quad \tau_2 = \frac{1}{R_B C_B} \qquad (3.12a)$$

and

$$\lambda_1 = \frac{R_A}{R_B}\,,\quad \lambda_2 = \frac{C_A}{C_B} \qquad (3.12b)$$

Then from (3.7), the expressions for the pole-Q and pole frequency are:

$$Q_{PN} = \frac{\sqrt{\lambda_1\lambda_2}\ \sqrt{1-\beta_1\delta_1-\beta_2\delta_2}}{(\lambda_1\lambda_2 + \lambda_1 + 1 + \beta_1\delta_1)} \qquad (3.13a)$$

and

$$\omega_{PN} = \frac{\sqrt{1 - \beta_1\delta_1 - \beta_2\delta_2}}{R_A R_B\, C_A C_B} \qquad (3.13b)$$

It is noted that at the nominal values $R_A = R_B = R$ and $C_A = C_B = C$ equations (3.11) and (3.13) reduce to (3.9) and (3.10), respectively.

From (3.13) the Q_{PN} and ω_{PN} sensitivities with respect to various parameters may be shown to be

$$S_{R_A}^{Q_{PN}} = -S_{R_B}^{Q_{PN}} = \tfrac{1}{2} - \frac{\lambda_1\lambda_2 + \lambda_1}{1 + \lambda_1\lambda_2 + \lambda_1 - \beta_1\delta_1} \tag{3.14a}$$

$$S_{C_A}^{Q_{PN}} = -S_{C_B}^{Q_{PN}} = \tfrac{1}{2} - \frac{\lambda_1\lambda_2}{1 + \lambda_1\lambda_2 + \lambda_1 - \beta_1\delta_1} \tag{3.14b}$$

$$S_{\beta_2}^{Q_{PN}} = S_{\delta_2}^{Q_{PN}} = S_{\beta_2}^{\omega_{PN}} = S_{\delta_2}^{\omega_{PN}} = \tfrac{1}{2} - \frac{1 - \beta_1\delta_1}{2(1 + \lambda_1\lambda_2 + \lambda_1 - \beta_1\delta_1)^2 Q_p^2} \tag{3.14c}$$

$$S_{\beta_1}^{Q_{PN}} = S_{\delta_1}^{Q_{PN}} - \frac{\beta_1\delta_1}{2(1+\lambda_1\lambda_2+\lambda_1-\beta_1\delta_1)^2 Q_p^2} + \frac{\beta_1\delta_1}{(1+\lambda_1\lambda_2+\lambda_1-\beta_1\delta_1)} \tag{3.14d}$$

$$S_{\beta_1}^{\omega_{PN}} = S_{\delta_1}^{\omega_{PN}} - \frac{\beta_1\delta_1}{2(1+\lambda_1\lambda_2+\lambda_1-\beta_1\delta_1)^2 Q_p^2} \tag{3.14e}$$

$$S_{R_A}^{\omega_{PN}} = S_{R_B}^{\omega_{PN}} = S_{C_A}^{\omega_{PN}} = S_{C_B}^{\omega_{PN}} = -\tfrac{1}{2} - \tag{3.14f}$$

The first order deviation of Q_{PN} and ω_{PN} are given by

$$\frac{\Delta Q_{PN}}{Q_{PN}} = \Sigma\, S_{\beta_i}^{Q_{PN}} \frac{\Delta\beta_i}{\beta_i} + \Sigma\, S_{\delta_i}^{Q_{PN}} \frac{\Delta\delta_i}{\delta_i} + \Sigma\, S_{R_i}^{Q_{PN}} \frac{\Delta R_i}{R_i} + \Sigma\, S_{C_i}^{Q_{PN}} \frac{\Delta C_i}{C_i} \tag{3.15a}$$

and

$$\frac{\Delta\omega_{PN}}{\omega_{PN}} = \Sigma\, S_{\beta_i}^{\omega_{PN}} \frac{\Delta\beta_i}{\beta_i} + \Sigma\, S_{\delta_i}^{\omega_{PN}} \frac{\Delta\delta_i}{\delta_i} + \Sigma\, S_{R_i}^{\omega_{PN}} \frac{\Delta R_i}{R_i} + \Sigma\, S_{C_i}^{\omega_{PN}} \frac{\Delta C_i}{C_i} \tag{3.15b}$$

where $\frac{\Delta e_i}{e_i}$ is the fractional change in the element e_i.

Assuming the maximum deviations in the values of the gains,

resistors and capacitors to be respectively, $|\frac{\Delta g}{g}|$, $|\frac{\Delta R}{R}|$ and $|\frac{\Delta C}{C}|$, it may be shown, from (3.14), (3.15) and setting $\lambda_1 = \lambda_2 = 1$, that the worst case changes in Q_{PN} and ω_{PN} are:

$$|\frac{\Delta Q_{PN}}{Q_{PN}}|_{WC} = (F_1 + F_2)\,|\frac{\Delta g}{g}| + F_3\,|\frac{\Delta R}{R}| + F_4\,|\frac{\Delta C}{C}| \tag{3.16a}$$

and

$$|\frac{\Delta \omega_{PN}}{\omega_{PN}}|_{WC} = F_1\,|\frac{\Delta g}{g}| + |\frac{\Delta R}{R}| + |\frac{\Delta C}{C}| \tag{3.16b}$$

where

$$F_1 = 2\left|\tfrac{1}{2} - \frac{1 - \beta_1\delta_1}{2(3-\beta_1\delta_1)^2\,Q_P^2}\right| + 2\left|\frac{\beta_1\delta_1}{2(3-\beta_1\delta_1)^2\,Q_P^2}\right| \tag{3.17a}$$

$$F_2 = 2\left|\frac{\beta_1\delta_1}{3-\beta_1\delta_1}\right| \tag{3.17b}$$

$$F_3 = 2\left|\tfrac{1}{2} - \frac{2}{3-\beta_1\delta_1}\right| \tag{3.17c}$$

$$F_4 = 2\left|\tfrac{1}{2} - \frac{1}{3-\beta_1\delta_1}\right| \tag{3.17d}$$

Let us define a figure of merit F as:

$$F = |\frac{\Delta Q_{PN}}{Q_{PN}}|_{WC} + |\frac{\Delta \omega_{PN}}{\omega_{PN}}|_{WC} \tag{3.18a}$$

It is now observed that minimizing F simultaneously minimizes $|\frac{\Delta Q_{PN}}{Q_{PN}}|_{WC}$ and $|\frac{\Delta \omega_{PN}}{\omega_{PN}}|_{WC}$.

From (3.16) and (3.18), F can be written as

$$F = \left\{2\left|1 - \frac{1-\beta_1\delta_1}{(3-\beta_1\delta_1)^2\,Q_P^2}\right| + 2\left|\frac{\beta_1\delta_1}{(3-\beta_1\delta_1)^2\,Q_P^2}\right| + 2\left|\frac{\beta_1\delta_1}{3-\beta_1\delta_1}\right|\right\}|\frac{\Delta g}{g}| + \left\{2\left|\tfrac{1}{2} - \frac{2}{3-\beta_1\delta_1}\right| + 1\right\}|\frac{\Delta R}{R}|$$

$$+ \left\{2\left|\tfrac{1}{2} - \frac{1}{3-\beta_1\delta_1}\right| + 1\right\}|\frac{\Delta C}{C}| \tag{3.18b}$$

It is noted that F can be controlled by varying only $\beta_1\delta_1$. Ideally, the minimum value of F is zero, failing which the individual components of F should be separately minimized. It is seen from (3.17) and (3.18) that neither of the objectives is feasible. However, normally the gains are realized as resistor ratios which can be controlled within 0.1% in thin film technology. On the other hand, tolerances of capacitors are higher than those of resistors. Thus, it is logical to choose $\beta_1\delta_1$ such that the components of F due to $|\frac{\Delta C}{C}|$ has a minimum value. This happens when

$$F_4 = 0 \tag{3.19a}$$

or

$$\beta_1\delta_1 = 1 \tag{3.19b}$$

From (3.10) and (3.19)

$$-\beta_2\delta_2 = 4Q_P^2 \tag{3.20}$$

In order now to reduce the gain spread and hence the spread in the corresponding resistor values, which is desirable for thin film implementation, it is seen from 3.21 that we require

$$\beta_2 = -\delta_2 = 2Q_P \tag{3.21}$$

where the gain β_2 has been chosen to be positive for the purpose of better isolation. For the same reason β_1 is chosen to be unity. Using OA's, δ_1 and δ_2 are obtained as shown in Figure 3.3 while the gains β_1 and β_2 may be realized as shown in Figures 3.4a and 3.4b, respectively.

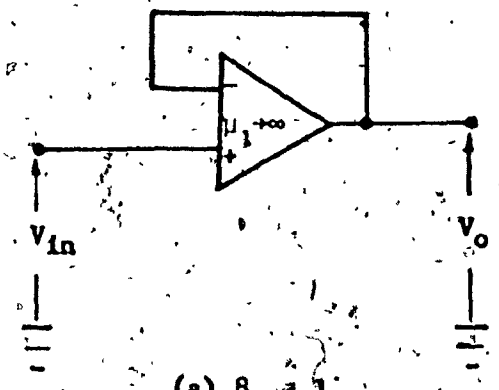

(a) $\beta_1 = 1$

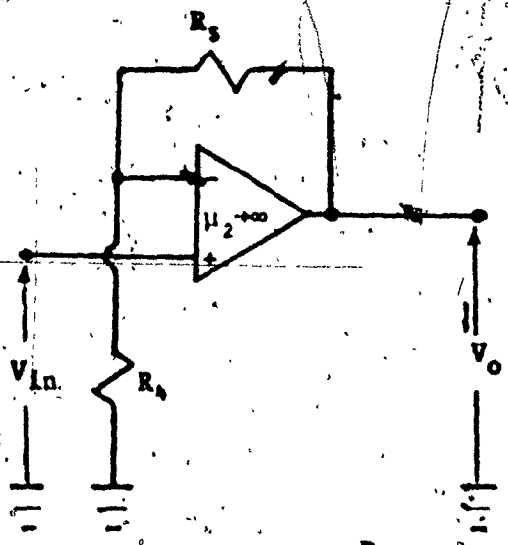

(b) $\beta_2 = 1 + \frac{R_s}{R_A}$

Fig. 3.4: a) OA Realization of Gain β_1
b) OA Realization of Gain β_2

From (3.16) and (3.17) and (3.19) the worst case deviations in Q_{PN} and ω_{PN} may now be expressed as

$$\left|\frac{\Delta Q_{PN}}{Q_{PN}}\right|_{WC} = \left(2 + \frac{1}{4Q_P^2}\right)\left|\frac{\Delta g}{g}\right| + \left|\frac{\Delta R}{R}\right| \qquad (3.22a)$$

$$\left|\frac{\Delta \omega_{PN}}{\omega_{PN}}\right|_{WC} = \left(1 + \frac{1}{4Q_P^2}\right)\left|\frac{\Delta g}{g}\right| + \left|\frac{\Delta R}{R}\right| + \left|\frac{\Delta C}{C}\right| \qquad (3.22b)$$

For $Q_P \gg 1$, the above expressions reduce to

$$\left|\frac{\Delta Q_{PN}}{Q_{PN}}\right|_{WC} \simeq 2\left|\frac{\Delta g}{g}\right| + \left|\frac{\Delta R}{R}\right| \qquad (3.22c)$$

$$\left|\frac{\Delta \omega_{PN}}{\omega_{PN}}\right|_{WC} \simeq \left|\frac{\Delta g}{g}\right| + \left|\frac{\Delta R}{R}\right| + \left|\frac{\Delta C}{C}\right| \qquad (3.22d)$$

3.3.3 The Effect of Finite Open Loop Gains

If the open loop gains μ, μ_1 and μ_2, of the input summer and the isolating amplifiers β_1 and β_2, respectively, are assumed to be finite, then the different gains become

$$\delta_{1\mu} = \frac{\mu}{1 + \mu + \frac{R_f}{R_1}}\ \delta_1 \qquad (3.23a)$$

$$\delta_{2\mu} = \frac{\mu}{1 + \mu + \frac{R_f}{R_1}}\ \delta_2 \qquad (3.23b)$$

$$\beta_{1\mu} = \frac{\mu_1}{1 + \mu_1} \qquad (3.23c)$$

$$\beta_{2\mu} = \frac{\mu_2\ \beta_2}{\beta_2 + \mu_2} \qquad (3.23d)$$

and the expressions (3.13) become

$$Q_{P\mu} = \frac{\sqrt{\lambda_1\lambda_2}\ \sqrt{1-\beta_{1\mu}\delta_{1\mu}-\beta_{2\mu}\delta_{2\mu}}}{(\lambda_1\lambda_2 + \lambda_1 + 1-\beta_{1\mu}\delta_{1\mu})}, \quad \omega_{P\mu} = \frac{\sqrt{1-\beta_{1\mu}\delta_{1\mu}-\beta_{2\mu}\delta_{2\mu}}}{R_A R_B\ C_A C_B} \qquad (3.23e)$$

Using the relation

$$S_z^Y = S_x^Y S_z^x \qquad x = f(z) \qquad (3.24)$$

and equations (3.14), (3.19), (3.21) and (3.23) it may be shown, for $Q_p >> 1$ and $\mu(\mu_1 \text{ or } \mu_2) >> Q_p$, that

$$S_\mu^{Q_{P\mu}} \simeq \frac{2Q_p}{\mu} \qquad (3.25a)$$

$$S_{\mu_1}^{Q_{P\mu}} \simeq \frac{1}{2\mu_1} \qquad (3.25b)$$

$$S_{\mu_2}^{Q_{P\mu}} \simeq \frac{Q_p}{\mu_2} \qquad (3.25c)$$

and

$$S_\mu^{\omega_{P\mu}} \simeq \frac{Q_p}{\mu} \qquad (3.26a)$$

$$S_{\mu_1}^{\omega_{P\mu}} \simeq -\frac{1}{16Q_p^2\mu_1} \qquad (3.26b)$$

$$S_{\mu_2}^{\omega_{P\mu}} \simeq \frac{Q_p}{\mu_2} \qquad (3.26c)$$

As seen from equations (3.25) and (3.26), the proposed design results in very low pole-Q and pole-frequency sensitivities with respect to the active elements.

3.3.4 The Effect of the Minimum Worst Case Deviation and Gain Spread Design on the Notch and All Pass Sections

It was pointed out earlier in this section that, in addition to the properties of ω_p and Q_p, the properties of the notch frequency ω_N,

the Q_Z and ω_Z should be studied for the Notch and AP section, respectively. These properties are now examined for the design developed in section 3.3.2.

A) The Notch Section

Using (3.9), (3.19b) and setting

$$\gamma_1\beta_1 S_o = -2\gamma_o$$

a notch section can be obtained with a notch frequency ω_N given by

$$\omega_N = \frac{\{\gamma_o(\gamma_1\beta_1 + \gamma_2\beta_2) - \gamma_o\beta_2\delta_2\}^{\frac{1}{2}}\,\tau}{\gamma_o^{\frac{1}{2}}} \qquad (3.27)$$

where the gains δ_1, β_1, β_2 and δ_2 are chosen as in section 3.3.2.

In order to study the effect of the design discussed in the previous section on the response of the notch filter, we have to consider the transfer function given by (3.11). This may be written in the form:

$$T(s) = \frac{s^2 + \varepsilon s + \omega_{ZN}^2}{s^2 + \frac{\omega_P}{Q_P}s + \omega_P^2} \qquad (3.28a)$$

where

$$\varepsilon = \tau_1\left[\lambda_2 + \lambda_1 + 1 - \delta_1\beta_1 + \frac{\gamma_1\beta_1\delta_o}{\gamma_o}\right] \qquad (3.28b)$$

and

$$\omega_{ZN} = \frac{\{\delta_o(\gamma_1\beta_1 + \gamma_2\beta_2) + \gamma_o(1-\delta_1\beta_1-\beta_2\delta_2)\}^{\frac{1}{2}}(\tau_1\tau_2)^{\frac{1}{2}}}{\gamma_o^{\frac{1}{2}}} \qquad (3.28c)$$

Ideally $\varepsilon = 0$ and $\omega_{ZN} = \omega_N$. From earlier discussions, it is seen that these are satisfied when

$$\delta_1 = \beta_1 = 1\,,\ \beta_2 = -\delta_2 = 2Q_p\,,\ \lambda_1 = \lambda_2 = 1 \qquad (3.28d)$$

and

$$\gamma_1\beta_1\delta_o = -2\gamma_o \tag{3.28e}$$

In practice this may not be the case due to manufacturing tolerances and temperature effects. However, for the notch section to be at all useful, the deviation $\Delta\varepsilon$ of ε from zero must be within acceptable limits. Thus, before examining the properties of ω_{ZN}, an upper bound on $|\Delta\varepsilon|$ is desirable.

From (3.28b) it may be shown that

$$|\Delta\varepsilon| \leq (\lambda_1\lambda_2 + \lambda_1)\left|\frac{\Delta\lambda_1}{\lambda_1}\right| + \lambda_1\lambda_2\frac{\Delta\lambda_2}{\lambda_2} + \delta_1\beta_1\left|\frac{\Delta\delta_1}{\delta_1}\right|$$

$$+\left|\left(\frac{\gamma_1\beta_1\delta_o}{\gamma_o} - \delta_1\beta_1\right)\frac{\Delta\beta_1}{\beta_1}\right| + \left|\frac{\gamma_1\beta_1\delta_o}{\gamma_o}\frac{\Delta\gamma_1}{\gamma_1}\right| + \left|\frac{\gamma_1\beta_1\delta_o}{\gamma_o}\frac{\Delta\delta_o}{\delta_o}\right|$$

$$+\left|\frac{\gamma_1\beta_1\delta_o}{\gamma_o}\frac{\Delta\gamma_o}{\gamma_o}\right| \tag{3.29a}$$

Thus, assuming $\pm$ 0.1% change in resistor ratios and $\pm$ 1% change in capacitor ratios and using (3.28d) and (3.28e), the worst case deviation, $|\Delta\varepsilon|_{WC}$, of ε from zero may be shown to be

$$|\Delta\varepsilon|_{WC} = 0.022 \tag{3.29b}$$

Therefore, even for a notch frequency of 10Hz,

$$\left|\frac{\omega_N}{\Delta\varepsilon}\right|_{WC} = 2860 \tag{3.29c}$$

Hence, it is expected that the network of Figure 3.3 may be used to realize notch sections with reasonably deep notches.

The sensitivities of ω_{ZN} with respect to the various parameters may be shown to be

$$S_{R_A}^{\omega_{ZN}} = S_{R_B}^{\omega_{ZN}} = S_{C_A}^{\omega_{ZN}} = S_{C_B}^{\omega_{ZN}} = -\tfrac{1}{2} \qquad (3.30a)$$

$$S_{\delta_o}^{\omega_{ZN}} = 2 \quad S_{\delta_1}^{\omega_{ZN}} = -\frac{1}{4aQ_p^2}, \quad S_{\delta_2}^{\omega_{ZN}} = \frac{1}{2a} \qquad (3.30b)$$

$$S_{\beta_1}^{\omega_{ZN}} = -\frac{3}{8aQp^2}, \quad S_{\beta_2}^{\omega_{ZN}} = \frac{1}{2a} + \frac{1}{4aQp^2} \qquad (3.30c)$$

$$S_{\gamma_o}^{\omega_{ZN}} = \tfrac{1}{2}\frac{1-a}{a}, \quad S_{\gamma_1}^{\omega_{ZN}} = -\frac{1}{4Q_p^2}, \quad S_{\gamma_2}^{\omega_{ZN}} = \frac{a-1}{2a} + \frac{1}{4aQ_p^2} \qquad (3.30d)$$

where

$$\frac{\omega_N}{\omega_P} = a \qquad (3.30e)$$

In most practical applications a is in the vicinity of unity. For a = 1 the fractional change in ω_{ZN} may be shown to be

$$\left|\frac{\Delta\omega_{ZN}}{\omega_{ZN}}\right| \leq \left(1 + \frac{5}{2Q_p^2}\right)\left|\frac{\Delta g}{g}\right| + \left|\frac{\Delta C}{C}\right| + \left|\frac{\Delta R}{R}\right| \qquad (3.31a)$$

where $\left|\frac{\Delta g}{g}\right|$, $\left|\frac{\Delta C}{C}\right|$ and $\left|\frac{\Delta R}{R}\right|$ are as defined in section 3.3.2.

For $Q_p >> 1$ (3.31a) reduces to

$$\left|\frac{\Delta\omega_{ZN}}{\omega_{ZN}}\right|_{WC} \approx \left|\frac{\Delta g}{g}\right| + \left|\frac{\Delta C}{C}\right| + \left|\frac{\Delta R}{R}\right| \qquad (3.31b)$$

B) The All Pass Section

The transfer function given by (3.9) can be written in the form (3.8a). For an AP section, $Q_Z = -Q_P$ and $\omega_Z = \omega_P$. Therefore, the design equations for this section are

$$\gamma_1\beta_1\delta_o = -4\gamma_o \tag{3.32a}$$

$$\delta_o\gamma_2\beta_2 = 4\gamma_o \tag{3.32b}$$

and $\beta_1\delta_1$, $\beta_2\delta_2$ are as in (3.19) and (3.20), respectively.

Now in order to study the properties of the numerator of the AP transfer function, under the constraints of the design proposed in section 3.3.2, equation (3.11) has to be considered. We then have,

$$Q_{ZN} = \frac{\{\gamma_o\lambda_1\lambda_2\ [\delta_o(\gamma_1\beta_1+\beta_2\gamma_2) + \gamma_o(1 - \beta_1\delta_1 - \beta_2\delta_2)]\}^{\frac{1}{2}}}{\gamma_o(\lambda_1 + \lambda_1\lambda_2 + 1 - \beta_1\delta_1) + \gamma_1\beta_1\delta_o} \tag{3.33a}$$

and

$$\omega_{ZN} = \frac{\{\delta_o(\gamma_1\beta_1 + \gamma_2\beta_2) + \gamma_o(1 - \beta_1\delta_1 - \beta_2\delta_2)\}^{\frac{1}{2}}}{\{\gamma_o R_A R_B C_A C_B\}^{\frac{1}{2}}} \tag{3.33b}$$

The sensitivities of Q_{ZN} and ω_{ZN} with respect to the various elements may be shown to be:

$$S_{\delta_o}^{Q_{ZN}} = -2\ ,\quad S_{\delta_1}^{Q_{ZN}} = -\tfrac{1}{2} - \frac{1}{8Q_P^2}\ ,\quad S_{\delta_2}^{Q_{ZN}} = \tfrac{1}{2} \tag{3.34a}$$

$$S_{\beta_1}^{Q_{ZN}} = -2 - \frac{5}{8Q_P^2}\ ,\quad S_{\beta_2}^{Q_{ZN}} = \tfrac{1}{2} + \frac{1}{2Q_P^2} \tag{3.34b}$$

$$S_{\gamma_o}^{Q_{ZN}} = 2 \quad , \quad S_{\delta_1}^{Q_{ZN}} = -\left[2 + \frac{1}{2Q_p^2}\right] \quad , \quad S_{\delta_2}^{Q_{ZN}} = \frac{1}{2Q_p^2} \tag{3.34c}$$

$$S_{R_A}^{Q_{ZN}} = -S_{R_B}^{Q_{ZN}} = 3/2 \quad , \quad S_{C_A}^{Q_{ZN}} = -S_{C_B}^{Q_{ZN}} = 1 \tag{3.34d}$$

and

$$S_{R_A}^{\omega_{ZN}} = S_{R_B}^{\omega_{ZN}} = S_{C_A}^{\omega_{ZN}} = S_{C_B}^{\omega_{ZN}} = -1/2 \tag{3.35a}$$

$$S_{\delta_o}^{\omega_{ZN}} = -\frac{1}{2Q_p^2} \quad , \quad S_{\delta_1}^{\omega_{ZN}} = -\frac{1}{8Q_p^2} \quad , \quad S_{\delta_2}^{\omega_{ZN}} = 1/2 \tag{3.35b}$$

$$S_{\beta_1}^{\omega_{ZN}} = -\frac{5}{8Q_p^2} \quad , \quad S_{\beta_2}^{\omega_{ZN}} = 1/2 + \frac{1}{2Q_p^2} \tag{3.35c}$$

$$S_{\gamma_o}^{\omega_{ZN}} = 0 \quad , \quad S_{\gamma_1}^{\omega_{ZN}} = -\frac{1}{2Q_p^2} \quad , \quad S_{\gamma_2}^{\omega_{ZN}} = \frac{1}{2Q_p^2} \tag{3.35d}$$

From (3.34) and (3.35) it may be shown that

$$\left|\frac{\Delta Q_{ZN}}{Q_{ZN}}\right| \leq \left(9\tfrac{1}{2} + \frac{9}{4Q_p^2}\right)\left|\frac{\Delta g}{g}\right| + 3\left|\frac{\Delta R}{R}\right| + 2\left|\frac{\Delta C}{C}\right| \tag{3.36a}$$

and

$$\left|\frac{\Delta \omega_{ZN}}{\omega_{ZN}}\right| \leq \left(1 + \frac{11}{4Q_p^2}\right)\left|\frac{\Delta g}{g}\right| + \left|\frac{\Delta R}{R}\right| + \left|\frac{\Delta C}{C}\right| \tag{3.36b}$$

For $Q_p >> 1$ these expressions become

$$\left|\frac{\Delta Q_{ZN}}{Q_{ZN}}\right|_{WC} = \left(9\tfrac{1}{2}\right)\left|\frac{\Delta g}{g}\right| + 3\left|\frac{\Delta R}{R}\right| + 2\left|\frac{\Delta C}{C}\right| \tag{3.36c}$$

and

$$\left|\frac{\Delta \omega_{ZN}}{\omega_{ZN}}\right|_{WC} = \left|\frac{\Delta g}{g}\right| + \left|\frac{\Delta R}{R}\right| + \left|\frac{\Delta C}{C}\right|$$

3.4 CONCLUSIONS

A grounded capacitor RC active network capable of realizing any transfer function has been developed. This network can be utilized

to implement the $\overline{\text{URC}}$ realization technique presented in Chapter 2. A design procedure that simultaneously minimizes the worst case deviations in Q_p and ω_p has been derived. Thus, it can be used to obtain LP, BP and HP responses. This design is also utilized to obtain N and AP filters. The effect of the design on ω_N (ω_Z and Q_Z) for Notch (All Pass) sections has been investigated and it is found that the worst case deviations for these quantities are low.

The purpose of the next chapter is to derive another network, by modifying the one presented in this chapter, which possesses a better performance capability and has, in addition, a lower element spread.

CHAPTER IV

AN EASILY INTEGRABLE RC ACTIVE FILTER

4.1 INTRODUCTION

The purpose of this chapter is to present a significant improvement of the second order network developed in Chapter 3. The new network offers a simpler configuration, while retaining all the attractive features of the preceeding one. Further, it achieves a lower value for the gain spread as well as for the different worst case deviations.

4.2 THE MODIFIED CONFIGURATION

It may be seen, from (3.14a), (3.14b), (3.15) and (3.16) that the expressions for F_3 and F_4 as given by (3.17c) and (3.17d), are respectively $F_3 = 2|S_{R_A}^{Q_{PN}}| = 2|S_{R_B}^{Q_{PN}}|$ and $F_4 = 2|S_{C_A}^{Q_{PN}}| = 2|S_{C_B}^{Q_{PN}}|$ with $\lambda_1 = \lambda_2 = 1$. The values of F_3 and F_4 are different because of the presence of the term λ_1 separately in F_3. This, in turn, is due to the presence of this term, as a separate parameter, in the coefficient of s in the denominator polynomial of the transfer function, given by (3.11). Consequently, the contributions by $|\frac{\Delta R}{R}|$ and $|\frac{\Delta C}{C}|$ to F cannot be minimized simultaneously. However, this term disappears from the transfer function, as a separate parameter, when the network of Figure 3.3 is modified to that of Figure 4.1 [61]. Thus, it may be expected that, in the modified network, the components of F due to $|\frac{\Delta R}{R}|$ and $|\frac{\Delta C}{C}|$ can be minimized simultaneously. This will result in a lower value of F. Moreover, since now the gains δ_2, β_1 and β_2 will appear as a product, it may also be expected, from (3.9), that, for a given Q_p, the modified network can be designed with a lower gain spread. The above features of the modified network are established in what follows.

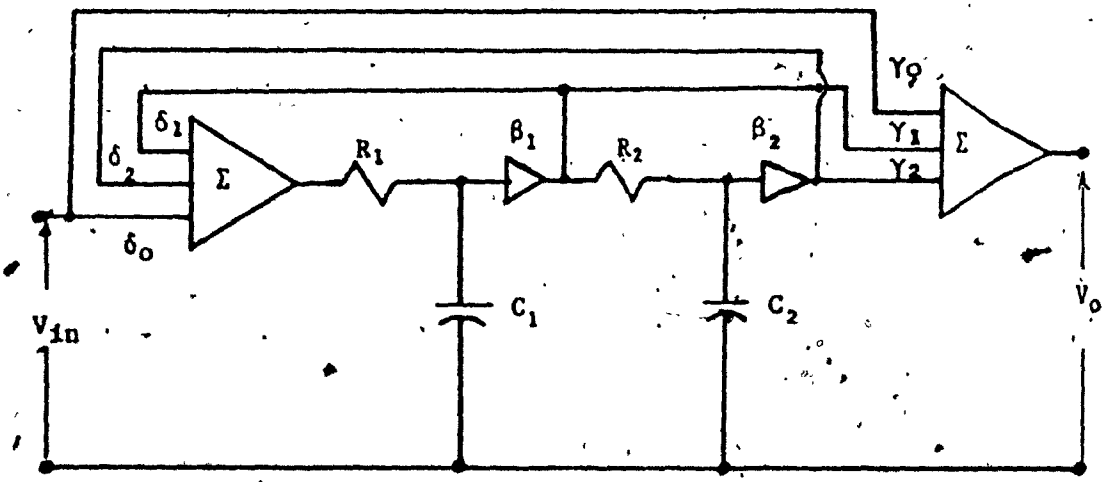

Fig. 4.1: Modified Configuration

4.3 An Optimum Design for the Modified Configuration

Analysis of the network of Figure 4.1 yields

$$T(s)=\frac{V_{out}}{V_{in}} = \frac{\{\gamma_o R_1C_1R_2C_2s^2+s[\gamma_1\beta_1\delta_oR_2C_2+\gamma_o(R_1C_1+R_2C_2-\beta_1\delta_1R_2C_2)] + [\gamma_1\beta_1\delta_o+\gamma_2\beta_1\beta_2\delta_o+\gamma_o(1-\beta_1\delta_1-\beta_1\beta_2\delta_2)]\}}{[R_1R_2C_1C_2s^2+s(R_1C_1+R_2C_2-\beta_1\delta_1R_2C_2)+1-\beta_1\delta_1-\beta_1\beta_2\delta_2]} \quad (4.1)$$

The pole Q_p and the pole frequency ω_p are given by

$$Q_p = \sqrt{\{\lambda_1\lambda_2(1-\beta_1\delta_1-\beta_1\beta_2\delta_2)\}}/(\lambda_1\lambda_2+1-\beta_1\delta_1) \quad (4.2a)$$

$$\omega_p = \sqrt{(1-\beta_1\delta_1-\beta_1\beta_2\delta_2)/(R_1R_2C_1C_2)} \quad (4.2b)$$

where $\lambda_1 = R_1/R_2$, $\lambda_2 = C_1/C_2$ (4.3)

The Q_p and ω_p sensitivities with respect to the various parameters may be shown to be

$$S^{Q_p}_{R_1} = S^{Q_p}_{C_1} = -S^{Q_p}_{R_2} = -S^{Q_p}_{C_2} = \tfrac{1}{2} - \frac{\lambda_1\lambda_2}{\lambda_1\lambda_2+1-\beta_1\delta_1}$$

$$S^{Q_p}_{\beta_2} = S^{Q_p}_{\delta_2} = S^{\omega_p}_{\delta_2} = S^{\omega_p}_{\beta_2} = \tfrac{1}{2} - \frac{1-\beta_1\delta_1}{2K^2Q_p^2}, \quad K = \frac{\lambda_1\lambda_2+1-\beta_1\delta_1}{\sqrt{\lambda_1\lambda_2}}$$

$$S^{Q_p}_{\delta_1} = \frac{-\beta_1\delta_1}{2K^2Q_p^2} + \frac{\beta_1\delta_1}{K\sqrt{\lambda_1\lambda_2}}, \quad S^{Q_p}_{\beta_1} = \tfrac{1}{2} - \frac{1}{2K^2Q_p^2} + \frac{\beta_1\delta_1}{K\sqrt{\lambda_1\lambda_2}} \quad (4.4)$$

$$S^{\omega_p}_{\delta_1} = \frac{-\delta_1\beta_1}{2K^2Q_p^2}, \quad S^{\omega_p}_{\beta_1} = \tfrac{1}{2} - \frac{1}{2K^2Q_p^2}$$

Now

$$\frac{\Delta Q_p}{Q_p} = \Sigma\, S^{Q_p}_{\beta_1}\,\Delta\beta_1/\beta_1+\Sigma S^{Q_p}_{\delta_1}\,\Delta\delta_1/\delta_1+\Sigma S^{Q_p}_{R_1}\,\Delta R_1/R_1+\Sigma S^{Q_p}_{C_1}\,\Delta C_1/C_1 \quad (4.5a)$$

$$\frac{\Delta\omega_o}{\omega_o} = \Sigma\, S^{\omega_p}_{\beta_1}\,\Delta\beta_1/\beta_1+\Sigma S^{\omega_p}_{\delta_1}\,\Delta\delta_1/\delta_1+\Sigma S^{\omega_p}_{R_1}\,\Delta R_1/R_1+\Sigma S^{\omega_p}_{C_1}\,\Delta C_1/C_1 \quad (4.5b)$$

Assuming, as in Chapter 3, the maximum deviations in the values of the gains, resistors, and capacitors to be, respectively, $|\frac{\Delta g}{g}|$, $|\frac{\Delta R}{R}|$, and $|\frac{\Delta C}{C}|$. We may show, from (4.4), that first order worst case changes in Q_p and ω_p are:

$$|\frac{\Delta Q_p}{Q_p}|_{WC} = (F_1+F_2)\ |\frac{\Delta g}{g}| + F_3|\frac{\Delta R}{R}| + F_3|\frac{\Delta C}{C}| \qquad (4.6)$$

and

$$|\frac{\Delta \omega_p}{\omega_p}|_{WC} = F_1|\frac{\Delta g}{g}| + |\frac{\Delta R}{R}| + |\frac{\Delta C}{C}| \qquad (4.7)$$

where

$$F_1 = |\frac{\delta_1\beta_1}{2K^2Q_p^2}| + |\frac{1}{2} - \frac{1}{2K^2Q_p^2}| + 2\ |\frac{1}{2} - \frac{1-\delta_1\beta_1}{2K^2Q_p^2}| \qquad (4.8a)$$

$$F_2 = 2\ |\frac{\delta_1\beta_1}{K\sqrt{\lambda_1\lambda_2}}|, \quad F_3 = 2\ |\frac{1}{2} - \frac{\lambda_1\lambda_2}{1+\lambda_1\lambda_2\ \beta_1\delta_1}| \qquad (4.8b)$$

$$F = |\frac{\Delta Q_p}{Q_p}|_{WC} + |\frac{\Delta \omega_p}{\omega_p}|_{WC} \qquad (4.9a)$$

$$= (2F_1+F_2)\ |\frac{\Delta g}{g}| + (F_3+1)\ \{|\frac{\Delta R}{R}| + |\frac{\Delta C}{C}|\} \qquad (4.9b)$$

As discussed in Chapter 3, ideally F = 0. It is readily observed from (4.8) and (4.9b) that this is not possible. However, deviations in $|\frac{\Delta R}{R}|$ and $|\frac{\Delta C}{C}|$ are expected to be more than those in $|\frac{\Delta g}{g}|$. Thus, it is natural to seek a minimum value for F_3. This occurs when $F_3 = 0$ or

$$\lambda_1\lambda_2 = 1-\beta_1\delta_1 \qquad (4.10)$$

Hence F is minimum when

$$f = 2F_1+F_2 = (1 + \frac{1}{4Q_p^2})\left|\frac{1-\lambda_1\lambda_2}{\lambda_1\lambda_2}\right| + \frac{1}{4Q_p^2}\left|\frac{4Q_p^2\lambda_1\lambda_2-1}{\lambda_1\lambda_2}\right| + \left|1 - \frac{1}{4Q_p^2}\right| \quad (4.11)$$

is minimum.

It can easily be shown that $\partial f/\partial(\lambda_1\lambda_2)$ is negative for $\lambda_1\lambda_2 < 1$ and positive for $\lambda_1\lambda_2 > 1$. Hence f is minimum when

$$\lambda_1\lambda_2 = 1 \quad \text{or} \quad \beta_1\delta_1 = 0 \quad (4.12)$$

and the corresponding bounds on $\left|\frac{\Delta Q_p}{Q_p}\right|$ and $\left|\frac{\Delta\omega_p}{\omega_p}\right|$ are

$$\left|\frac{\Delta Q_p}{Q_p}\right| \leq 3\left|\frac{1}{2} - \frac{1}{8Q_p^2}\right| \left|\frac{\Delta g}{g}\right| \quad (4.13a)$$

$$\left|\frac{\Delta\omega_p}{\omega_p}\right| \leq 3\left|\frac{1}{2} - \frac{1}{8Q_p^2}\right| \left|\frac{\Delta g}{g}\right| + \left|\frac{\Delta R}{R}\right| + \left|\frac{\Delta C}{C}\right| \quad (4.13b)$$

For $Q_p >> 1$, these values reduce to

$$\left|\frac{\Delta Q_p}{Q_p}\right|_{WC} \simeq \frac{3}{2}\left|\frac{\Delta g}{g}\right| \quad (4.13c)$$

$$\left|\frac{\Delta\omega_p}{\omega_p}\right|_{WC} \simeq \frac{3}{2}\left|\frac{\Delta g}{g}\right| + \left|\frac{\Delta R}{R}\right| + \left|\frac{\Delta C}{C}\right| \quad (4.13d)$$

From (4.2), (4.10) and (4.12)

$$-\beta_1\beta_2\delta_2 = (4Q_p^2-1) \quad (4.14)$$

Now in order to reduce the gain spread and hence the spread in the corresponding resistor values, it is seen from (4.14) that

$$\beta_1 = \beta_2 = -\delta_2 = (4Q_p^2-1)^{1/3} = (2Q_p)^{2/3}, \text{ for } Q_p >> 1 \quad (4.15)$$

where the gains β_1 and β_2 have been chosen positive to provide better isolation.

It should be noted that for variations due to temperature, the expression for the bound on $|\frac{\Delta Q_p}{Q_p}|$ remains the same as in (4.13) while that for $|\frac{\Delta\omega_p}{\omega_p}|$ may be shown to be

$$|\frac{\Delta\omega_p}{\omega_p}| \leq 3\,|\tfrac{1}{2} - \frac{1}{8Q_p^2}|\;\;|\frac{\Delta g}{g}| \qquad (4.16a)$$

or

$$|\frac{\Delta\omega_p}{\omega_p}|_{WC} = \frac{3}{2}\,|\frac{\Delta g}{g}|, \quad \text{for } Q_p >> 1 \qquad (4.16b)$$

This is in view of the excellent tracking properties of thin film resistors and capacitors and the fact that the variations in the resistors and capacitors may be made to cancel each other [22].

From (4.14), β_1 cannot be zero unless $Q_p = \frac{1}{2}$; hence from (4.12) $\delta_1 = 0$. Thus one of the feedback loops, namely the one from the output of β_2 is eliminated. Further, it is desirable to have equal valued capacitors, that is, $\lambda_2 = 1$. Therefore, from (4.14), $\lambda_1 = 1$ or the resistors R_1 and R_2 are of equal value, thus facilitating thin film fabrication.

If OA's are used to realize the finite grains, then it is reasonable to assume that $(2Q_p)^{2/3} << \mu$ (the open loop gain of any of the OA's), in which case the gains can be controlled by resistor ratios. Since the resistor ratios can be controlled to within less than 0.1%, the changes in gains are expected to be small. Thus, the changes of Q_p and ω_p given by (4.13c) and (4.16b) are good measures of the actual changes.

Using OA's, the optimum design of the configuration of Figure 4.1 reduces to the one shown in Figure 4.2a, where

$$-\delta_2 = \frac{R_f}{R_3} = (2Q_p)^{2/3} \tag{4.17}$$

and the amplifiers β_1 and β_2 are realized as in Figures 4.2b and 4.2c, respectively.

4.3.1 The Effect of the Finite Open Loop Gains of the Operational Amplifiers

If the finite open loop gains μ, μ_1 and μ_2 of the input summer and the amplifiers β_1 and β_2 respectively are considered, then we have, for the different gains

$$\delta_{2\mu} = \frac{\mu\delta_2}{1+\mu+\frac{R_f}{R_3}} \tag{4.18a}$$

$$\beta_{2\mu} = \frac{\mu_2\beta_2}{\mu_2 + \beta_2} \tag{4.18b}$$

$$\beta_{1\mu} = \frac{\mu_1\beta_1}{\mu_1 + \beta_1} \tag{4.18c}$$

and the expressions for the pole-Q and pole frequency, using the optimum design, become

$$Q_{p\mu} = \frac{\sqrt{1 - \beta_{1\mu}\,\beta_{2\mu}\,\delta_{2\mu}}}{2}, \quad \omega_{p\mu} = \frac{\sqrt{1 - \beta_{1\mu}\,\beta_{2\mu}\,\delta_{2\mu}}}{R\,C}$$

Hence, it may be shown, using 4.18, that for $Q_p >> 1$ and μ (μ_1 or μ_2) $>> Q_p$

$$S_{\mu}^{Q_p} = S_{\mu}^{\omega_p} = \frac{(2Q_p)^{2/3}}{2\mu}, \quad S_{\mu_1}^{Q_p} = S_{\mu_1}^{\omega_p} = \frac{(2Q_p)^{2/3}}{\mu_1} \tag{4.19a}$$

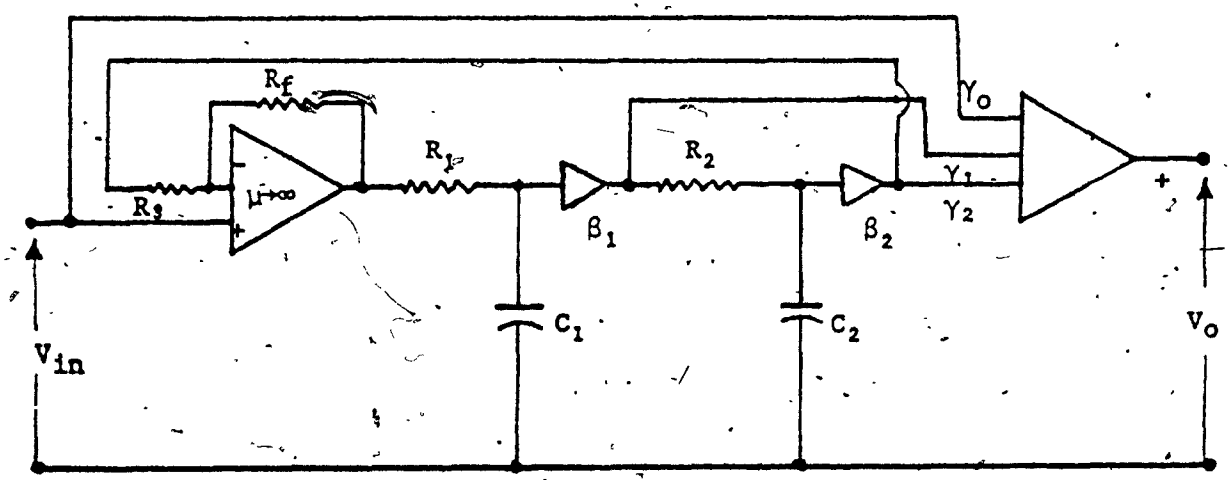

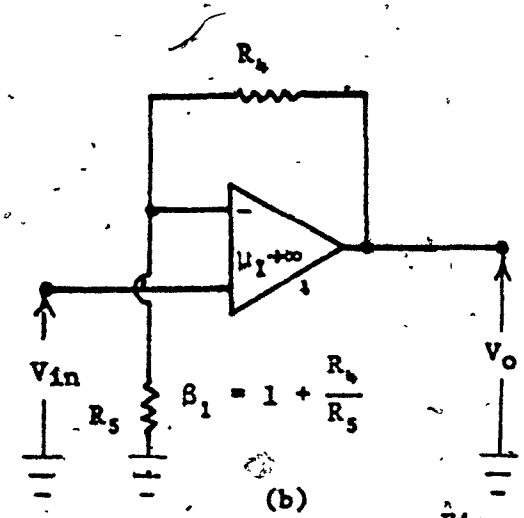

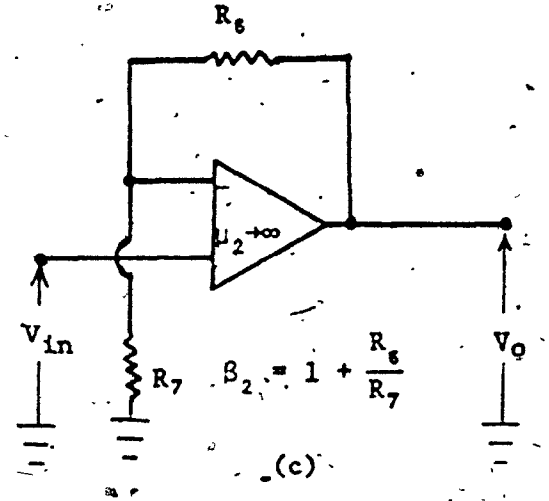

Fig. 4.2: a) Modified Network
b) OA Realization of Gain β_1
c) OA Realization of Gain β_2

$$S_{\mu_2}^{Q_p} = S_{\mu_2}^{\omega_p} = \frac{(2Q_p)^{2/3}}{\mu_2} \qquad (4.19b)$$

It is seen that these values are lower than those of the network of Chapter 3.

4.3.2 The Effect of the Optimum Design on the Notch and All Pass Sections

As discussed in the previous chapter, the optimum design will yield suitable sections for LP, HP and BP responses. However, if this design is used for N and AP responses, then the effect of this design on the numerator polynomial of the transfer functions of these two sections must also be studied.

A) Notch Section

Using the design conditions of section 4.3 and setting

$$\gamma_1 \beta_1 \delta_o = -2\gamma_o \qquad (4.20a)$$

in (4.1), a notch filter may be derived from the network of Figure 4.1. The notch frequency ω_N is given by

$$\omega_N = \frac{\{\beta_1\delta_o(\gamma_1+\gamma_2\beta_2) + \gamma_o(1-\beta_1\beta_2\delta_2)\}^{\frac{1}{2}}}{\gamma_o^{\frac{1}{2}} RC} \qquad (4.20b)$$

where β_1, β_2 and δ_2 are as chosen by (4.15)

However, as pointed out in Chapter 3, it is difficult to obtain an ideal notch response, in practice, due to manufacturing tolerances and temperature coefficients of the components. Also, the quality of the notch filters can be investigated, as discussed in that chapter,

by examining $|\Delta\varepsilon|_{WC}$, the worst case deviation of ε from zero, and ω_{ZN}; where ε and ω_{ZN} have the same significance as in section 3.3.4. In this case

$$\omega_{ZN} = \frac{\{\beta_1\delta_o(\gamma_1+\gamma_2\beta_2) + \gamma_o(1-\beta_1\beta_2\delta_2)\}^{\frac{1}{2}}}{\{\gamma_o R_1R_2C_1C_2\}^{\frac{1}{2}}} \qquad (4.21a)$$

and

$$\varepsilon = \frac{1}{R_1C_1}\left\{\frac{\gamma_1\beta_1\delta_o}{\gamma_o} + 1 + \lambda_1\lambda_2\right\} \qquad (4.21b)$$

It is observed that if

$$\lambda_1 = \lambda_2 = 1\ , \quad \beta_1 = \beta_2 = -\delta_2 = (4Q_p^2-1)^{1/3} \qquad (4.21c)$$

that is, when the design conditions of section 4.3 are satisfied, and if (4.20a) holds, then $\varepsilon = 0$ and $\omega_{ZN} = \omega_N$.

Assuming, as before, that resistor and capacitor ratios change by 0.1% and 1%, respectively, it may be shown from (4.21b) that

$$|\Delta\varepsilon|_{WC} = 0.019 \qquad (4.21d)$$

Therefore, again considering a notch frequency of 10 HZ

$$\frac{\omega_N}{|\Delta\varepsilon|_{WC}} = 3141 \qquad (4.21e)$$

Comparing (4.21e) and (3.29c), it is expected that filters derived from the network of Figure 4.1 will yield deeper notches than those obtained from the network of Figure 3.3.

The sensitivities of ω_{ZN} with respect to the various parameters are:

$$S_{R_i}^{\omega_{ZN}} = S_{C_i}^{\omega_{ZN}} = -\tfrac{1}{2} \quad (i = 1,2) \qquad (4.22a)$$

$$S_{\beta_1}^{\omega_{ZN}} = \tfrac{1}{2}\left(1 - \frac{1}{4aQ_p^2}\right), \quad S_{\beta_2}^{\omega_{ZN}} = \tfrac{1}{2}\left(1 + \frac{1}{4aQ_p^2}\right) \tag{4.22b}$$

$$S_{\gamma_o}^{\omega_{ZN}} = \frac{a-1}{a}, \quad S_{\delta_2}^{\omega_{ZN}} = \frac{1}{2a}\left(1 - \frac{1}{4Q_p^2}\right) \tag{4.22c}$$

$$S_{\gamma_o}^{\omega_{ZN}} = \tfrac{1}{2}\left(\frac{1}{a} - 1\right), \quad S_{\gamma_1}^{\omega_{ZN}} = -\frac{1}{4aQ_p^2}, \quad S_{\gamma_2}^{\omega_{ZN}} = \frac{1}{2a}\left(a - 1 + \frac{1}{2Q_p^2}\right) \tag{4.22d}$$

As mentioned in section 3.3.4, $a = \left(\frac{\omega_N}{\omega_p}\right)$ is in the vicinity of unity in practice. From (4.22) and for $a = 1$ and $Q_p >> 1$ it may be shown that

$$\left|\frac{\Delta\omega_{ZN}}{\omega_{ZN}}\right|_{WC} = \frac{3}{2}\left|\frac{\Delta g}{g}\right| + \left|\frac{\Delta R}{R}\right| + \left|\frac{\Delta C}{C}\right| \tag{4.23a}$$

Equation (4.23a) is a good measure for manufacturing tolerances. However, for variations due to temperature this figure reduces to

$$\left|\frac{\Delta\omega_{ZN}}{\omega_{ZN}}\right|_{WC} = \frac{3}{2}\left|\frac{\Delta g}{g}\right| \tag{4.23b}$$

B) <u>The AP Section</u>

As discussed in Chapter 3, for an AP section $Q_Z = -Q_p$ and $\omega_Z = \omega_p$. These conditions may be satisfied, as seen from (4.1), by setting

$$\gamma_1\beta_1\delta_o = -4\gamma_o \tag{4.24}$$

$$\gamma_2\beta_1\beta_2\delta_o = 4\gamma_o \tag{4.25}$$

provided that the design conditions presented in section 4.3 are also used.

However, in the event that these conditions are not exactly satisfied, Q_Z and ω_Z have to be replaced by

$$Q_{ZN} = \frac{\{\beta_1\delta_0(\gamma_1+\gamma_2\beta_2)+\gamma_0(1-\beta_1\beta_2\delta_2)\}^{\frac{1}{2}}\ \gamma_0^{\frac{1}{2}}\ \sqrt{\lambda_1\lambda_2}}{\{\gamma_0\lambda_1\lambda_2+\gamma_0+\gamma_1\beta_1\delta_0\}} \tag{4.26}$$

and

$$\omega_{ZN} = \{\beta_1\delta_0(\gamma_1+\gamma_2\beta_2)+\gamma_0(1-\beta_1\beta_2\delta_2)\}^{\frac{1}{2}}/\{\gamma_0 R_1 R_2 C_1 C_2\}^{\frac{1}{2}} \tag{4.27}$$

It is observed that when the conditions given in (4.21c) along with equations (4.24) and (4.25) are satisfied then, $Q_{ZN} = Q_Z = -Q_p$ and $\omega_{ZN} = \omega_N = \omega_p$.

The sensitivities of Q_{ZN} and ω_{ZN} with respect to the various parameters are:

$$S_{R_i}^{Q_{ZN}} = S_{C_i}^{Q_{ZN}} = (-1)^{i+1} \quad (i = 1,2) \tag{4.28a}$$

$$S_{\beta_1}^{Q_{ZN}} = -\left[2 + \frac{1}{2Q_p^2}\right], \quad S_{\beta_2}^{Q_{ZN}} = \tfrac{1}{2}\left[1 - \frac{10}{8Q_p^2}\right] \tag{4.28b}$$

$$S_{\delta_0}^{Q_{ZN}} = -2, \quad S_{\delta_2}^{Q_{ZN}} = -\frac{1}{2Q_p^2} \tag{4.28c}$$

$$S_{\gamma_0}^{Q_{ZN}} = 2, \quad S_{\gamma_1}^{Q_{ZN}} = \tfrac{1}{2}\left[2 + \frac{1}{Q_p^2}\right], \quad S_{\gamma_2}^{Q_{ZN}} = \frac{1}{2Q_p^2} \tag{4.28d}$$

and

$$S_{R_i}^{\omega_{ZN}} = S_{C_i}^{\omega_{ZN}} = -\tfrac{1}{2} \quad (i = 1,2) \tag{4.29a}$$

$$S_{\beta_1}^{\omega_{ZN}} = \tfrac{1}{2}\left[1 - \frac{1}{4Q_p^2}\right], \quad S_{\beta_2}^{\omega_{ZN}} = -\frac{1}{2Q_p^2} \tag{4.29b}$$

$$S_{\delta_o}^{\omega_{ZN}} = 0 \quad , \quad S_{\delta_2}^{\omega_{ZN}} = \tfrac{1}{2}\left(1 - \frac{1}{4Q_p^2}\right) \tag{4.29c}$$

$$S_{\gamma_o}^{\omega_{ZN}} = 0 \quad , \quad S_{\gamma_1}^{\omega_{ZN}} = -\frac{1}{4Q_p^2} \quad , \quad S_{\gamma_2}^{\omega_{ZN}} = \frac{1}{2Q_p^2} \tag{4.29d}$$

For $Q_p >> 1$ it may be shown, using (4.28) and (4.29), that

$$\left|\frac{\Delta Q_{ZN}}{Q_{ZN}}\right|_{WC} \simeq (8\tfrac{1}{2}) \left|\frac{\Delta g}{g}\right| + 2\left|\frac{\Delta R}{R}\right| + 2\left|\frac{\Delta C}{C}\right| \tag{4.30a}$$

and

$$\left|\frac{\Delta \omega_{ZN}}{\omega_{ZN}}\right|_{WC} \simeq \frac{3}{2}\left|\frac{\Delta g}{g}\right| + \left|\frac{\Delta R}{R}\right| + \left|\frac{\Delta C}{C}\right| \tag{4,30b}$$

For variations due to temperature, the above expressions reduce to, for $Q_p >> 1$,

$$\left|\frac{\Delta Q_{ZN}}{Q_{ZN}}\right|_{WC} \simeq \frac{17}{2}\left|\frac{\Delta g}{g}\right| \tag{4.31a}$$

and

$$\left|\frac{\Delta \omega_{ZN}}{\omega_{ZN}}\right|_{WC} \simeq \frac{3}{2}\left|\frac{\Delta g}{g}\right| \tag{4.31b}$$

4.4 STABILITY

It has been shown [62] - [63], that some networks using OA's can attain a low frequency unstable mode of operation during activation, that is, just after switching on the power supply. It is the purpose of this section to study such stability properties for the configuration of Figure 4.2 under the constraints of the optimum design developed in section 4.3.

The characteristic polynomial of (4.1), considering finite open loop gains of the OA's is

$$D(s) = R_1R_2C_1C_2s^2 + s[R_1C_1 + R_2C_2] + 1 - \beta_{1\mu}\beta_{2\mu}\delta_{2\mu} \tag{4.32}$$

where $\beta_{1\mu}$, $\beta_{2\mu}$ and $\delta_{2\mu}$ are given by equation (4.18). As the μ's tend to infinity, $\beta_{1\mu}$, $\beta_{2\mu}$ and $\delta_{2\mu}$ tend to β_1, β_2 and δ_2 respectively. In practice, the amplifier gains can assume any value in the range $0 < (|\mu_1|, |\mu_2|, |\mu|) < |\mu_{max}|$, where $|\mu_{max}| < \infty$, since these rise from zero just after activation.

The differential open loop gain of a frequency compensated operational amplifier, in a bounded frequency range $0 < \omega \leq \omega_m$ is given by (1.1). In the low frequency range, that is for $|s| << \omega_c$ the amplifier gains μ, μ_1 and μ_2 in (4.18) may be assumed real. For any attainable gains in the range $0 \leq (\mu, \mu_1, \mu_2) \leq \mu_{max}$, it may be shown from (4.32) that the zeros of D(s) are always in the left half plane. Therefore, the d.c. (or low frequency) unstable mode of operation cannot arise during activation.

4.5 THE INFLUENCE OF THE FINITE BANDWIDTH OF THE AMPLIFIER

The finite bandwidth (B.W) of the OA's used in active filters may result in drastic deviation of the actual performance of active filters from what is expected [64] - [65]. In this section, the effect of the OA's finite B.W on Q_p and ω_p is studied. It is shown that ω_p is relatively independent of B, the finite gain bandwidth product of the OA's, while the effect on Q_p is an enhancement.

When the one pole model as given in (1.1), is used for the amplifiers, the resulting fifth order denominator polynomial may be written in the form

$$D_1(s) = b_5 s^5 + b_4 s^4 + b_3 s^3 + b_2 s^2 + b_1 s + b_0 \qquad (4.33)$$

where for $Q_p >> 1$

$$b_o = 1$$

$$b_1 = \frac{1}{4Q_p^2}\left(\frac{\beta_1}{B_2} + \frac{\beta_2}{B_3} - \frac{\delta_2}{B_1}\right) + \frac{1}{Q_p\omega_p}$$

$$b_2 = \frac{1}{4Q_p^2}\left(\frac{\beta_1\beta_2}{B_2B_3} - \frac{\beta_1\delta_2}{B_1B_2} - \frac{\beta_2\delta_2}{B_1B_3}\right) + \frac{1}{\omega_pQ_p}\left(\frac{\beta_1}{B_2} + \frac{\beta_2}{B_3} - \frac{\delta_2}{B_1}\right) + \frac{1}{\omega_p^2}$$

$$b_3 = \frac{1}{B_1B_2B_3} + \frac{1}{Q_p\omega_p}\left(\frac{\beta_1\beta_2}{B_2B_3} - \frac{\beta_1\delta_2}{B_1B_2} - \frac{\beta_2\delta_2}{B_1B_3}\right)$$

$$+ \frac{1}{\omega_p^2}\left(\frac{\beta_1}{B_2} + \frac{\beta_2}{B_3} - \frac{\delta_2}{B_1}\right) \qquad (4.34)$$

$$b_4 = \frac{4Q_p}{\omega_pB_1B_2B_3} + \frac{1}{\omega_p^2}\left(\frac{\beta_1\beta_2}{B_2B_3} - \frac{\beta_1\delta_2}{B_1B_2} - \frac{\beta_2\delta_2}{B_1B_3}\right)$$

$$b_5 = \frac{4Q_p^2}{\omega_p^2B_1B_2B_3}$$

and B_1, B_2, B_3 are the gain-bandwidth products of the input summer and the amplifiers β_1 and β_2 respectively.

Equation (4.33) can be expressed in factored form as

$$D_1(s) = \left(\frac{1}{p_1}s+1\right)\left(\frac{1}{p_2}s+1\right)\left(\frac{1}{p_3}s+1\right)\left(\frac{1}{\omega_{pB}^2}s^2 + \frac{1}{\omega_{pB}Q_{pB}}s+1\right) \qquad (4.35)$$

Comparing the coefficients of (4.35) and (4.33), it can be shown that

$$\frac{1}{\omega_{pB}^2} = b_2 - \frac{\omega_{pB}}{Q_{pB}}b_3 - \omega_{pB}^2\,b_4\left(1 - \frac{1}{Q_{pB}^2}\right)$$

$$+ \frac{\omega_{pB}^3}{Q_{pB}}b_5\left(2 - \frac{1}{Q_{pB}^2}\right) \qquad (4.36)$$

and

$$\frac{1}{\omega_{PB}Q_{PB}} = b_1 - \omega_{PB}^2 b_3 + \frac{\omega_{PB}^3}{Q_{PB}} b_4 + \omega_{PB}^4 b_5 \left[1 - \frac{1}{Q_{PB}^2}\right] \qquad (4.37)$$

As shown in Appendix A.1, for $\mu_o \gg 1$ and $Q_p \gg 1$ and neglecting second and higher order terms of (1/B)

$$\omega_{PB} \simeq \omega_p \qquad (4.38a)$$

$$Q_{PB} \simeq \frac{Q_p}{1 - Q_p\omega_p X} \qquad (4.38b)$$

where

$$X = \frac{\beta_2}{B_3} + \frac{\beta_1}{B_2} + \frac{1 - \delta_2}{B_1} \qquad (4.38c)$$

As seen from (4.38a) ω_p is independent of B, at least as far as first order effects are concerned. In view of this and of equation (4.16), it is expected that, once the filter is tuned, it will experience negligible frequency shift. The fact that ω_p is independent of B is a desirable feature, particularly for highly selective responses.

The effect of the finite bandwidth of the OA's on Q_{PB} is shown by (4.38b). To minimize this effect, X has to be minimized subject to the constraint (4.14). Assuming the amplifiers to be identical, that is, $B_1 = B_2 = B_3 = B$, X is minimum when

$$\beta_1 = \beta_2 = -\delta_2 = (4Q_p^2 - 1)^{1/3} \simeq (2Q_p)^{2/3} \qquad (4.39)$$

It is interesting to note that this condition was also derived earlier in section 4.3.1 from an entirely different consideration.

It is observed from (4.38) that the effect of B on Q_{PB} is an enhancement. This enhancement is shown in Figure 4.3 for a Q_p of 10, for identical amplifiers and using Fairchild μA741 OA's.

In order to study the exact effect of B on pole-Q and pole-frequency for any particular filter, using the design of section 4.3.1, equation (4.33) has to be simulated on the computer. This was done (Appendix A.2), using typical data values for Fairchild μA741 OA's (B = 1MHZ), for Q_p's and ω_p's in the range (10-100) and (100-10^5) respectively. The results of the computer runs were in close agreement to the values calculated from equations (4.38); as seen from Figure 4.3.

In the following section, a method that compensates for Q_p-enhancement is presented. The compensated network is then studied in detail.

4.6 THE COMPENSATED NETWORK

In this section a simple technique for compensating for the effect of the finite bandwidth of the OA's on Q_p is first presented. The effect of compensation on ω_p is then examined. The sensitivity properties of the compensated network are also presented. Finally, a tuning procedure for the compensated network is given.

4.6.1 The Compensation Scheme

Equation (4.38b) may be derived by another method, that is, by evaluating the phase shift of the loop gain at ω_p. As shown in Appendix B, this approach shows that Q-factor enhancement is due to a phase lag introduced by the finite pole of the OA's. Therefore, Q-levelling

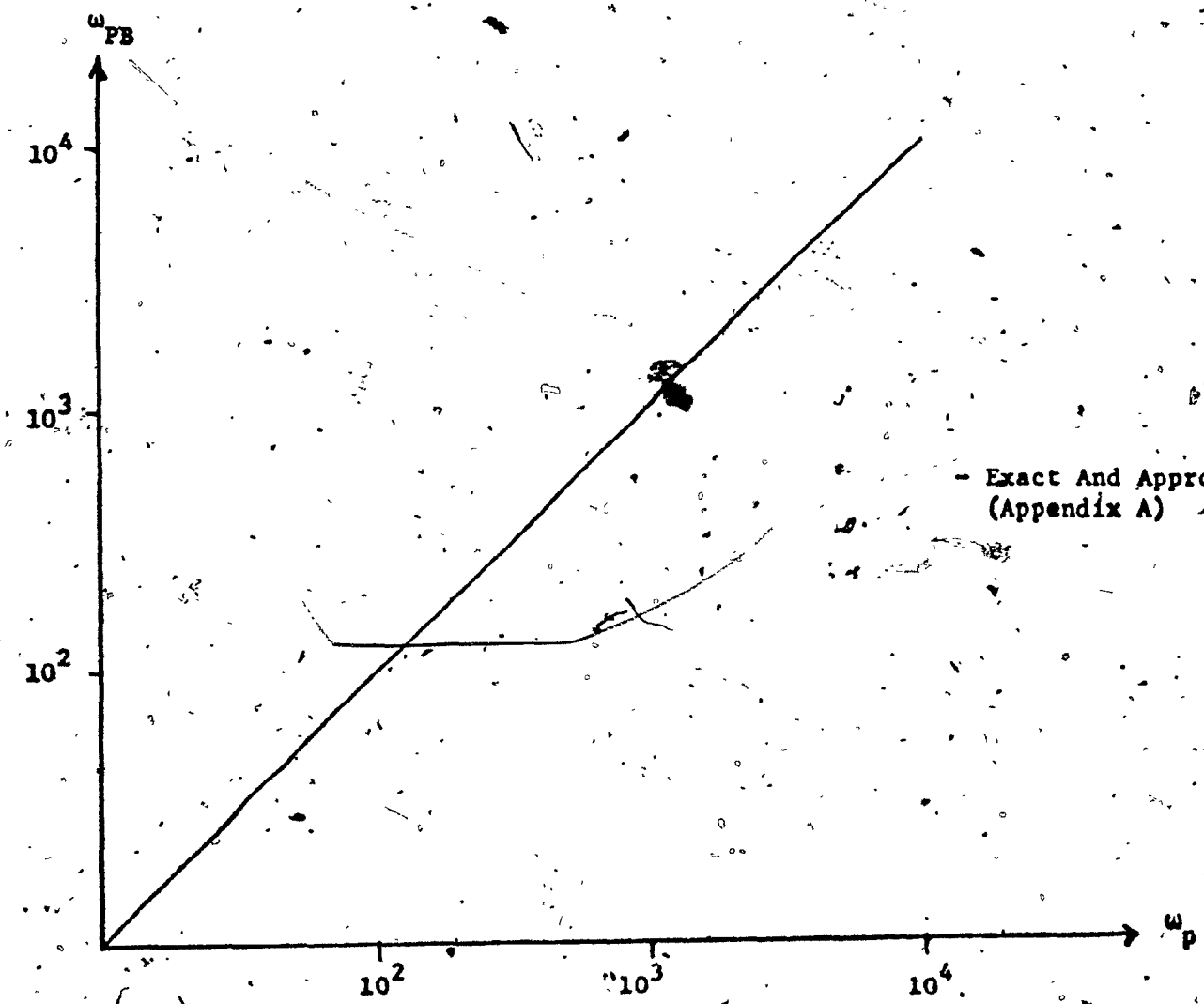

Fig. 4.3a: Plot of ω_{PB} Versus ω_p for $Q_p = 10$

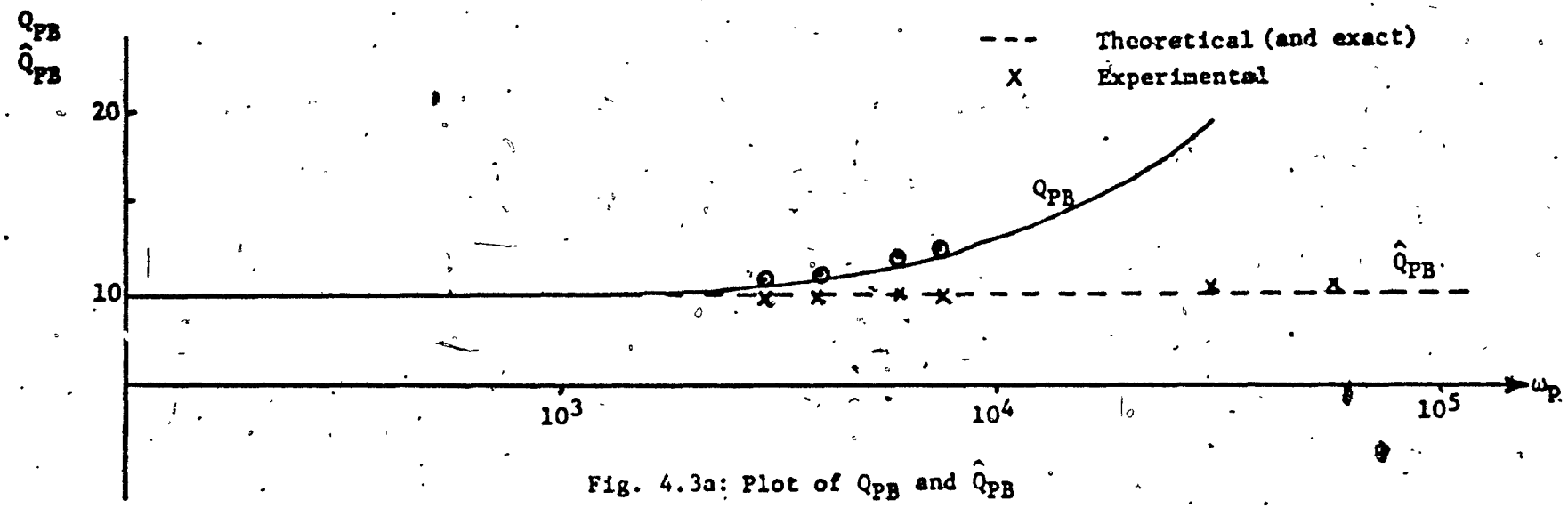

Fig. 4.3a: Plot of Q_{PB} and $\hat{Q}_{PB}$

may be accomplished by introducing a phase lead. The phase lead network should be such that the capacitors remain grounded and minimum in number. This may be easily achieved by connecting a resistor R_c as shown in Figure 4.4.

The pole-Q for the compensated circuit may be shown to be (Appendix B).

$$\hat{Q}_{PB} \simeq \frac{Q_p}{1 - Q_p\omega_p (X-R_c C)} \tag{4.40}$$

Thus, compensation may be accomplished by setting

$$R_c = X/C \tag{4.41}$$

in which case

$$\hat{Q}_{PB} = Q_P$$

It may be also shown that the pole frequency of the compensated network is

$$\hat{\omega}_{PB} \simeq \frac{\omega_p}{1 + \frac{\omega_p R_c C}{2Q_p}} = \frac{\omega_p}{1 + \frac{3\omega_p}{(2Q_p)^{1/3} B}} \tag{4.42}$$

Thus the effect of compensation on $\hat{\omega}_{PB}$ is negligible, provided that $(2Q_p)^{1/3} B >> \omega_p$, which is normally satisfied in practice.

Using a computer program, the exact values of $\hat{Q}_{PB}$ and $\hat{\omega}_{PB}$ were calculated from the resulting fifth order denominator polynomial of the compensated network. These values were in close agreement with those provided by equations (4.40) and (4.41). Figure 4.3 shows variations of the compensated $\hat{Q}_p$ versus ω_p (for $Q_p = 10$).

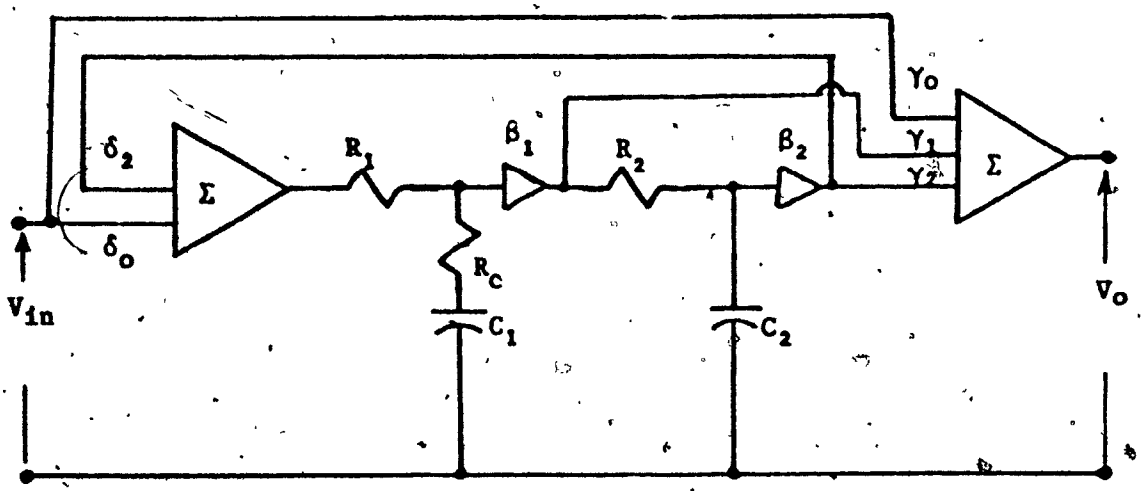

Fig. 4.4: Compensated Network

4.6.2 The Sensitivity Properties of the Compensated Network

(A) $\hat{\omega}_{PB}$ Sensitivity

From (4.42) and (4.41), it may be shown that

$$S_B^{\hat{\omega}_{PB}} = 0, \quad S_{R_c}^{\hat{\omega}_{PB}} = \frac{\omega_p R_c C}{2(2Q_p + \omega_p R_c C)} \tag{4.43a}$$

For μA741 OA's, it may be shown that

$$S_{R_c}^{\hat{\omega}_p} = (0.215 \times 10^{-6}) \cdot \frac{\omega_p}{Q_p^{1/3}} \tag{4.43b}$$

Thus, for most filter applications, $S_{R_c}^{\hat{\omega}_{PB}}$ may be regarded negligible. Therefore, in view of (4.16) and (4.43), once the pole frequency of the compensated network is tuned for manufacturing tolerances, the frequency shift due to temperature will be almost negligible.

(B) $\hat{Q}_{PB}$ Sensitivities

From (4.40) and (4.41) it may be shown that

$$S_{B_1}^{\hat{Q}_{PB}} = S_{B_2}^{\hat{Q}_{PB}} = S_{B_3}^{\hat{Q}_{PB}} = -\frac{\omega_p (2Q_p)^{5/3}}{2B} \tag{4.44a}$$

and

$$S_{R_c}^{\hat{Q}_{PB}} = -\frac{3}{2} \frac{\omega_p (2Q_p)^{5/3}}{B} \tag{4.44b}$$

After the filter is tuned, variations of $\hat{Q}_{PB}$ with respect to temperature may be estimated from

$$S_B^{\hat{Q}_{PB}} = \sum_{i=1}^{3} S_{B_i}^{\hat{Q}_{PB}} = -\frac{3}{2} \cdot \frac{\omega_p (2Q_p)^{5/3}}{B} \tag{4.45}$$

This is due to the fact that the OA's track very closely with temperature. The temperature dependence of $\hat{Q}_{PB}$ on R_C can be estimated from (4.44b).

It is observed from (4.44b) and (4.45) that the sensitivities of $\hat{Q}_{PB}$ with respect to B and R_C are identical. This fact, along with equation (4.40), may be used to advantage to make the pole Q of the compensated network insensitive to temperature variations by replacing R_C by a temperature dependent resistor (for example a thermistor) such that the temperature coefficients of B and R_C are equal and opposite.

4.6.3 The Tuning of the Compensated Network

A simple three step tuning procedure is now described for the compensated network.

(1) For any response, starting with the basic LP section, the pole frequency is first adjusted by trimming R_1 and R_2.

(2) The pole-Q is next adjusted by trimming R_C. As seen from (4.43b) this will not affect ω_p.

(3) Any numerator coefficient may be independently controlled by trimming resistors as observed from (4.1).

4.7 INFLUENCE OF THE AMPLIFIER BANDWIDTH ON THE ZEROS OF NOTCH AND ALL PASS RESPONSES OF THE COMPENSATED CIRCUIT

The finite bandwidth of the OA may also affect the zeros of a notch or an all pass filter. The purpose of this section is to investigate this effect.

Assuming all the OA's to be identical and the constraints of the design presented in section 4.3 , the following fifth order polynomial results

$$N_1(s) = a_5 s^5 + a_4 s^4 + a_3 s^3 + a_2 s^2 + a_1 s + a_0 \qquad (4.46)$$

where

$$a_0 = 1$$

$$a_1 = \{[\frac{2Q_D}{\omega_p} + \frac{2Q_p}{\omega_p}(1 - \frac{\rho\beta_1\delta_o}{\gamma_o}) + R_c C\,(1 + \beta_1\beta_2\delta - \frac{\rho\beta_1\delta_o}{\gamma_o} + \frac{\gamma_2\beta_1\beta_2\delta_o}{\gamma_o})]B^3 + (3 - \frac{\rho\beta_1\delta_o}{\gamma_o})\eta B^2\}$$

$$a_2 = \{[\frac{2Q_p}{\omega_p} + (1 - \frac{\rho\beta_1\delta_o}{\gamma_o})\,R_c C\,\frac{2Q_D}{\omega_p}B^3 + \frac{10Q_p}{\omega_p} + (1 - \frac{\rho\beta_1\delta_o}{\gamma_o})\frac{2Q_p}{\omega_p} + R_c C\,(3 - \frac{\rho\beta_1\delta_o}{\gamma_o})]\,\eta B^2 + 3\eta^2 B\}\,\frac{1}{\nu}$$

$$a_3 = \{[\frac{12Q_D^2}{\omega_p^2} + (1 - \frac{\rho\beta_1\delta_o}{\gamma_o})\frac{2Q_p}{\omega_p}R_c C + \frac{4Q_p}{\omega_p}R_c C]\,\eta B^2 + (\frac{12Q_D}{\omega_p} + 3R_c C)\,\eta^2 B + \eta^3\}\,\frac{1}{\nu} \qquad (4.47)$$

$$a_4 = [(\frac{12Q_p^2}{\omega_p^2} + \frac{6Q_p}{\omega_p}R_c C)\,\eta^2 B + (\frac{4Q_p}{\omega_p} + \frac{2Q_p}{\omega_p}R_c C + R_c G)\eta^3]\frac{1}{\nu}$$

$$a_5 = (\frac{4Q_p^2}{\omega_p^2} + \frac{2Q_p}{\omega_p}R_{oo}C)\,\frac{\eta^3}{\nu}$$

and

$$\eta = \beta_1 = \beta_2 = -\delta_2$$
$$\delta = |\delta_2| \qquad (4.48)$$
$$\rho = |\gamma_1|$$
$$\nu = (1 + \beta_1\beta_2\delta - \frac{\rho\beta_1\delta_o}{\gamma_o} + \frac{\gamma_2\beta_1\beta_2\delta_o}{\gamma_o})\,B^3$$

(A) The Notch Section

Using equations (4.20a), (4.46),(4.47) and (4.48) along with the design constraints of section 4.3.1 and the procedure of Appendix A, the effect of B on the notch response of the compensated network may be shown to be

$$\frac{1}{\hat{\omega}_{NB}^2} \simeq \frac{1}{\omega_N^2}\left[1 + \frac{4\omega_p}{(2Q_p)^{1/3}B} + \frac{R_c C\,\omega_p^2}{B(2Q_p)^{4/3}}\right] \tag{4.49}$$

$$\frac{1}{\hat{Q}_{ZB}} \simeq \frac{\omega_N}{(2Q_p)^{4/3}B} \tag{4.50}$$

where

$$R_c C = \frac{3(2Q_p)^{2/3}}{B} \tag{4.51}$$

Thus,we observe, from (4.49) and (4.50), that the effect of B on the notch section is almost negligible, provided

$$(2Q_p)^{1/3}B \gg 4\omega_p \tag{4.52}$$

(B) All Pass Section

Using equations (4.46), (4.47) and (4.48) along with the design equations of the AP response, it may be shown that

$$\frac{1}{\hat{Q}_{ZB}} \simeq -\frac{1}{Q_p} + \frac{\omega_p}{(2Q_p)^{4/3}B} - \frac{3\omega_p(2Q_p)^{2/3}}{GB} + \omega_p R_c$$

$$\simeq -\frac{1}{Q_p} + \frac{\omega_p}{(2Q_p)^{4/3}B} \tag{4.53}$$

and

$$\frac{1}{\hat{\omega}_{ZB}} \simeq \frac{1}{\omega_p^2}\left[1 + \frac{2\omega_p}{(2Q_p)^{1/3}B} - \frac{R_c C\omega_p^2}{(2Q_p)^{4/3}B}\right] \tag{4.54}$$

where $R_c C$ is as in (4.51)

It is observed from (4.53) and (4.54) that the effect of the finite bandwidth of the OA on the zeros of the compensated AP section is negligible provided $(2Q_p)^{1/3}GB >> 2\omega_p$, which is normally the case.

From (4.53), and (4.51) it is also observed that the effect of B on $\hat{Q}_{ZB}$ may be compensated in an identical manner as in the case of $\hat{Q}_p$. Therefore, R_c may be used to tune simultaneously $\hat{Q}_p$ and $\hat{Q}_Z$ for the AP section.

4.8 THE EFFECT OF THE OA'S INPUT AND OUTPUT RESISTANCES ON THE RESPONSE OF THE COMPENSATED CIRCUIT

It has been shown that the output impedance of an OA might limit the usefulness of active filters [66]. In this section the effect of the differential input and output resistances of the OA's on the response of the compensated filter is studied for a Q_p of 10.

The filter of Figure 4.4 was used to realize a band pass section with a Q_p of 10 at f_p = 1.01 KHZ. Using Fairchild μA741C OA's (GB = 1MHZ, differential input impedance = 1MΩ, output impedance = 75Ω) and a computer program based on [67], the filter was analyzed. The results of the analysis indicated that the deviation in pole-Q as well as in pole frequency were within 1%.

4.9 EXPERIMENTAL RESULTS

A second order low pass section and a second order band pass section were built and tested, using the proposed design along with the compensation scheme. Finally, a sixth order band pass filter with a very

narrow band was also built and tested.

The low pass section has a Q_p = 10 and f_p = 1KHZ and gain of - 8.7 db at f_p. The band pass section has a Q_p = 50 and f_p = 1.13 KHZ and a unity centre frequency gain.

The sixth order filter has a centre frequency f_p = 100HZ. The pass band is 10HZ and the stop band attenuation is greater than 38 db outside the frequency range 85 - 115 HZ. The maximum permissible pass band ripple is 1.5 db.

Resistors (temperature coefficients = ±100 p.p.m/°C, tolerance < 1%), capacitors (temperature coefficient = -140 ± 40 p.p.m, tolerance < 2%), and μA741C OA's (fixed internal frequency compensation) were used.

4.9.1 The Q-enhancement and Compensation Scheme

The $\hat{Q}_p$-enhancement and the levelling scheme discussed in sections 4.5.1 and 4.5.2 respectively were experimentally verified for a Q_p of 10. Figure 4.3 shows the experimental plots which closely agree with the theoretical ones.

4.9.2 The Low Pass Filter

The realization and design values are shown in Figure 4.5a. The measured frequency response (input level = .2V) is shown in Figure 4.5b in logarithmic scale. The effect of the d.c. supply variations is illustrated in Figure 4.5c. The deviation in ω_p is negligible and the variation in Q_p is within the expected value in the range ± 7 (upper curve) to ± 17 volt. The effect of temperature is

illustrated in Figure 4.5d (70°C) and Figure 4.4e (0°C). The deviation in f_p can be shown to be within the range expected due to the temperature coefficients of the passive elements. The variations in Q_p are within the theoretical prediction.

4.9.3 The Band Pass Filter

The realization along with the element values are shown in Figure 4.6. The measured frequency response is shown in Figure 4.6b and is agreed with the theoretical response.

4.9.4 The Sixth Order Band Pass

The realization, transfer function and element values are shown in Figure 4.7a and table 4.1, respectively. It uses a cascade of a BP and two N-sections.

The measured frequency response is shown in Figure 4.7b, for an input level of $\frac{2}{3}$ volts, and is in close agreement with the theoretical one. Figure 4.7c shows the effect of variations of power supply voltage from ± 7 to ± 17 volts. The effect of temperature variations of the active element was studied by placing the active elements only in a constant temperature chamber and measuring the response. This effect is also shown in Figure 4.7c. As seen the effect of power supply and temperature variations of the active element, is negligible on the frequency response. The pass band ripple remains within 1.5 db and the deviation from the required specification in the stop band is negligible.

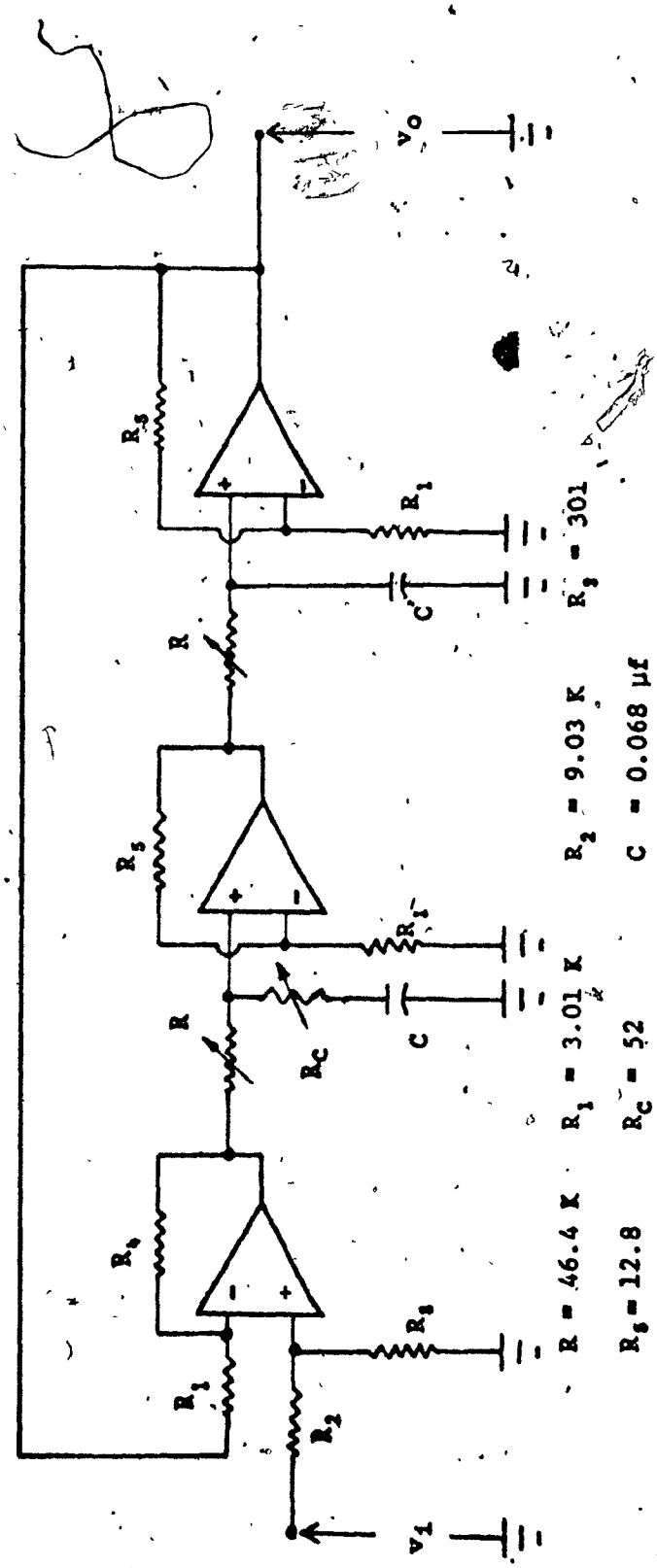

Fig. 4.5a: Low Pass Realization

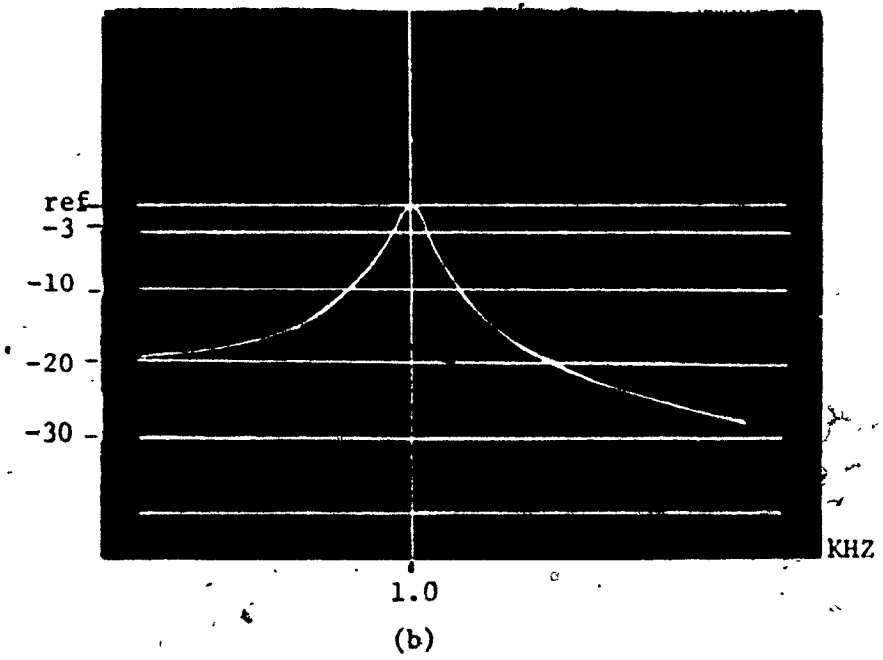

(b)

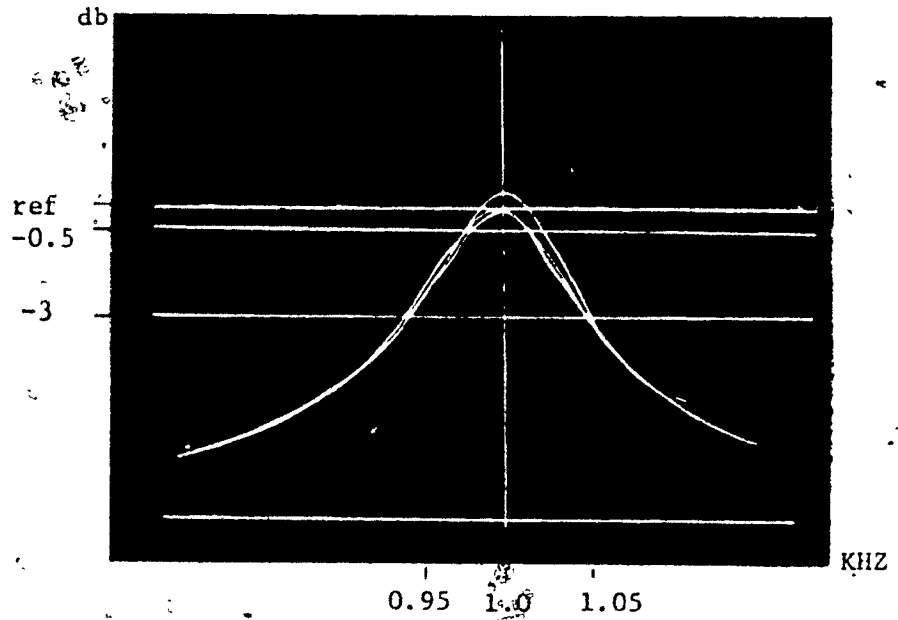

(c)

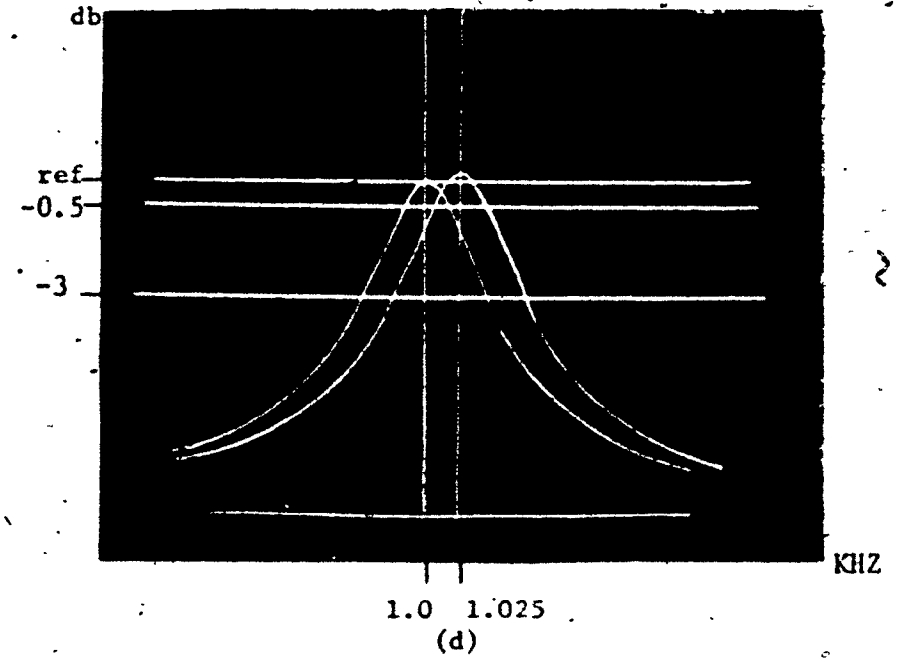

(d)

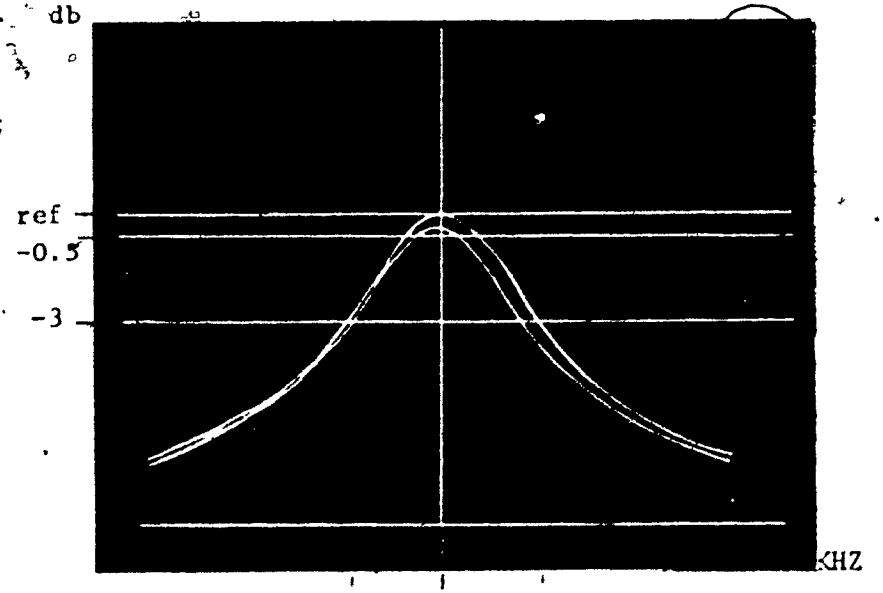

(e)

Fig. 4.5: (b) LP Response (c) Effect of Power Supply (d) Effect of Temperature (70°C), (e) Effect of Temperature(0°

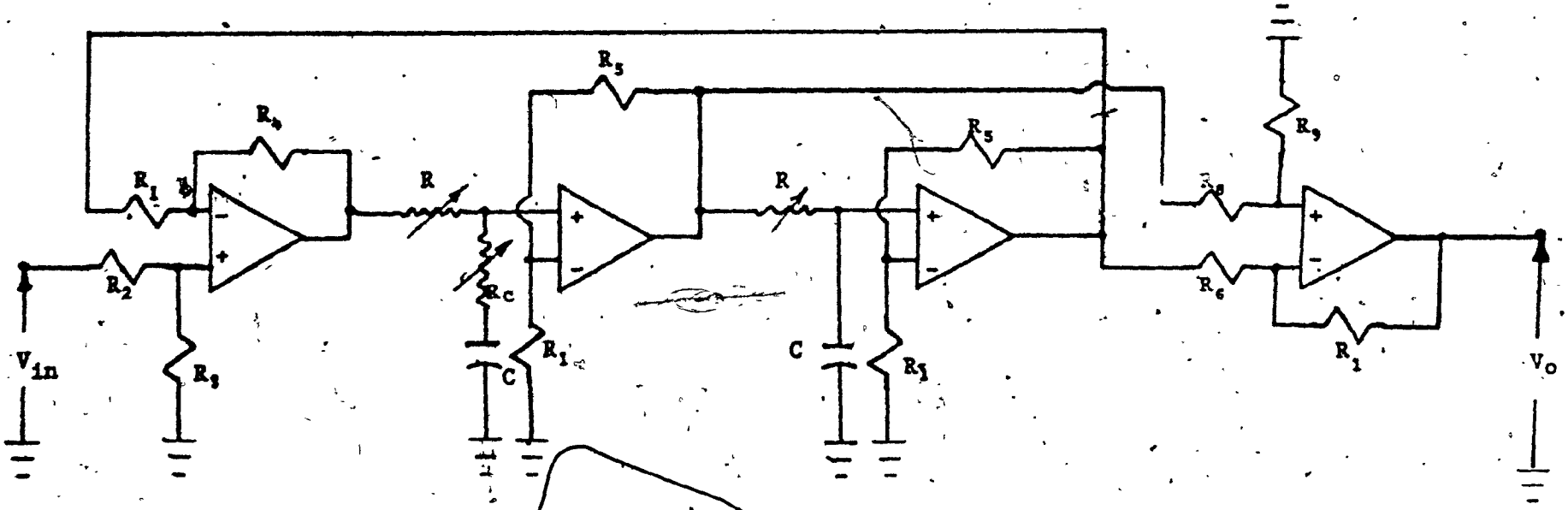

R = 94 K R_1 = 2.15 K R_2 = 55 K R_3 = 511 R_4 = 46.3 K R_5 = 44.4 K

R_6 = 46.3K R_8 = 10.93 K R_9 = 10 R_c = 68.5 C = .15 µf

Fig. 4.6a: Band Pass Realization

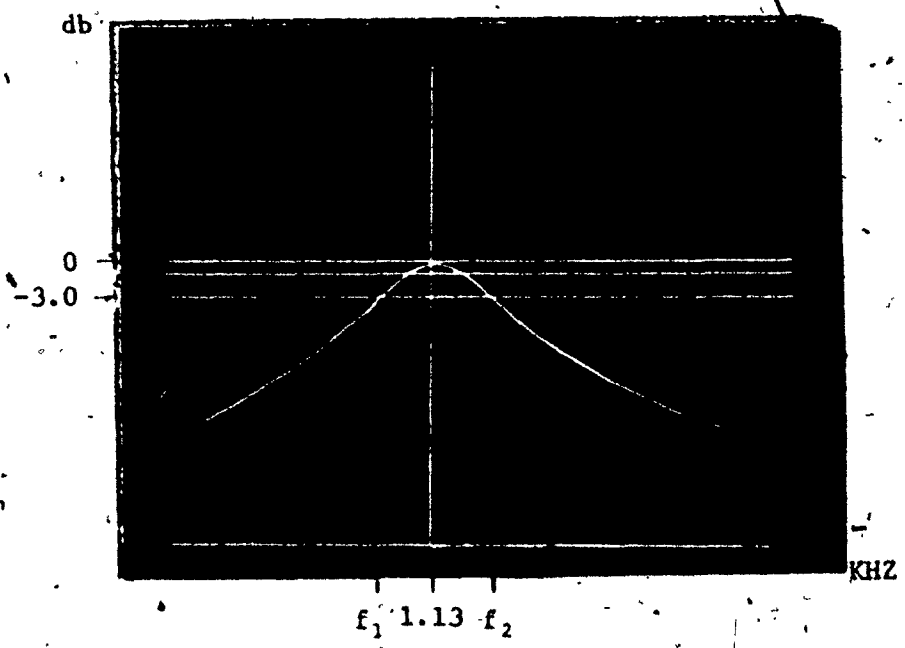

(b)

Fig. 4.6: b), Band pass response, Q_p = 50, f_p = 1.13 KHZ (f_1 = 1.119 KHZ, f_2 = 1.141 KHZ)

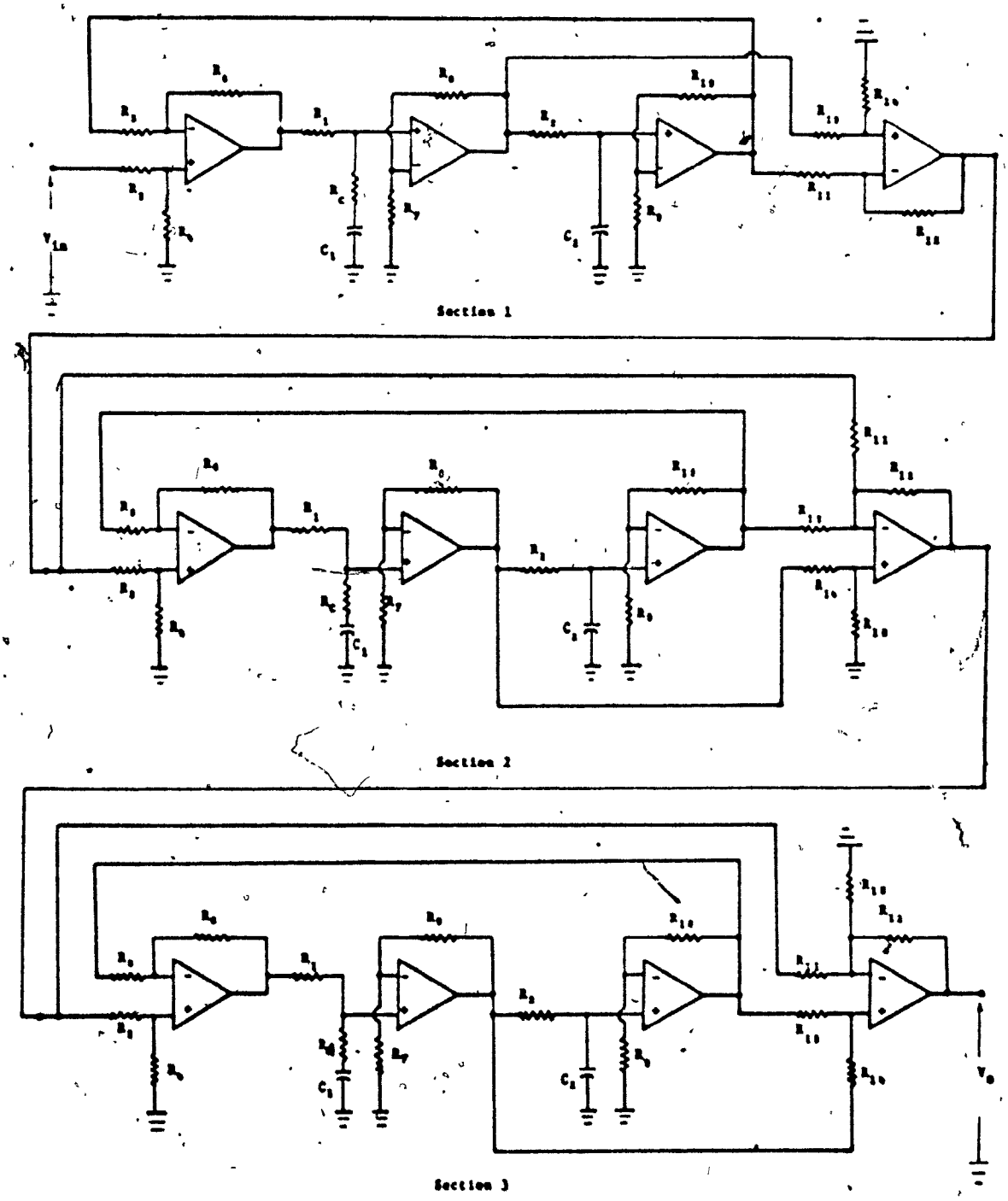

Fig. 4.7a: Realization of $T(s) = \frac{0.003s}{s^2+0.03s+1} = \frac{s^2 + 1.327}{s^2 + 0.0258s + (1.051)^2} = \frac{s^2 + 0.753}{s^2 + 0.0233s + (0.931)^2}$

Table 4.1 Element Values for the Sixth Order BP Filter

Element	Section 1	Section 2	Section 3
R_1, R_2	935	805	893
R_3	330	91	91
R_4	0.438	2.22	2.22
R_5	3.32	2.15	2.15
R_6	39.2	39.8	39.8
R_7	2	2.15	2.15
R_8	21.6	37.6	37.6
R_9	2	2.15	2.15
R_{10}	21.6	37.6	37.6
R_{11}	23.6	40.2	5.9
R_{12}	2	40.2	5.9
R_{13}	—	5.025	2
R_{14}	—	84	58.4
R_{15}	—	2	1.175
R_C	0.0829	0.059	0.059
C_1, C_2	0.068	0.15	0.15

All R's in KΩ and C's in μf.

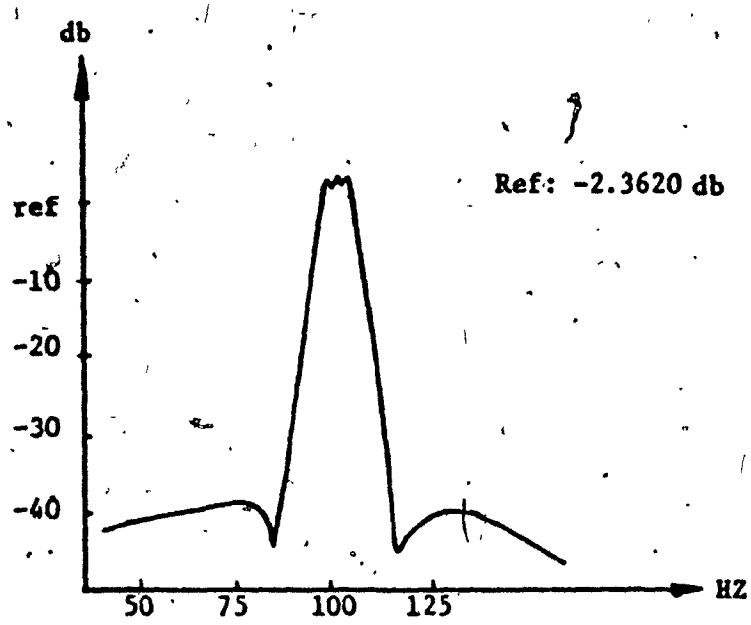

(b)

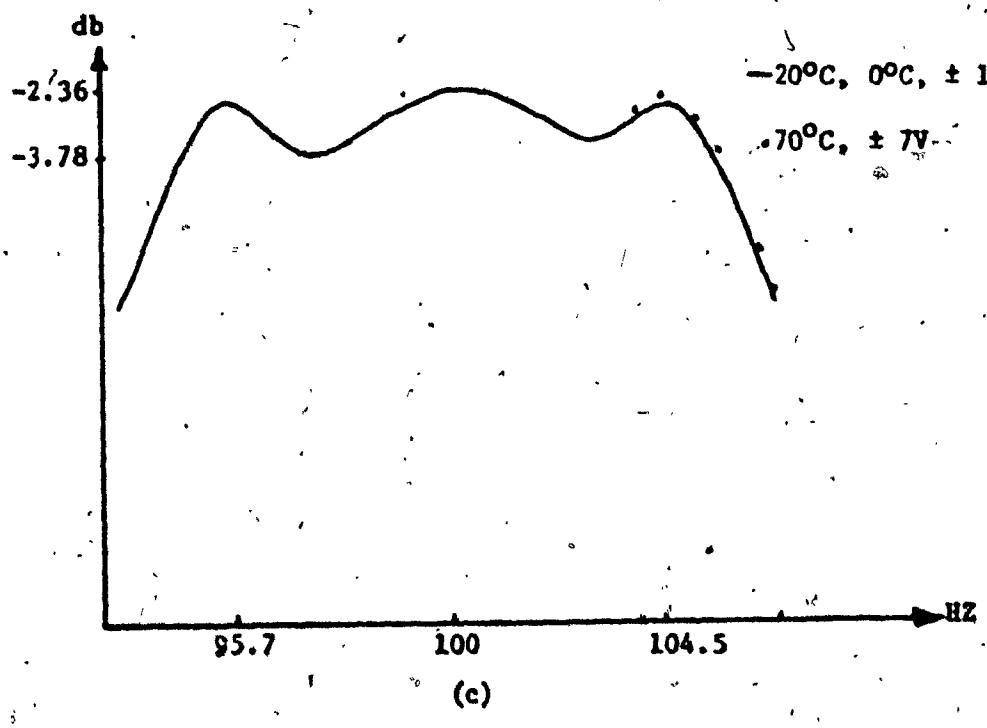

(c)

Fig. 4.7: b) Sixth Order Band Pass Response
c) The Pass Band

4.10 CONCLUSIONS

A significant improved design of the grounded capacitor RC active filter reported in the previous chapter has been presented. The design presented minimizes simultaneously the worst case changes in ω_p and Q_p due to variations in passive and active components. The feedback gains have all been made equal to $(2Q_p)^{2/3}$. This compares very favourably with several other designs which require a gain of Q_p. It is shown that this network is always stable during activation. The effect of the finite bandwidth of the OA on ω_p has also been shown to be negligible, while that on Q_p is an enhancement. It is shown that the above choice of gains also minimizes the Q_p-enhancement.

A simple scheme has been proposed to compensate for the effect of the bandwidth of the OA on Q_p without affecting ω_p, thus improving the useful frequency range of operation of the circuit. The effect of compensation on the zeros of the notch and all pass sections has also been studied. It is found that ω_N and ω_Z are negligibly affected, while compensating for Q_p automatically compensates for Q_Z. The parasitic effect of the input and output impedances of the OA on the compensated filter is studied for a band pass section of $Q_p = 10$ and $f_p = 1.01$ KHZ and found to be negligible for μA741 OA. Finally, detailed experimental results are given that are in close agreement with theory.

In the following chapter, the optimum design developed in section 4.3 is used to study in detail the properties of the second order band pass and low pass $\overline{\text{URC}}$ realizations derived from the synthesis procedure proposed in Chapter 2.

CHAPTER V

ACTIVE URC REALIZATIONS

5.1 INTRODUCTION

In Chapter 2, a synthesis procedure has been proposed that can realize any rational transfer function by using, as unit elements, a short circuited $\overline{\text{URC}}$, an ideal gyrator terminated by an open circuited $\overline{\text{URC}}$ and, in general, finite gain amplifiers. The purpose of this chapter is to illustrate this procedure by first designing second order band pass filters, using the configuration of Figure 4.2 along with the optimum design of section 4.3.

The effects of the non-commensurate behaviour of the $\overline{\text{URC}}$'s on the resulting realizations are also studied. The influence of gyrator imperfections on the transformation u(s) as well as on the band pass filters is next examined. The dependance of the Q-factor and pole frequency on the finite bandwidth of the OA's, that determine the finite gains, is then investigated. Finally, the practical feasibility of the proposed synthesis technique is demonstrated by designing a second order Butterworth low pass filter, and showing that the entire filter can be fabricated by hybrid IC technology.

5.2 DESIGN OF A BAND PASS FILTER

For a second order BP filter with selectivity Q_p, resonant frequency ω_p and gain H at resonance, the open circuit voltage transfer function may be written as

$$T(s) = H \frac{\frac{\omega_p}{Q_p} s}{s^2 + \frac{\omega_p}{Q_p} s + \omega_p^2} \qquad (5.11)$$

The distributed realization may be obtained as follows:

Step 1

Use (2.3) to obtain from (5.1)

$$G(u) = T\left(\frac{1}{R_T C_T u}\right) = H \frac{\frac{1}{Q_p \omega_p R_T C_T} u}{u^2 + \frac{u}{Q_p \omega_p R_T C_T} + \frac{1}{(\omega_p R_T C_T)^2}} \qquad (5.2)$$

Step 2

Set

$$\gamma_0 = 0, \ \gamma_2 = -\gamma_1, \ \gamma_1 \beta_1 \delta_0 = 2H \qquad (5.3)$$

in the network of Figure 4.2. Further, let

$$R_i = R_{ui}, \ C_i = C_{ui} \quad (i = 1,2) \qquad (5.4a)$$

$$R_{ui} C_{ui} = R_u C_u = 2 Q_p (\omega_p R_T C_T) \quad (i = 1,2) \qquad (5.4b)$$

$$\beta_1 = \beta_2 = -\delta_2 = (2 Q_p)^{2/3} \qquad (5.4c)$$

Figure 4.2 then reduces to Figure 5.1 and realizes G(u) as given by (5.2) where

$$\beta_1 = \beta_2 = 1 + R_5/R_6, \ \delta_2 = -R_4/R_1 \qquad (5.4d)$$

$$\gamma_1 = \frac{R_{10}}{R_9 + R_{10}} \left(1 + \frac{R_8}{R_7}\right), \ \gamma_2 = -\frac{R_8}{R_7}$$

Step 3

Replace in Figure 5.1 each lumped resistor R_{ui} by the one port represented by Figure 2.7a and each lumped capacitor C_{ui} by the one port of the network shown in Figure 2.7b, that is, the resistor R_{ui}

in the u-plane is replaced by a short circuited $\overline{\text{URC}}$ with a total resistance R_{2Ti}, while the capacitor C_{ui} is replaced by an ideal gyrator, of gyration constant K_i, terminated by an open circuited $\overline{\text{URC}}$ with a total resistance R_{2Ti}, such that

$$R_{1Ti} = R_{ui} \quad , \quad C_{ui} = (R_{2Ti}/K_i) \quad (i = 1,2) \tag{5.5a}$$

Thus, from (5.4) and (5.5a) we obtain,

$$R_{1Ti}\, R_{2Ti} = 2\, Q_p\, (\omega_p R_T C_T) K_i \quad (i = 1,2) \tag{5.5b}$$

Since $R_{u_1} = R_{u_2} = C_u$ and $C_{u_1} = C_{u_2} = C_u$, we note that $R_{1T1} = R_{1T2}$, while $\frac{R_{2T1}}{K_1} = \frac{R_{2T2}}{K_2}$. However, R_{1Ti} need not necessarily be equal to R_{2Ti}. In fact, it will be shown later that it is of advantage not to choose them to be equal. While it is not necessary for the gyrators to be identical, it is so desirable for thin film implementation. For identical gyrators, $R_{2T1} = R_{2T2}$.

Step 4

The value of total capacitors C_{1Ti}'s and C_{2Ti}'s of the lines can be determined once the commensurate RC product of the lines is chosen. The resulting $\overline{\text{URC}}$ realization of T(s) is shown in Figure 5.2 where

$$R_{1Ti}C_{1Ti} = R_{2Ti}C_{2Ti} = R_TC_T \quad (i = 1,2) \tag{5.5c}$$

$$R_{1T1} = R_{1T2} \ , \ R_{2T1} = R_{2T2} \ , \ K_1 = K_2 \tag{5.5d}$$

$$C_{1T1} = C_{1T2} \ , \ C_{2T1} = C_{2T2} \tag{5.5e}$$

The commensurate R_TC_T product of the lines is not chosen arbitrarily, but should be selected from either of the regions $\omega_pR_TC_T \leq 0.01$ or $\omega_pR_TC_T \geq 30$, such that, as discussed in Chapter 2,

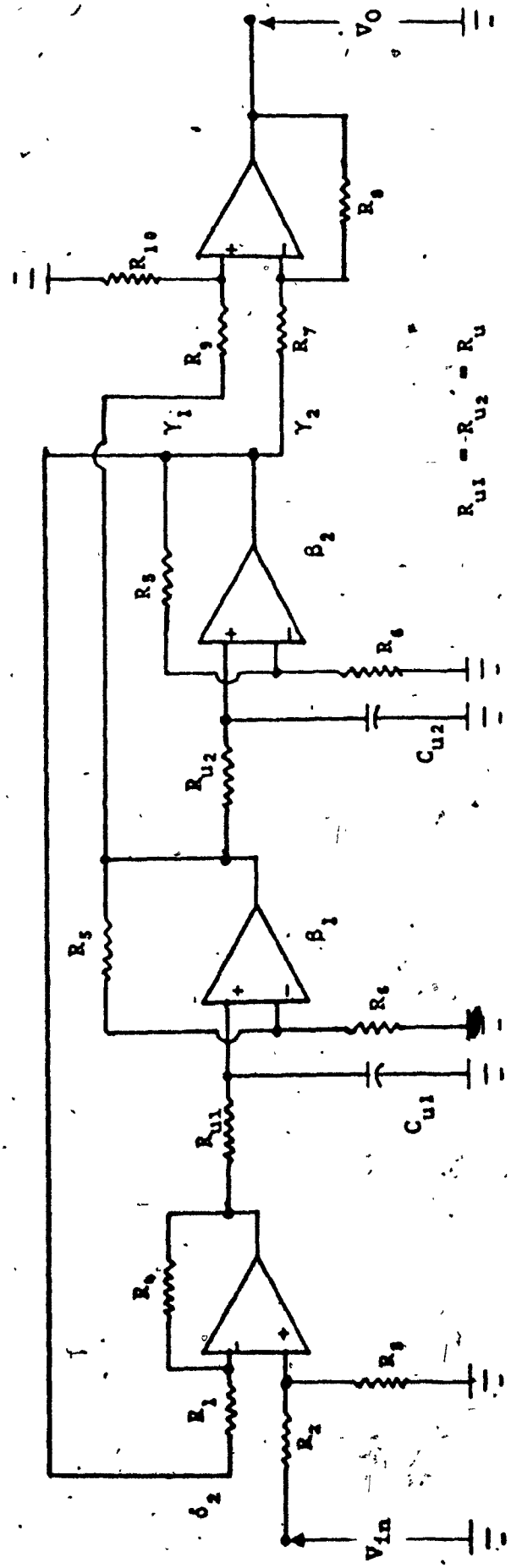

$$\frac{\left(\frac{1}{Q_p R_T C_T}\right) u}{u^2 + \left(\frac{1}{Q_p \omega_p R_T C_T}\right) u + \frac{1}{(\omega_p R_T C_T)^2}}$$

Fig. 5.1: Realization of $G(u) = H \cdot$

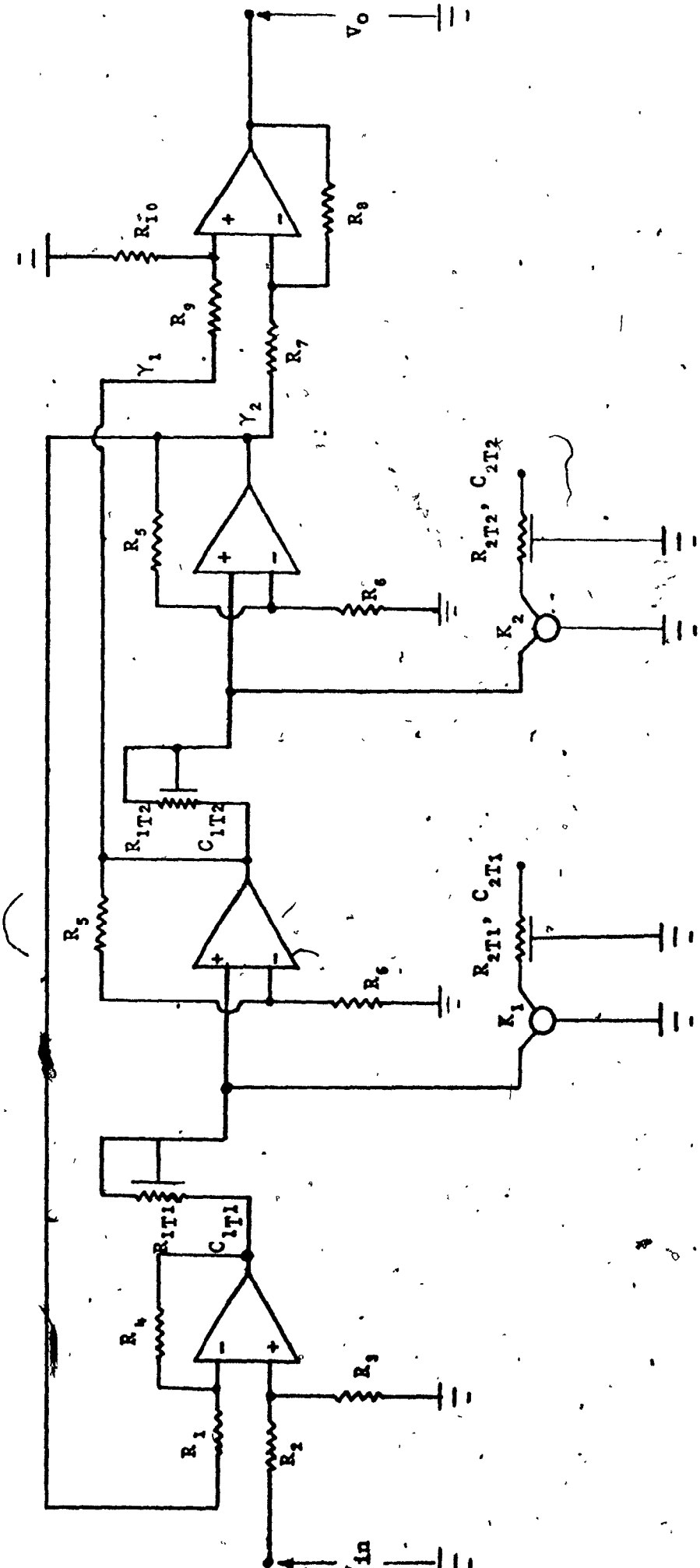

Fig. 5.2: Distributed Band Pass Realization

even if the RC product of any of the lines deviates from its nominal value, the effect on the realized response is negligible.

It is obvious that the value of the RC product and hence the substrate area required in thin film implementation is less, for the same ω_p°, in the first region than in the other. Also, the second region is suitable only for frequencies such that $\omega_p > .30 \times 10^3$. This is because the maximum RC product available at present, in thin film technology, is of the order of 10^{-3}. On the other hand, the lowest value for the RC product in the same technology is of the order of 10^{-9}. Thus, using the first region, pole frequencies up to 10^7 rad can be adequately covered. Currently, active filter applications are below this range. Thus the region $\omega_p R_T C_T \leq 0.01$ appears to be more desirable at present than the region $\omega_p R_T C_T > 30$.

5.3 NON COMMENSURATE BEHAVIOUR OF THE URC'S AND THE BP RESPONSE

If the $\overline{\text{URC}}$'s in Figure 5.2 are not commensurate the resulting transfer function is given by

$$T_{nc} = \frac{2H\, k_2 u_2(s)}{k_1 k_2 u_1(s) u_2(s) + k_1 u_1(s) + k_2 u_2(s) + 1 - \beta_1\beta_2\delta_2} \qquad (5.6)$$

where

$$k_i = \frac{R_{1Ti}\, R_{2Ti}}{K_i}, \quad i = 1,2 \qquad (5.7a)$$

$$u_1 = \frac{1}{s\sqrt{\alpha_1\alpha_2}} \; \frac{\tanh\sqrt{\alpha_1 s}}{\tanh\sqrt{\alpha_2 s}} \qquad (5.7b)$$

$$u_2 = \frac{1}{s\sqrt{\alpha_3\alpha_4}} \; \frac{\tanh\sqrt{\alpha_3 s}}{\tanh\sqrt{\alpha_4 s}} \qquad (5.7c)$$

and

$$\alpha_i = R_{1Ti}C_{1Ti} = R_{2Ti}C_{2Ti} = R_TC_T \quad (i = 1,2) \qquad (5.7d)$$

It is noted that at nominal values (5.6) reduces to (5.1)

A computer program was written (Appendix C.1) to calculate Q_R, the ratio of the realized Q_p to the one designed for Q_p = 10, 50 and 90, for ± 5 variation in any of the α's with all others at their nominal values and with $\omega_pR_TC_T$ in the range 0.01 to 100. These three values of Q were chosen to reflect the behaviour of the filter at low, medium and high Q-factors. Similarly ω_R, the ratio of the realized ω_p to the designed one was calculated in the same frequency range. These values are given in Tables 5.1, 5.2 and 5.3, respectively. It is seen that the variations in Q_p and ω_p are low either in the range $\omega_pR_TC_T < 0.02$ or in the range $\omega_pR_TC_T > 30$, and relatively large in the range $0.05 \leq \omega_pR_TC_T > 30$. This agrees with the conclusions drawn in section 2.5.

Figure 5.3a shows a normalized band pass response with Q_p = 10 realized by commensurate URC's such that $\omega_pR_TC_T = 0.01$. On the same figure the normalized responses of (5.6) are also plotted with the product of each of the URC's varying separately by + 5%. Figure 5.3b shows the same responses for $\omega_pR\,C = 1$, where we expect the response to be more sensitive to the distributed parameters. However, even in this case, the departure from the rational response is seen to be not very significant.

TABLE 5.1a: Q_R FOR ±5% VARIATIONS IN ANY OF THE DISTRIBUTED PARAMETERS, $Q_p = 10$

$\omega_p R_T C_T$	Q_R															
	+ 5% change in								− 5% change in							
	R_{1T1}	R_{2T1}	R_{1T2}	R_{2T2}	C_{1T1}	C_{2T1}	C_{1T2}	C_{2T2}	R_{1T1}	R_{2T1}	R_{1T2}	R_{2T2}	C_{1T1}	C_{2T1}	C_{1T2}	C_{2T2}
0.01	1.004	1.001	1.004	1.001	1.004	1.001	1.004	1.001	1.001	1.004	1.001	1.004	1.001	1.004	1.001	1.004
0.03	1.005	0.997	1.005	0.997	1.007	0.998	1.007	0.998	0.995	1.007	0.995	1.007	0.997	1.004	0.997	1.008
0.05	1.01	0.994	1.01	0.994	1.011	0.994	1.011	0.994	0.993	1.011	0.993	1.011	0.994	1.011	0.994	1.011
0.1	1.006	0.986	1.006	0.986	1.019	0.994	1.019	0.984	0.973	1.019	0.973	1.019	0.986	1.017	0.986	1.017
0.3	1.056	0.955	1.056	0.955	1.055	0.946	1.055	0.946	0.836	1.055	0.896	1.055	0.956	1.056	0.956	1.056
0.5	1.092	0.927	1.092	0.927	1.09	0.929	1.09	0.929	0.928	1.091	0.928	1.093	0.927	1.093	0.927	1.093
0.7	1.127	0.904	1.127	0.904	1.124	0.905	1.124	0.905	0.905	1.125	0.905	1.125	0.903	1.128	0.903	1.128
0.9	1.157	0.884	1.157	0.884	1.154	0.886	1.154	0.886	0.886	1.157	0.886	1.157	0.883	1.160	0.883	1.160
1	1.171	0.876	1.171	0.876	1.168	0.855	1.168	0.855	0.876	1.171	0.876	1.171	0.875	1.174	0.875	1.174
2	1.222	0.847	1.223	0.847	1.233	0.847	1.233	0.847	0.850	1.237	0.850	1.237	0.840	1.232	0.840	1.237
3	1.177	0.871	1.177	0.871	1.181	0.869	1.181	0.869	0.858	1.201	0.858	1.201	0.860	1.197	0.860	1.197
5	1.065	0.948	1.065	0.948	1.07	0.943	1.07	0.944	0.932	1.086	0.932	1.086	0.936	1.08	0.936	1.08
9	0.458	0.481	0.458	0.481	0.369	0.344	0.369	0.383	0.383	0.366	0.383	0.367	0.456	0.460	0.485	0.460
15	0.986	0.019	0.986	1.019	0.995	1.02	0.985	1.02	1.023	0.982	1.023	0.982	1.022	0.983	1.022	0.983
20	0.99	1.006	0.998	1.006	0.998	1.007	0.998	1.007	1.01	0.995	1.01	0.995	1.008	0.996	1.008	0.996
30	1.004	1.000	1.004	1.000	1.004	1.000	1.004	1.0	1.0	1.004	1.0	1.004	1.0	1.005	1.0	1.004
50	1.002	1.002	1.002	1.002	1.002	1.002	1.002	1.002	1.002	1.002	1.002	1.002	1.002	1.002	1.002	1.002
100	1.002	1.002	1.002	1.002	1.002	1.002	1.002	1.002	1.002	1.002	1.002	1.002	1.002	1.002	1.002	1.002

TABLE 3.1b: ω_R FOR ± 5% VARIATIONS IN ANY OF THE DISTRIBUTED PARAMETERS, $Q_p = 10$

$\omega_p R_1 C_1$	ω_R															
	+ 5% Change in								-5% Change in							
	R_{1T_1}	R_{2T_1}	R_{1T_2}	R_{2T_2}	C_{1T_1}	C_{2T_1}	C_{1T_2}	C_{2T_2}	R_{1T_1}	R_{2T_1}	R_{1T_2}	R_{2T_2}	C_{1T_1}	C_{2T_1}	C_{1T_2}	C_{2T_2}
0.01	1.025	1.0	1.025	1.0	1.0	0.976	1.0	0.976	0.975	1.0	0.975	1.0	1.0	1.026	1.0	1.026
0.03	1.023	1.0	1.023	1.0	1.0	0.977	1.0	0.977	0.973	1.0	0.973	1.0	1.0	1.027	1.0	1.027
0.05	1.024	1.0	1.024	1.0	1.0	0.976	1.0	0.976	0.974	1.0	0.974	1.0	1.0	1.026	1.0	1.026
0.1	1.02	1.0	1.02	1.0	1.0	0.980	1.0	0.980	0.970	1.0	0.970	1.0	1.0	1.03	1.0	1.03
0.3	1.024	1.0	1.024	1.0	1.0	0.99	1.0	0.99	0.99	1.0	0.99	1.0	1.0	1.026	1.0	1.026
0.5	1.024	1.001	1.024	1.001	0.999	0.977	0.999	0.977	0.975	0.999	0.975	0.999	1.0	1.025	1.0	1.025
0.7	1.023	1.002	1.023	1.002	0.998	0.977	0.998	0.977	0.976	0.998	0.976	0.998	1.001	1.024	1.001	1.024
0.9	1.022	1.003	1.022	1.003	0.997	0.978	0.997	0.978	0.977	0.998	0.977	0.998	1.002	1.023	1.002	1.023
1	1.021	1.003	1.021	1.003	0.997	0.990	0.997	0.990	0.99	0.997	0.99	0.997	1.003	1.023	1.003	1.023
2	1.015	1.009	1.015	1.009	0.991	0.984	0.991	0.984	0.983	0.991	0.983	0.991	1.009	1.017	1.009	1.017
3	1.011	1.014	1.011	1.014	0.987	0.989	0.987	0.989	0.988	0.987	0.988	0.987	1.014	1.012	1.014	1.012
5	1.008	1.016	1.008	1.014	0.984	0.992	0.984	0.992	0.991	0.983	0.991	0.983	1.017	1.009	1.017	1.009
9	1.089	1.089	1.089	1.089	1.089	1.089	1.089	1.089	1.089	1.089	1.089	1.089	1.089	1.089	1.089	1.089
15	1.012	1.012	1.012	1.012	0.988	0.988	0.988	0.988	0.987	0.987	0.987	0.987	1.013	1.013	1.013	1.013
20	1.013	1.012	1.013	1.012	0.988	0.988	0.988	0.988	0.987	0.988	0.987	0.988	1.013	1.013	1.013	1.013
30	1.012	1.012	1.012	1.012	0.988	0.988	0.988	0.988	0.987	0.987	0.987	0.987	1.013	1.013	1.013	1.013
50	1.012	1.012	1.012	1.012	0.988	0.988	0.988	0.988	0.987	0.987	0.987	0.987	1.013	1.013	1.013	1.013
100	1.012	1.012	1.012	1.012	0.988	0.988	0.988	0.988	0.987	0.987	0.987	0.987	1.013	1.013	1.013	1.013

TABLE 5.2a: Q_R FOR ±5% VARIATION IN ANY OF THE DISTRIBUTED PARAMETERS, Q_p = 50

$\omega_p R_T C_T$	Q_R															
	+ 5% change in								- 5% change in							
	R_{1T1}	R_{2T1}	R_{1T2}	R_{2T2}	C_{1T1}	C_{2T1}	C_{1T2}	C_{2T2}	R_{1T1}	R_{2T1}	R_{1T2}	R_{2T2}	C_{1T1}	C_{2T1}	C_{1T2}	C_{2T2}
0.01	1.01	0.994	1.01	0.994	1.011	0.994	1.011	0.994	0.993	1.01	0.993	1.01	0.994	1.01	0.994	1.01
0.03	1.029	0.978	1.028	0.978	1.028	0.978	1.028	0.978	0.972	1.028	0.972	1.028	0.978	1.028	0.978	1.024
0.05	1.047	0.962	1.047	0.962	1.046	0.962	1.047	0.962	0.953	1.046	0.953	1.046	0.962	1.047	0.962	1.047
0.1	0.891	0.925	0.891	0.925	1.093	0.817	1.093	0.817	0.773	1.093	0.779	1.093	0.925	0.939	0.925	0.939
0.3	1.339	0.806	1.339	0.806	1.329	0.806	1.329	0.816	0.508	1.330	0.605	1.330	0.806	1.34	0.854	1.34
0.5	1.68	0.717	1.685	0.717	1.692	0.721	1.692	0.721	0.22	1.692	0.22	1.692	0.716	1.692	0.716	1.692
0.7	2.128	0.653	2.128	0.653	2.131	0.658	2.131	0.653	0.158	2.131	0.158	2.131	0.653	2.205	0.653	2.205
0.9	2.872	0.604	2.872	0.604	2.789	0.612	2.789	0.612	0.133	2.961	0.133	2.961	0.604	2.961	0.604	2.961
1	3.312	0.590	3.312	0.590	4.202	0.438	3.202	0.438	0.113	3.329	0.113	3.329	0.586	3.462	0.586	3.462
2	7.08	0.534	7.08	0.534	7.185	0.534	7.185	0.534	0.028	10.697	0.028	10.697	0.521	10.615	0.521	10.615
3	3.435	0.583	3.435	0.583	3.610	0.578	3.610	0.578	0.555	4.778	0.555	4.778	0.560	4.462	0.560	4.462
5	1.416	0.779	1.416	0.779	1.49	0.766	1.46	0.766	0.731	1.608	0.731	1.608	0.744	1.549	0.744	1.549
9	0.101	0.106	0.101	0.106	0.078	0.081	0.078	0.081	0.083	0.077	0.083	0.077	0.103	0.102	0.103	0.102
15	0.933	1.063	0.933	1.063	0.929	1.098	0.929	1.098	1.104	0.913	1.104	0.917	1.098	0.984	1.098	0.921
20	0.982	1.024	0.982	1.024	0.978	1.028	0.978	1.028	1.039	0.969	1.039	0.969	1.034	0.973	1.034	0.973
30	1.01	0.994	1.01	0.994	1.01	0.994	1.01	0.994	0.995	1.01	0.995	1.01	0.994	1.01	0.994	1.01
50	1.002	1.002	1.002	1.002	1.002	1.002	1.002	1.002	1.001	1.003	1.001	1.003	1.002	1.003	1.002	1.003
100	1.002	1.002	1.002	1.002	1.002	1.002	1.002	1.002	1.002	1.002	1.002	1.002	1.002	1.002	1.002	1.002

TABLE 5.2b: ω_R FOR ± 5% CHANGES IN ANY OF THE DISTRIBUTED PARAMETERS, $Q_p = 50$

$\omega_p R_T C_T$	ω_R															
	+ 5% Change in								-5% Change in							
	R_{1T1}	R_{2T1}	R_{1T2}	R_{2T2}	C_{1T1}	C_{2T1}	C_{1T2}	C_{2T2}	R_{1T1}	R_{2T1}	R_{1T2}	R_{2T2}	C_{1T1}	C_{2T1}	C_{1T2}	C_{2T2}
0.01	1.025	1.0	1.025	1.0	1.0	0.976	1.0	0.976	0.975	1.0	0.975	1.0	1.0	1.026	1.0	1.026
0.03	1.023	1.0	1.023	1.0	1.0	0.977	1.0	0.977	0.973	1.0	0.973	1.0	1.0	1.027	1.0	1.027
0.05	1.024	1.0	1.024	1.0	1.0	0.976	1.0	0.976	0.974	1.0	0.974	1.0	1.0	1.026	1.0	1.026
0.1	1.02	1.0	1.02	1.0	1.0	0.980	1.0	0.980	0.970	1.0	0.970	1.0	1.0	1.03	1.0	1.03
0.3	1.024	1.0	1.024	1.0	1.0	0.99	1.0	0.99	0.99	1.0	0.99	1.0	1.0	1.026	1.0	1.026
0.5	1.023	1.001	1.023	1.001	0.999	0.977	0.999	0.977	0.975	0.999	0.975	0.999	1.0	1.025	1.0	1.025
0.7	1.023	1.002	1.023	1.002	0.998	0.978	0.998	0.978	0.976	0.998	0.976	0.998	1.002	1.024	1.002	1.024
0.9	1.022	1.003	1.022	1.003	0.997	0.978	0.997	0.978	0.977	0.977	0.977	0.977	1.003	1.023	1.003	1.023
1	1.021	1.003	1.021	1.003	0.997	0.99	0.997	0.99	0.99	0.997	0.99	0.997	1.003	1.021	1.003	1.023
2	1.015	1.009	1.015	1.009	0.991	0.985	0.991	0.985	0.983	0.991	0.983	0.991	1.009	1.017	1.009	1.017
3	1.011	1.013	1.011	1.013	0.987	0.987	0.987	0.987	0.989	0.987	0.988	0.987	1.014	1.012	1.014	1.012
5	1.009	1.014	1.009	1.014	0.98	0.991	0.986	0.991	0.991	0.985	0.991	0.984	1.017	1.009	1.012	1.009
9	1.089	1.089	1.089	1.089	1.089	1.089	1.089	1.089	1.089	1.089	1.089	1.089	1.089	1.089	1.089	1.089
15	1.012	1.012	1.012	1.012	0.988	0.988	0.988	0.988	0.987	0.987	0.987	0.987	1.013	1.013	1.013	1.013
20	1.012	1.012	1.012	1.012	0.988	0.988	0.988	0.988	0.987	0.988	0.987	0.988	1.013	1.013	1.013	1.013
30	1.012	1.012	1.012	1.012	0.988	0.988	0.988	0.988	0.987	0.987	0.987	0.987	1.013	1.013	1.013	1.013
50	1.012	1.012	1.012	1.012	0.988	0.988	0.988	0.988	0.987	0.987	0.987	0.987	1.013	1.013	1.013	1.013
100	1.012	1.012	1.012	1.012	0.988	0.988	0.988	0.988	0.987	0.987	0.987	0.987	1.013	1.013	1.013	1.013

TABLE 5.3a: Q_R FOR ± 5% VARIATIONS IN ANY OF THE DISTRIBUTED PARAMETERS, $Q_p = 90$.

$\omega_p R_T C_T$	Q_R															
	+ 5% Change in								- 5% Change in							
	R_{1T1}	R_{2T1}	R_{1T2}	R_{2T2}	C_{1T1}	C_{2T1}	C_{1T1}	C_{2T1}	R_{1T1}	R_{2T1}	R_{1T2}	R_{2T2}	C_{1T1}	C_{2T1}	C_{1T2}	C_{2T2}
0.01	1.015	0.988	1.015	0.988	1.018	0.987	1.018	0.987	0.985	1.018	0.985	1.018	1.018	0.988	0.988	1.018
0.03	0.989	0.959	0.989	0.959	1.059	0.944	1.049	0.954	0.908	1.049	0.918	1.059	0.959	1.035	0.959	1.035
0.05	1.067	0.932	1.067	0.932	1.084	0.934	1.084	0.934	0.920	1.044	0.920	1.084	0.932	1.086	0.932	1.086
0.1	0.694	0.871	0.694	0.871	1.179	0.645	1.179	0.645	0.592	1.179	0.592	1.179	0.872	0.765	0.872	0.765
0.3	1.830	0.695	1.83	0.695	1.799	0.264	1.796	0.264	0.245	1.799	0.245	1.799	0.694	1.834	0.694	1.834
0.5	3.678	0.584	3.678	0.584	3.485	0.589	3.485	0.589	0.588	3.518	0.588	3.518	0.593	3.749	0.593	3.749
0.7	28.46	0.511	28.46	0.511	19.145	0.516	19.145	0.516	0.515	24.701	0.515	24.70	0.509	48.92	0.509	48.82
0.9	5.951	0.461	5.951	0.461	6.224	0.467	6.224	0.467	0.466	6.056	0.466	6.056	0.459	5.362	0.459	5.362
1	3.996	0.445	3.996	0.445	4.312	0.281	4.312	0.281	0.449	3.950	0.260	3.95	0.441	1.65	0.441	3.65
2	1.866	0.390	1.866	0.390	1.852	0.389	1.852	0.389	0.377	1.609	0.377	1.609	0.377	1.612	0.377	1.612
3	3.737	0.438	3.737	0.438	3.364	0.433	3.364	0.433	0.411	2.414	0.411	2.414	0.415	2.60	0.415	2.60
5	2.109	0.662	2.109	0.662	2.293	0.645	2.293	0.645	0.601	3.095	0.601	3.095	0.617	2.737	0.617	2.737
9	0.056	0.059	0.056	0.059	0.064	0.065	0.064	0.065	0.065	0.063	0.063	0.063	0.06	0.057	0.06	0.057
15	0.845	1.155	0.881	1.155	0.879	1.116	0.879	1.116	1.198	0.861	1.198	0.861	1.187	0.867	1.187	0.867
20	0.966	1.041	0.966	1.041	0.960	1.049	0.960	1.049	1.069	0.943	1.069	0.943	1.060	0.951	1.06	0.941
30	1.016	0.989	1.016	0.989	1.016	0.989	1.016	0.989	0.989	1.011	0.989	1.015	0.988	1.017	0.988	1.017
50	1.002	1.002	1.002	1.002	1.002	1.002	1.002	1.002	1.001	1.001	1.001	1.001	1.001	1.003	1.001	1.003
100	1.002	1.002	1.002	1.002	1.002	1.002	1.002	1.002	1.002	1.002	1.002	1.002	1.002	1.002	1.002	1.002

TABLE 5.3b: ω_R FOR ± 5% VARIATIONS IN ANY OF THE DISTRIBUTED PARAMETERS, $Q_p = 90$

$\omega_p R_T C_T$	ω_R															
	+ 5% Change in								- 5% Change in							
	R_{1T1}	R_{2T1}	R_{1T2}	R_{2T2}	C_{1T1}	C_{2T1}	C_{1T2}	C_{2T2}	R_{1T1}	R_{2T1}	R_{1T2}	R_{2T2}	C_{1T1}	C_{2T1}	C_{1T2}	C_{2T2}
0.01	1.025	1.0	1.025	1.0	1.0	0.976	1.0	0.976	0.975	1.0	0.975	1.0	1.0	1.026	1.0	1.026
0.03	1.023	1.0	1.023	1.0	1.0	0.977	1.0	0.976	0.973	1.0	0.973	1.0	1.0	1.027	1.0	1.027
0.05	1.024	1.0	1.024	1.0	1.0	0.976	1.0	0.976	0.974	1.0	0.974	1.0	1.0	1.026	1.0	1.026
0.1	1.02	1.0	1.02	1.0	1.0	0.980	1.0	0.976	0.970	1.0	0.970	1.0	1.0	1.03	1.0	1.03
0.3	1.024	1.0	1.024	1.0	1	0.990	1.0	0.99	0.99	1.0	0.99	1.0	1.0	1.026	1.0	1.026
0.5	1.023	1.001	1.023	1.001	0.999	0.992	0.999	0.977	0.975	0.999	0.975	0.999	1.001	1.025	1.001	1.025
0.7	1.023	1.002	1.023	1.002	0.998	0.978	0.998	0.978	0.976	0.998	0.976	0.998	1.002	1.024	1.002	1.024
0.9	1.022	1.003	1.022	1.003	0.997	0.978	0.997	0.978	0.977	0.997	0.997	0.997	1.003	1.023	1.003	1.023
1	1.021	1.003	1.021	1.003	0.997	0.99	0.997	0.99	0.99	0.997	0.99	0.997	1.003	1.023	1.003	1.023
2	1.015	1.009	1.015	1.009	0.991	0.985	0.991	0.985	0.98	0.991	0.98	0.991	1.009	1.017	1.009	1.017
3	1.011	1.013	1.011	1.013	0.987	0.989	0.987	0.987	0.988	0.987	0.988	0.987	1.014	1.012	1.014	1.012
5	1.009	1.016	1.009	1.016	0.985	0.991	0.985	0.991	0.991	0.983	0.991	0.983	1.017	1.009	1.017	1.009
9	1.089	1.089	1.089	1.089	1.089	1.089	1.089	1.089	1.089	1.089	1.089	1.089	1.089	1.089	1.089	1.089
15	1.012	1.012	1.012	1.012	0.988	0.988	0.988	0.988	0.987	0.987	0.987	0.987	1.013	1.013	1.013	1.013
20	1.013	1.012	1.013	1.012	0.988	0.988	0.988	0.988	0.987	0.988	0.987	0.988	1.013	1.013	1.013	1.013
30	1.012	1.012	1.012	1.012	0.988	0.988	0.988	0.988	0.987	0.987	0.987	0.987	1.013	1.013	1.013	1.013
50	1.012	1.012	1.012	1.012	0.988	0.988	0.988	0.988	0.987	0.987	0.987	0.987	1.013	1.013	1.013	1.013
100	1.012	1.012	1.012	1.012	0.988	0.988	0.988	0.988	0.987	0.987	0.987	0.987	1.013	1.013	1.013	1.013

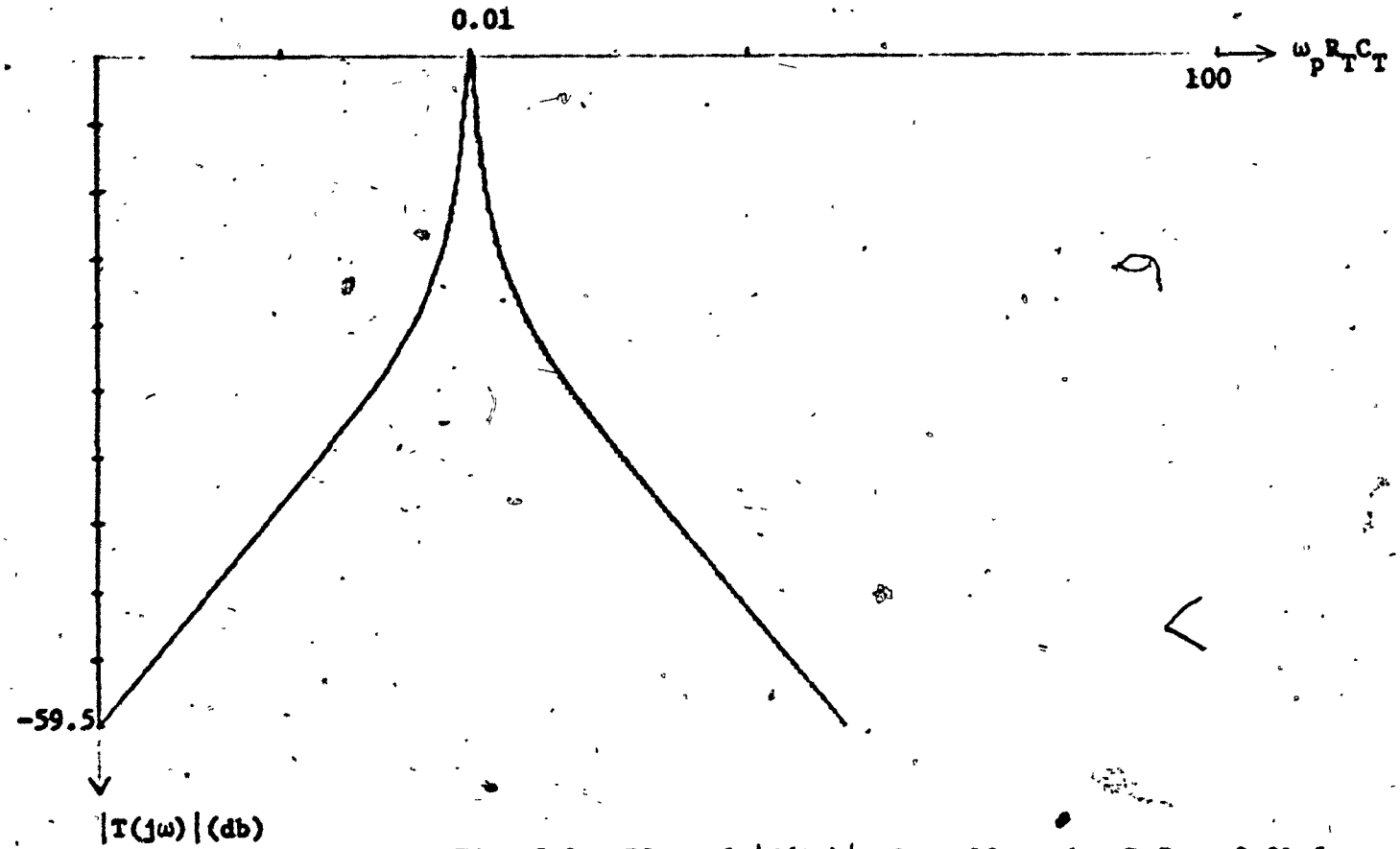

Fig. 5.3a: Plot of $|T(j\omega)|$, Q_p = 10, and [illegible] 0.01 for nominal values or + 5% variations in any of [illegible]ted parameters.

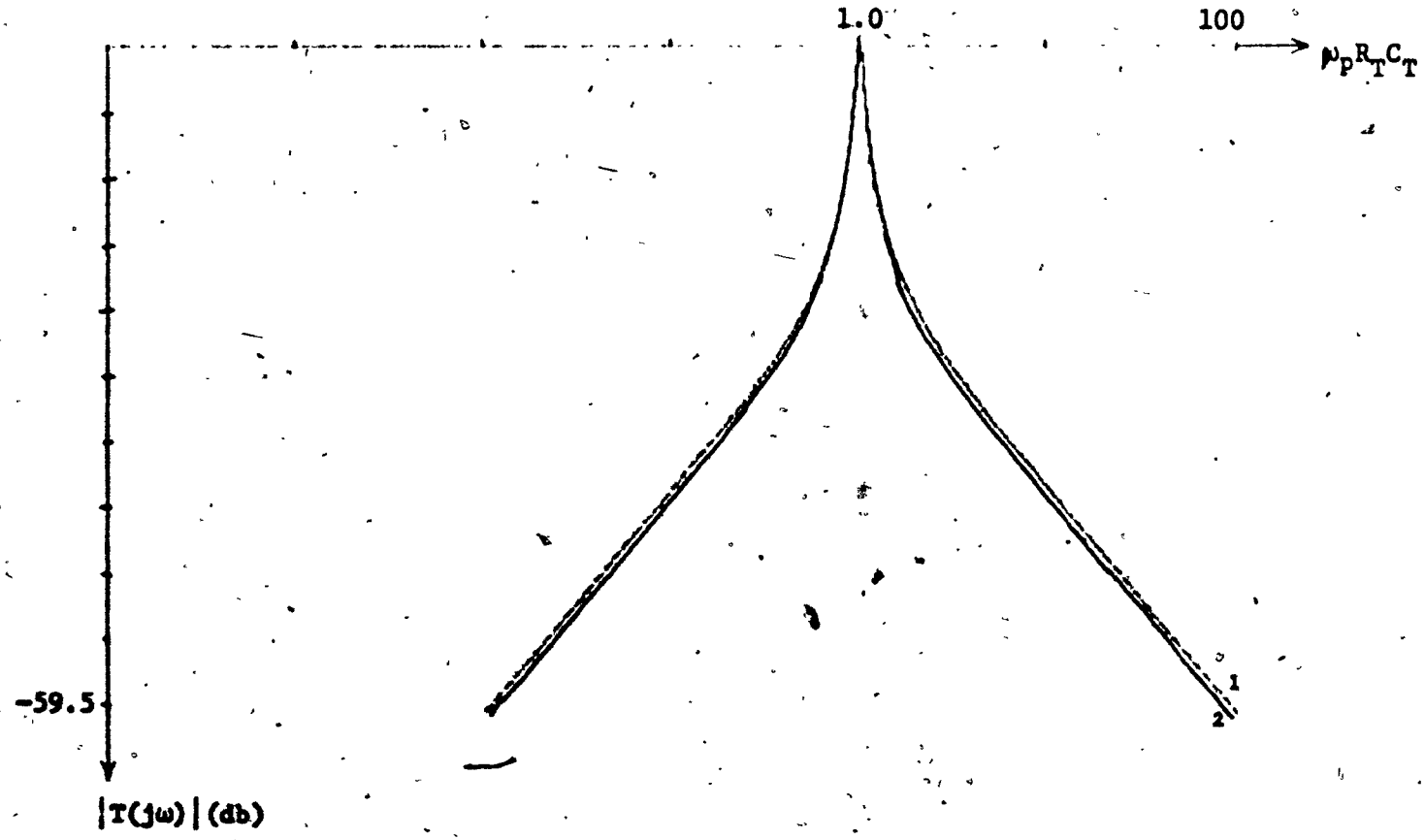

Fig. 5.3b: Plot of $|T(j\omega)|$, $Q_p = 10$, $\omega_p R_T C_T = 1.0$

Curve 1: Ideal Response or ± 5% Change in Any C_{iTj} or R_{iTi} or R_{2Ti}.

Curve 2: ± 5% Change in R_{iTi} or R_{2T2}

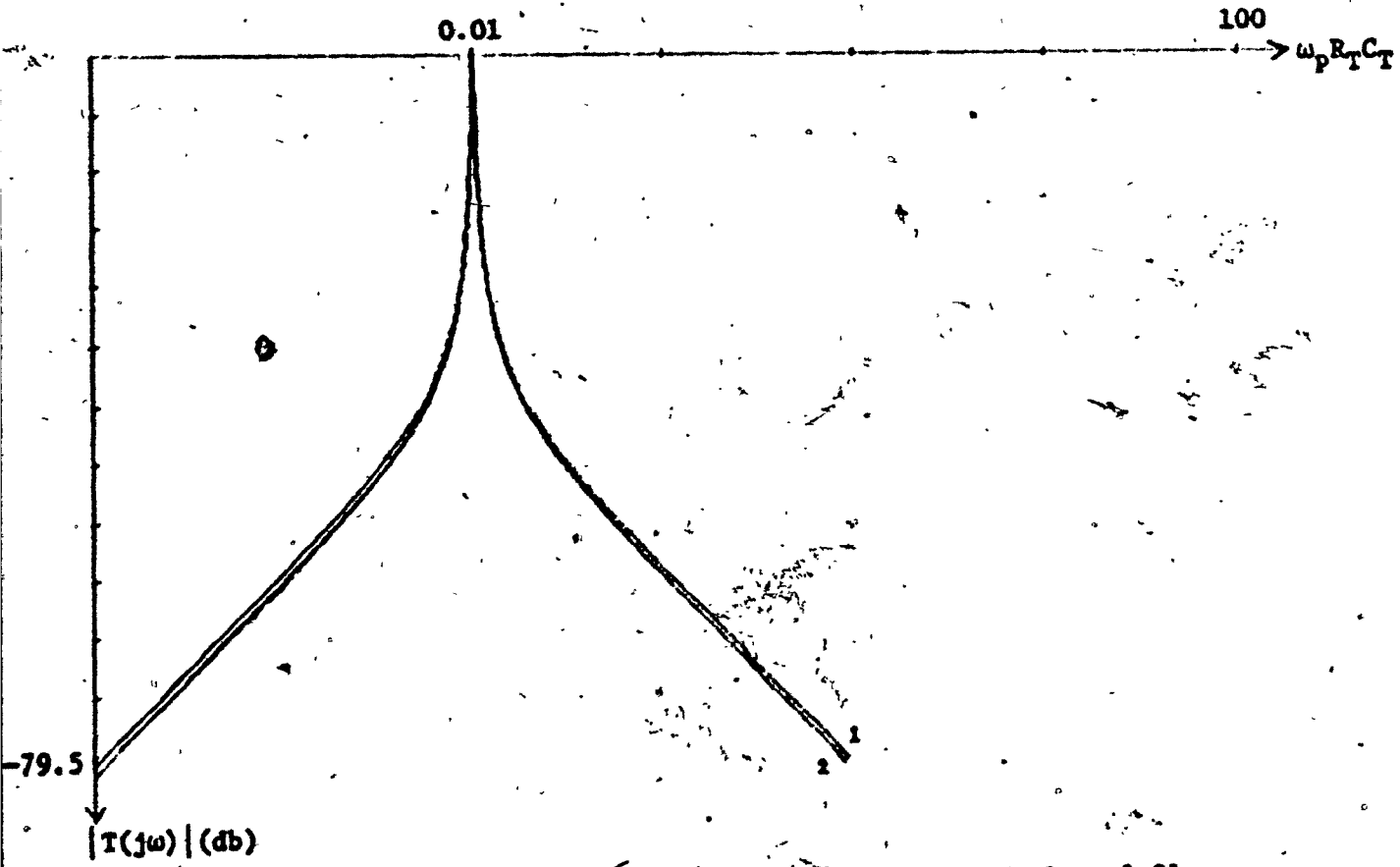

Fig. 5.4a: Plot of $|T(j\omega)|$, $Q_p = 50$, $\omega_p R_T C_T = 0.01$

Curve 1: Ideal Response or + 5% Change in any of the Parameters except R_{1T_2}

Curve 2: + 5% in R_{1T_2}

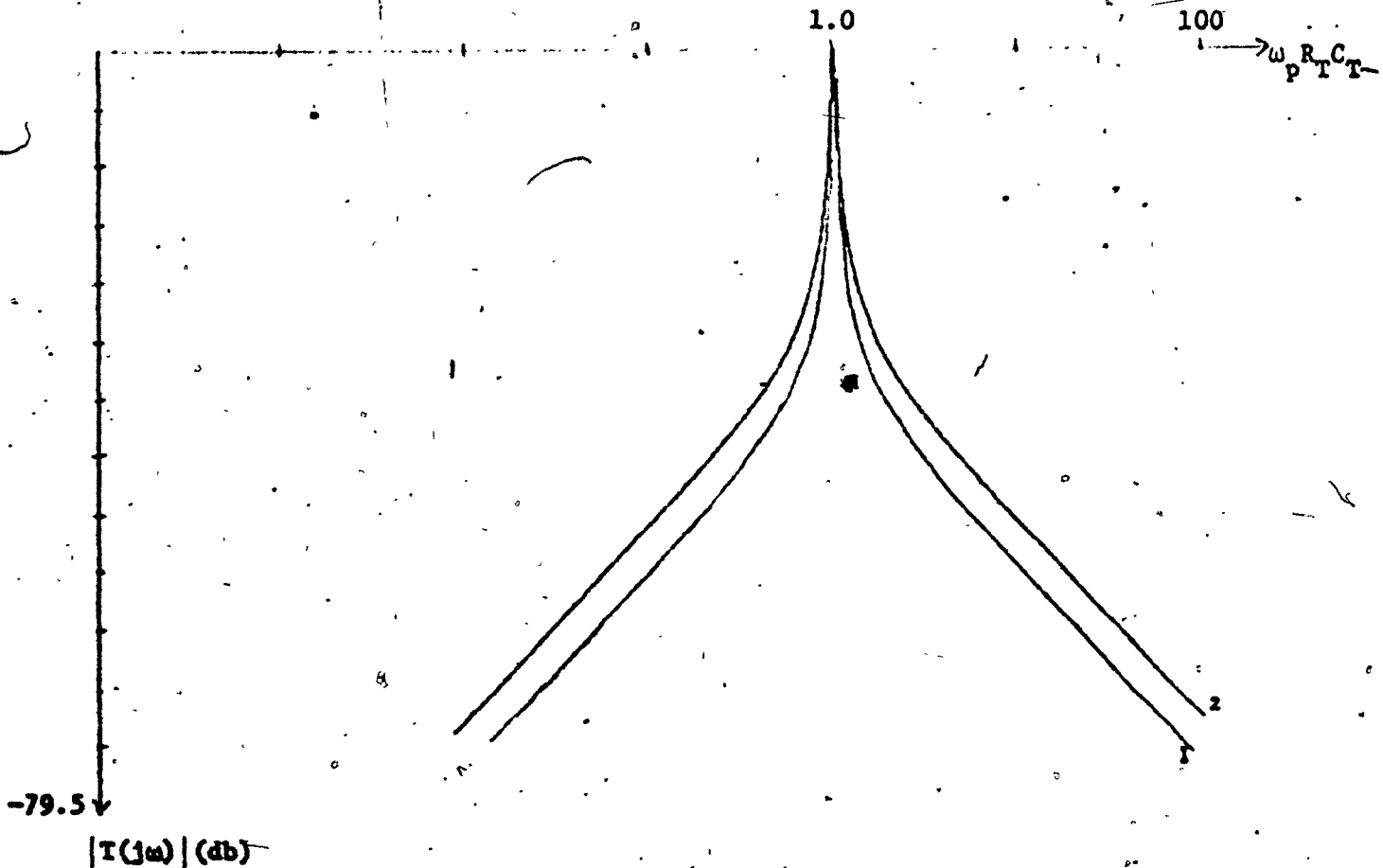

Fig. 54.b: Plot of $|T(j\omega)|$, $Q_p = 50$, $\omega_p R_T C_T = 1.0$

Curve 1: Ideal Response or + 5% Change in any C_{iTj}

Curve 2: + 5% Change in any of R_{iTj}'s.

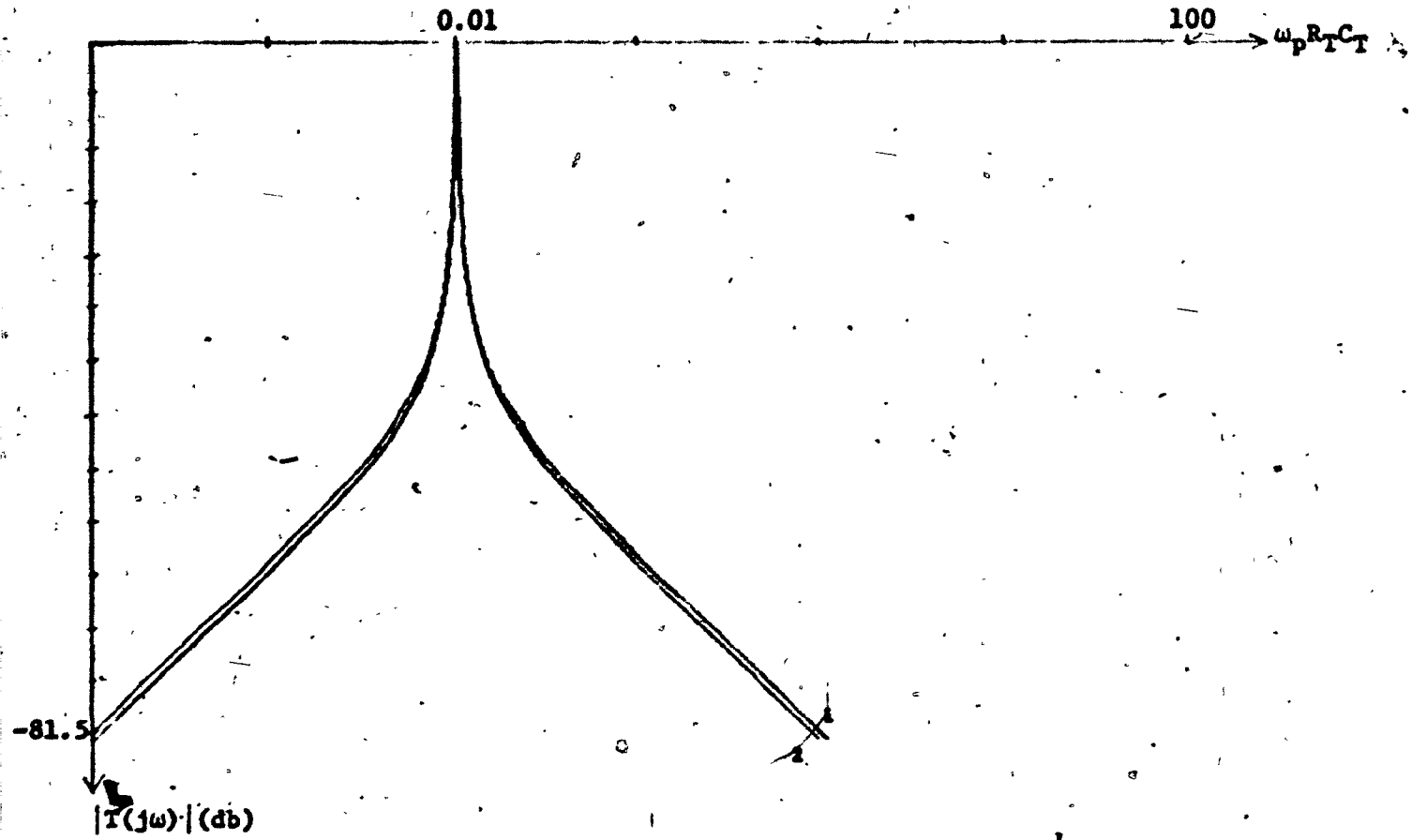

Fig. 5.5a: Plot of $|T(j\omega)|$, $Q_p = 90$, $\omega_p R_T C_T = 0.01$

Curve 1: Ideal Response or + 5% Change in any C_{1Tj} or R_{1T1} or R_{2T2}

Curve 2: + 5% Change in R_{1T2} or R_{2T2}

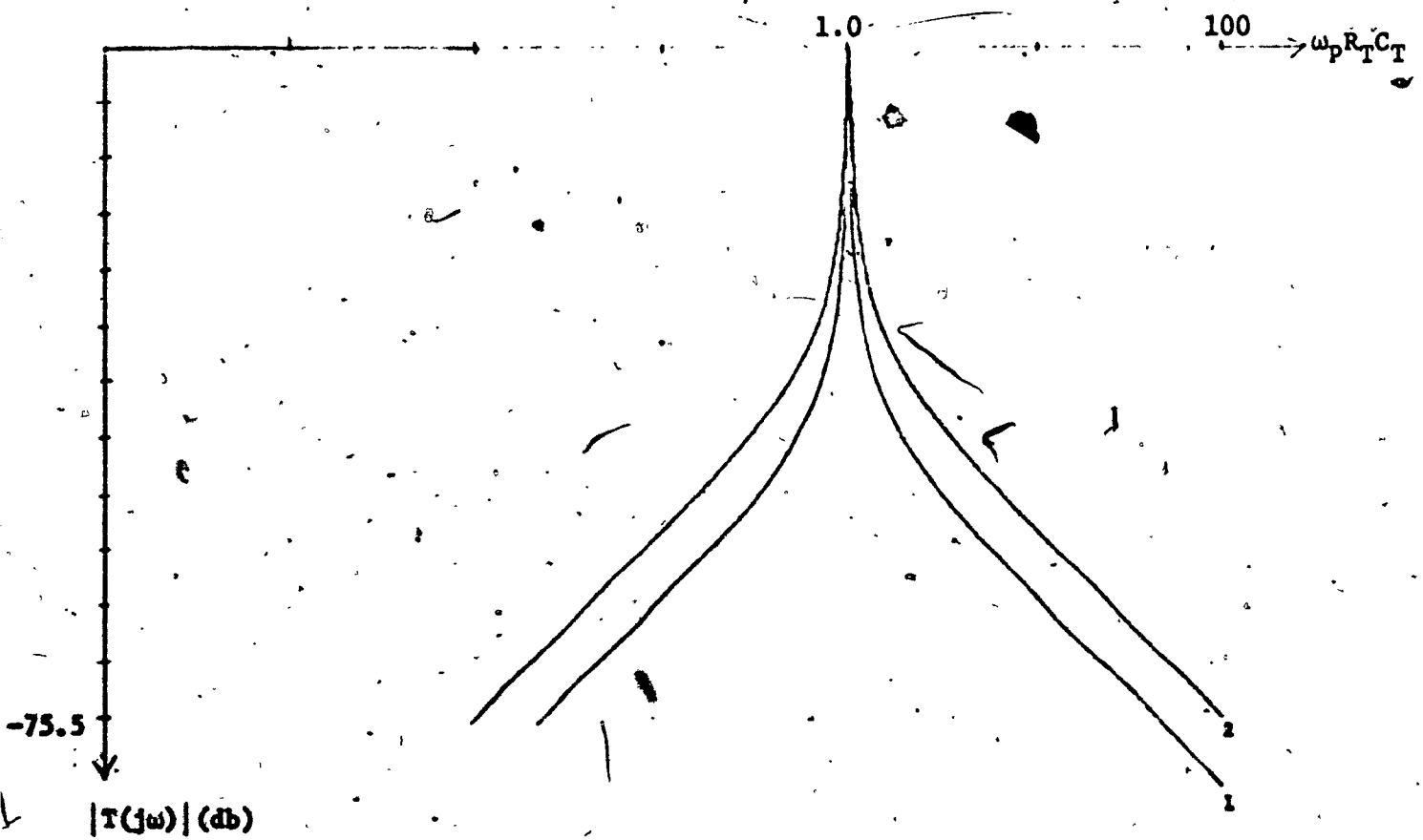

Fig. 5.5b: Plot of $|T(j\omega)|$, $Q_p = 90$, $\omega_p R_T C_T = 1.0$

Curve 1: Ideal Response or +5% Change in any C_{iTj}

Curve 2: + 5% Change in any R_{iTj}

Figures 5.4 and 5.5 show the same responses for Q_p = 50 and 90, respectively.

5.4 THE GYRATOR IMPERFECTIONS

The transformed frequency variable u(s) is rational in s if the URC's are commensurate and the gyrator is ideal. The effect of the non commensurate behaviour of the lines has been studied in sections 2.3.3 and 5.3. In this section, the influence of gyrator imperfections on u is examined. To this end, let us consider Antonious gyrator as shown in Figure 1.2.

Let the OA's in Figure 1.2 be identical and let them have an open gain μ, a gain bandwidth B, an input resistance R_I and output resistance R_o. Assuming $|\mu| >> 1$, $R_I >> r_g$, $r_g >> R_o$ and that the frequency of interest $\omega << B$, the y-parameters of the gyrator may be obtained as [9]:

$$y_{11}(\omega) \simeq G_a + G_c + \frac{j\omega}{Br_g}\left(2 + \frac{R_o}{r_g}\right) \tag{5.8a}$$

$$y_{12}(\omega) \simeq \frac{1}{r_g} + \frac{2\omega^2}{B^2 r_g^2}\left(1 - \frac{R_o}{r_g}\right) - \frac{j\omega R_o}{Br_g^2} \tag{5.8b}$$

$$y_{21}(\omega) \simeq -\frac{1}{r_g} - \frac{2\omega^2}{B^2 r_g^2}(r_g - R_o) + \frac{j\omega}{Br_g^2 R_I}(R_o R_I - r_g^2) \tag{5.8c}$$

$$y_{22}(\omega) \simeq \frac{2}{\mu r_g} + \frac{3R_o}{\mu r_g^2} + \frac{2\omega^2}{B^2 r_g^2}(r_g + 6R_o) + \frac{j\omega}{Br_g^2}(2r_g + 3R_o) \tag{5.8d}$$

where

$$R_1 = R_2 = R_3 = R_4 = r_g \tag{5.8e}$$

$$G_a = \frac{1}{\mu r_g}\left(2 + \frac{R_o}{r_g}\right), \quad G_c = \frac{2\omega^2}{B^2 r_g}\left(1 + \frac{4R_o}{r_g}\right) \tag{5.8f}$$

Therefore the OPI Z_2 of the network shown in Figure 2.7b becomes

$$\hat{Z}_2(j\omega) = \frac{y_{22} + q(j\omega)/R_{2T}}{y_{11}y_{22} + y_{11}q(j\omega)/R_{2T} - y_{12}y_{21}} \tag{5.9}$$

where $q(j\omega)$ is given by (2.29a) with $s = j\omega$.

For ideal gyrators and commensurate $\overline{\text{URC}}$'s we have from (2.30)

$$u(j\omega) = P(j\omega)/q(j\omega) = \frac{1}{j\omega RC} \tag{5.10}$$

where p and q are given in (2.29a) with $s = j\omega$. It may be noted from (2.28) that p represents the impedance Z_1 of the one port of Figure 2.7a normalized by the total resistance R_{1T} of the short circuited URC. Similarly, q represents the normalized OPI of Figure 2.7b, the normalizing constant being $\frac{K}{R_{2T}}$, where R_{2T} being the total resistance of the open circuited $\overline{\text{URC}}$ and K is the gyration constant. For the gyrator shown in Figure 1.2, it may be shown that [9]:

$$K = r_g^2 \tag{5.11}$$

where r_g is usually referred to as gyration resistance.

When the gyrators are non ideal p remains unchanged, but q becomes

$$\hat{q}(j\omega) = \frac{\hat{Z}_2(j\omega)}{(K/R_{2T})} = \hat{Z}_2(r_g^2/R_{2T}) \tag{5.12a}$$

where $\hat{Z}_2$ is given by (5.9). Hence, $u(j\omega)$ becomes

$$\hat{u}(j\omega) = \frac{p(j\omega)}{\hat{q}(j\omega)} \tag{5.12b}$$

It is seen from (5.9) and (5.12), that under ideal conditions, that is, for $\mu \to \infty$, $\beta \to \infty$, $R_I \to \infty$ and $R_o = 0$, $\hat{u}(j\omega)$ reduces to $u(j\omega)$.

The normalized magnitude and phase errors of $u(j\omega)$, given respectively, by

$$EM = \left| \frac{|\hat{u}(j\omega)| - |u(j\omega)|}{|u(j\omega)|} \right| , \quad EP = \left| \frac{/\hat{u}(j\omega) - /u(j\omega)}{/u(j\omega)} \right| \qquad (5.13a)$$

are of interest in a given frequency range.

An examination of the complete expressions for EM and EP shows that it is not possible to study EM and EP independently of any given design. This is because the total resistance R_{2T} of the open circuited $\overline{URC}$ appears in the expressions for $\hat{u}$ not only as the term $\omega_p R_{2T} C_{2T}$ but also as a separate parameter. It also turns out that a specific value for the gyrator resistance, r_g, has to be chosen in studying EM and EP. These, of course, mean that a specific design has to be considered. Further, it is obvious that the study will be for a particular OA.

Since the effect of non commensurate behaviour of $\overline{URC}$'s has been found to be negligible in the region $\omega_p R_T C_T \leq 0.01$ or $\omega_p R_T C_T \geq 30$, and since the former region has been found desirable for the present state of the art of active filters, the influence of gyrator imperfections is studied in the above region for two values of $\omega_p R_T C_T$, namely for $\omega_p R_T C_T = 0.001$ and 0.01. For any one of these values, a value for R_{2T} may be determined from (5.5b) once a set of values for R_{1T}, Q_p and $K = r_g^2$, is chosen.

Using a computer program (Appendix C.2) and typical data values for μA 741 OA's, EM and EP were computed for different Q_p's and ω_p's over a frequency range ω, where

$$\omega_p/10 \leq \omega \leq 10\,\omega_p \qquad (5.13b)$$

The normalized errors were also computed, assuming the μA 741 OA's to have infinite input resistance and zero output resistance but finite d.c. gains and bandwidth, respectively.

Finally, to study the relative influence of (R_{1T}/R_{2T}) and r_g, EM and EP were also calculated for $Q_p = 50$, $\omega_p = 150$ with R_{1T} varying in the range 200 to 5000 and r_g in the range 500 to 5000, subject to the design equation (5.5b).

The maximum values of EM and EP, in the frequency range $\frac{\omega_p}{10} \leq \omega \leq 10\,\omega_p$, for the above cases are listed in Tables 5.4 and 5.5.

The following can be concluded from an observation of the tables:

1) The effects of gyrator imperfections on u are negligible in the region $\omega_p R_T C_T \leq 0.01$. However, relatively speaking, the contributions to EM and EP by the input and output impedances of the OA's become important at only large values of (R_{1T}/R_{2T}). Also, the values for EM and EP increase (with or without OA impedances) for increasing Q_p and ω_p.

2) The values of EM and EP can be minimized by maximizing the value of (R_{1T}/R_{2T}) for a given r_g.

3) For different r_g's, a careful study of the tables will also show that for comparable values of (R_{1T}/R_{2T}), the design with the larger R_{1T} will have lowest values for EM and EP, while the one with the largest ratio for (R_{1T}/R_{2T}) will have minimum values for EM and EP.

The above study then suggests that, in order to reduce the influence of gyrator imperfections on any filter design, the filter be designed to have the main part of the response in the region $\omega_p R_T C_T \leq 0.01$. In addition, the gyration resistance r_g should be chosen suitably so as to have a large value for the ratio (R_{1T}/R_{2T}) as well as R_{1T}, compatible with thin film fabrication.

In order to verify these conclusions several BP sections were designed in the region $\omega_p R_T C_T \leq 0.01$ and their responses examined. In this study the OA's that determine the finite gains were assumed to be ideal. The results were in close agreement with the above conclusions.

5.5 THE EFFECT OF THE FINITE BANDWIDTH OF THE GAIN DETERMINING AMPLIFIERS

As mentioned in section 5.1, the network of Figure 4.2 is used to implement the URC synthesis procedure. The influence of amplifier bandwidths on the properties of realizations using the network of Figure 4.2 has been studied in section 4.5. The effect was shown to be an enhancement of the Q-factor, while the pole frequency was unaffected

TABLE 5.4a: EFFECT OF GYRATOR IMPERFECTIONS ON u, $\omega_p R_T C_T = 0.001$

Q_p	ω_p	$\omega_p R_T C_T = 0.001$, $R_{1T} = 1000\Omega$									
		$r_g = 100$				$r_g = 5000$					
		R_{1T}/R_{2T}	Effect of Bandwidth		Effect of Bandwidth, Input and Output Impedances		R_{1T}/R_{2T}	Effect of Bandwidth		Effect of Bandwidth, Input and Output Impedances	
			EM	EP	EM	EP		EM	EP	EM	EP
5	50	100	0.16×10^{-3}	0.62×10^{-4}	0.18×10^{-3}	0.679×10^{-4}	4	0.8×10^{-3}	0.3×10^{-3}	0.81×10^{-3}	0.312×10^{-3}
	150		0.48×10^{-3}	0.63×10^{-4}	0.54×10^{-3}	0.68×10^{-4}		0.238×10^{-2}	0.31×10^{-3}	0.24×10^{-2}	0.32×10^{-3}
	600		0.19×10^{-2}	0.64×10^{-4}	0.21×10^{-2}	0.62×10^{-4}		0.95×10^{-2}	0.31×10^{-3}	0.97×10^{-7}	0.32×10^{-3}
10	50	50	0.32×10^{-3}	0.12×10^{-3}	0.35×10^{-3}	0.14×10^{-3}	2	0.16×10^{-2}	0.61×10^{-3}	0.16×10^{-2}	0.62×10^{-3}
	150		0.96×10^{-3}	0.13×10^{-3}	0.1×10^{-2}	0.14×10^{-3}		0.48×10^{-2}	0.62×10^{-3}	0.49×10^{-2}	0.64×10^{-3}
	600		0.38×10^{-2}	0.13×10^{-3}	0.42×10^{-2}	0.13×10^{-3}		0.187×10^{-1}	0.62×10^{-3}	0.19×10^{-1}	0.63×10^{-3}
25	50	20	0.78×10^{-3}	0.31×10^{-3}	0.88×10^{-3}	0.34×10^{-3}	0.8	0.396×10^{-2}	0.152×10^{-2}	0.405×10^{-2}	0.156×10^{-2}
	150		0.24×10^{-2}	0.31×10^{-3}	0.27×10^{-2}	0.35×10^{-3}		0.118×10^{-1}	0.152×10^{-2}	0.121×10^{-1}	0.158×10^{-2}
	600		0.95×10^{-2}	0.31×10^{-2}	0.11×10^{-1}	0.34×10^{-3}		0.46×10^{-1}	0.151×10^{-2}	0.47×10^{-1}	0.154×10^{-2}
50	50	10	0.16×10^{-2}	0.61×10^{-3}	0.18×10^{-2}	0.678×10^{-3}	0.4	0.79×10^{-2}	0.3×10^{-2}	0.81×10^{-2}	0.31×10^{-2}
	150		0.48×10^{-2}	0.62×10^{-3}	0.53×10^{-2}	0.69×10^{-3}		0.23×10^{-1}	0.306×10^{-2}	0.20×10^{-1}	0.31×10^{-2}
	600		0.19×10^{-1}	0.61×10^{-3}	0.21×10^{-1}	0.68×10^{-3}		0.87×10^{-1}	0.28×10^{-2}	0.89×10^{-1}	0.29×10^{-2}

TABLE 5.4b: EFFECT OF GYRATOR IMPERFECTIONS ON $\omega_p R_T C_T = 0.01$

Q_p	ω_p	$\omega_p R_T C_T = 0.01$, $R_{1T} = 1000\Omega$								
		$r_R = 1000$				$r_R = 5000$				
		R_{1T}/R_{2T}	Effect of Bandwidth		Effect of Bandwidth, Input and Output Impedances		R_{1T}/R_{2T}	Effect of Bandwidth		Effect of Bandwidth, Input and Output Impedances	
			EM	EP	EM	EP		EM	EP	EM	EP
5	50	10	0.16×10^{-3}	0.62×10^{-4}	0.18×10^{-3}	0.68×10^{-4}	0.4	0.80×10^{-3}	0.3×10^{-3}	0.81×10^{-3}	0.31×10^{-3}
	150		0.48×10^{-3}	0.62×10^{-4}	0.54×10^{-3}	0.67×10^{-4}		0.24×10^{-2}	0.31×10^{-3}	0.24×10^{-2}	0.32×10^{-3}
	600		0.19×10^{-2}	0.6×10^{-4}	0.21×10^{-2}	0.58×10^{-4}		0.95×10^{-2}	0.29×10^{-3}	0.97×10^{-2}	0.3×10^{-3}
10	50	5	0.32×10^{-3}	0.12×10^{-3}	0.36×10^{-3}	0.14×10^{-3}	0.2	0.16×10^{-2}	0.61×10^{-3}	0.16×10^{-2}	0.62×10^{-3}
	150		0.95×10^{-3}	0.37×10^{-3}	0.1×10^{-2}	0.14×10^{-3}		0.48×10^{-2}	0.62×10^{-3}	0.49×10^{-2}	0.63×10^{-3}
	600		0.38×10^{-3}	0.12×10^{-3}	0.42×10^{-2}	0.12×10^{-3}		0.19×10^{-1}	0.58×10^{-3}	0.19×10^{-1}	0.60×10^{-3}
25	50	2	0.8×10^{-3}	0.3×10^{-3}	0.89×10^{-3}	0.34×10^{-3}	$\frac{1}{2}$	0.4×10^{-2}	0.15×10^{-2}	0.41×10^{-2}	0.16×10^{-2}
	150		0.24×10^{-2}	0.31×10^{-3}	0.27×10^{-2}	0.34×10^{-3}	0.08	0.12×10^{-1}	0.15×10^{-2}	0.12×10^{-1}	0.16×10^{-2}
	600		0.95×10^{-2}	0.29×10^{-3}	0.11×10^{-1}	0.32×10^{-3}		0.46×10^{-1}	0.14×10^{-2}	0.47×10^{-1}	0.15×10^{-2}
50	50	1	0.16×10^{-2}	0.61×10^{-3}	0.18×10^{-2}	0.66×10^{-3}	0.04	0.79×10^{-2}	0.3×10^{-2}	0.81×10^{-2}	0.31×10^{-2}
	150		0.48×10^{-2}	0.61×10^{-3}	0.53×10^{-2}	0.68×10^{-3}		0.23×10^{-1}	0.3×10^{-1}	0.24×10^{-1}	0.31×10^{-1}
	600		0.19×10^{-1}	0.58×10^{-3}	0.21×10^{-1}	0.64×10^{-3}		0.87×10^{-1}	0.27×10^{-2}	0.89×10^{-1}	0.28×10^{-2}

TABLE 5.5a: EFFECT OF DIFFERENT (R_{1T}/R_{2T}) ON EM AND EP FOR DIFFERENT r_g's, $\omega_p R_T C_T = 0.001$

R_{1T}	$\omega_p R_1 C_T = 0.001$, $Q_p = 50$, $\omega_p = 150$								
	$r_g = 500\Omega$			$r_g = 1000\Omega$			$r_g = 5000\Omega$		
	R_{1T}/R_{2T}	EM	EP	R_{1T}/R_{2T}	EM	EP	R_{1T}/R_{2T}	EM	EP
200	1.6	0.14×10^{-1}	0.19×10^{-2}	0.4	0.26×10^{-1}	0.34×10^{-2}	0.016	0.11	0.14×10^{-1}
600	14.4	0.485×10^{-2}	0.63×10^{-3}	3.6	0.89×10^{-2}	0.12×10^{-2}	0.144	0.39×10^{-1}	0.51×10^{-2}
1000	40	0.29×10^{-2}	0.38×10^{-3}	10	0.53×10^{-2}	0.69×10^{-3}	0.4	0.23×10^{-1}	0.31×10^{-2}
1400	78.4	0.21×10^{-2}	0.27×10^{-3}	19.6	0.38×10^{-2}	0.49×10^{-3}	0.78	0.17×10^{-1}	0.23×10^{-2}
1800	129.6	0.162×10^{-2}	0.21×10^{-3}	32.4	0.29×10^{-2}	0.38×10^{-3}	1.3	0.13×10^{-1}	0.18×10^{-2}
2000	160	0.15×10^{-2}	0.19×10^{-3}	40	0.26×10^{-2}	0.35×10^{-3}	1.6	0.12×10^{-1}	0.15×10^{-2}
3000	360	0.98×10^{-3}	0.12×10^{-3}	90	0.18×10^{-2}	0.23×10^{-3}	3.6	0.81×10^{-2}	0.11×10^{-2}
4000	640	0.73×10^{-3}	0.92×10^{-4}	160	0.13×10^{-2}	0.17×10^{-3}	6.4	0.61×10^{-2}	0.8×10^{-3}
5000	1000	0.59×10^{-3}	0.73×10^{-4}	250	0.11×10^{-2}	0.14×10^{-3}	10	0.49×10^{-2}	0.64×10^{-3}

TABLE 5.5b: EFFECT OF DIFFERENT (R_{1T}/R_{2T}) ON EM AND EP FOR DIFFERENT r_g's, $\omega_p R_T C_T = 0.01$

R_{1T}	$\omega_p R_T C_T = 0.01$, $Q_p = 50$, $\omega_p = 150$								
	$r_g = 500\Omega$			$r_g = 1000\Omega$			$r_g = 5000\Omega$		
	R_{1T}/R_{2T}	EM	EP	R_{1T}/R_{2T}	EM	EP	R_{1T}/R_{2T}	EM	EP
200	0.16	0.14×10^{-1}	0.19×10^{-2}	0.04	0.26×10^{-1}	0.34×10^{-2}	0.0016	0.11	0.14×10^{-1}
600	1.44	0.49×10^{-2}	0.62×10^{-3}	0.36	0.88×10^{-2}	0.11×10^{-2}	0.0144	0.39×10^{-1}	0.51×10^{-2}
1000	4	0.29×10^{-2}	0.37×10^{-3}	0.10	0.53×10^{-2}	0.68×10^{-3}	0.04	0.24×10^{-1}	0.31×10^{-2}
1400	7.84	0.21×10^{-2}	0.27×10^{-3}	1.96	0.38×10^{-2}	0.49×10^{-3}	0.078	0.17×10^{-1}	0.22×10^{-2}
1800	12.96	0.16×10^{-2}	0.21×10^{-3}	3.24	0.29×10^{-2}	0.38×10^{-3}	0.13	0.13×10^{-1}	0.17×10^{-2}
2000	16.0	0.15×10^{-2}	0.19×10^{-3}	4.0	0.27×10^{-2}	0.34×10^{-3}	0.16	0.12×10^{-1}	0.16×10^{-2}
3000	36.0	0.98×10^{-3}	0.12×10^{-3}	9.0	0.18×10^{-2}	0.23×10^{-3}	0.36	0.81×10^{-1}	0.1×10^{-2}
4000	64.0	0.73×10^{-3}	0.91×10^{-4}	16.0	0.13×10^{-2}	0.17×10^{-3}	0.64	0.61×10^{-1}	0.78×10^{-3}
5000	100	0.59×10^{-3}	0.72×10^{-4}	25.0	0.11×10^{-2}	0.14×10^{-3}	0.10	0.45×10^{-1}	0.63×10^{-3}

up to first order effects. However, in implementing the distributed synthesis procedure, we have first to move from the s-plane to the u-plane. A lumped realization is then obtained in the u-plane. The synthesis is completed by replacing appropriately the lumped element in the u-plane by distributed elements. The purpose of this section is to show that, in the resulting realizations, finite bandwidth of the gain determining OA's introduces a *de-enhancement* of the Q-factor and pole frequency, respectively. However, the effect on the pole frequency can, in practice, be ignored. For this purpose, the URC's are assumed commensurate, the gyrators ideal and that the frequency response of the OA's realizing the finite gains is given by (1.1).

The appropriate network to consider is now the one shown in Figure 5.2. The characteristic polynomial, or the denominator polynomial, D(s) is given by (5.6) with $u_1 = u_2 = \frac{1}{sR_TC_T}$. Under the one pole model of the OA's, the resulting polynomial is of fifth order and may be written in the form

$$\hat{D}(s) = b_5s^5 + b_4s^4 + b_3s^3 + b_2s^2 + b_1s + b_0 \qquad (5.14)$$

where

$$b_5 = \frac{1}{4Q_p^2\omega_p^2B^3}, \quad b_4 = \frac{4Q_p}{\omega_pB^3} + \frac{\beta_1\beta_2 + \beta_1\delta + \delta\beta_2}{4Q_p^2\omega_p^2B^2} \qquad (5.15a)$$

$$b_3 = \frac{(\beta_1 + \beta_2 + \delta)}{4Q_p^2\omega_p^2B} + \frac{(\beta_1\beta_2 + \beta_1\delta + \delta\beta_2)}{Q_p\omega_p^2B^2} + \frac{\beta_1\beta_2\delta}{B^3} \qquad (5.15b)$$

$$b_2 = \frac{1}{\omega_p^2} + \frac{\beta_1 + \beta_2 + \delta}{Q_p\omega_pB} + \frac{\beta_1\beta_2 + \beta_2\delta + \delta\beta_1}{B^3} \qquad (5.15c)$$

$$b_1 = \frac{\beta_1 + \beta_2 + \delta}{B} + \frac{1}{\omega_p Q_p} \tag{5.15d}$$

$$b_0 = 1 \tag{5.15e}$$

where

$$\delta = |\delta_2| \tag{5.15f}$$

using (5.15) and following the same procedure as given in Appendix A it may be shown that, for $Q_p >> 1$

$$\frac{1}{\hat{\omega}_{pd}} = \frac{1}{\omega_p^2} + \frac{\beta_1 + \beta_2 + \delta}{\omega_p Q_p B} \tag{5.16a}$$

and

$$\frac{1}{\hat{Q}_{pd}} = \frac{1}{Q_p} + \frac{(\beta_1 + \beta_2 + \delta)\omega p}{B} \tag{5.16b}$$

where $\hat{Q}_{pd}$ and $\hat{\omega}_{pd}$ are the Q-factor and pole frequency, respectively, actually realized by the distributed network.

It is thus seen from (5.15) and (5.16) that the design given by (4.39) may be used again to simultaneously minimize the effect of B on $\hat{Q}_{pd}$ and $\hat{\omega}_{pd}$, respectively. Using now (4.39), equations (5.15) and (5.16) reduce to

$$\frac{1}{\hat{\omega}_{pd}^2} = \frac{1}{\omega_p^2}\left[1 + \frac{6\omega_p}{(2Q_p)^{1/3}B}\right] \tag{5.17}$$

$$\frac{1}{\hat{Q}_{pd}} = \frac{1}{Q_p} + \frac{3(2Q)^{2/3}\omega_p}{B} \tag{5.18}$$

As seen from (5.17) and (5.18), the effect of the finite bandwidth on $\hat{Q}_{pd}$ and $\hat{\omega}_{pd}$ is a de-enhancement. However, the de-enhancement of $\hat{\omega}_{pd}$ is negligible, provided $(2Q_p)^{1/3}B >> 6\omega_p$ which is normally

satisfied in practice.

The transfer function given by equation (5.6) was simulated on the computer (Appendix C.3). In the simulation, the gyrator imperfections and the one pole model of the OA's determining the finite gains were considered.

Band pass filters having Q_p of 10 and 50 were studied in the region $\omega_p RC \leq 0.01$, using the design presented in section 5.2 for various values of $R_{1T1} = R_{1T2} = R_{1T}$, $R_{2T1} = R_{2T2} = R_{2T}$ and $r_{g_1} = r_{g_2} = r_g$. The study confirmed the denhancement suffered by both the Q-factor and the pole frequency ω_p. It also revealed the fact that this effect, particularly on $\hat{\omega}_{pd}$ is least when (R_{1T}/R_{2T}) is maximized. This may have to be limited due to considerations of a given design as well as those due to thin film technology. However, using typical data values for LM318 OA's (internally compensated, B = 15 MHZ), it was found that Q_p's up to 50 could be realized with less than 5% de-enhancement at ω_p = 1.2 K rad, the de-enhancement in ω_p being neligible (< 0.02%). The de-enhancement was also found to decrease with lower Q_p's.

5.6 THE DESIGN OF A BUTTERWORTH LOW PASS FILTER

Simple low pass filters having cut off frequencies in the range $0.1 < f < 100$ are frequently encountered in biomedical engineering applications [48]. It is difficult to fabricate these filters in hybrid IC form using the present RC active filter techniques [14-21], [31-43]. The purpose of this section is to demonstrate the feasibility of the proposed $\overline{\text{URC}}$ realization technique, by designing a second order

LP Butterworth filter with a cut off frequency of $\omega_p = 10$ and showing that the resulting network can be easily fabricated by hybrid IC technology. The effect of gyrator and gain determining OA's imperfections on the realized response is also studied and shown to be negligible.

5.6.1 The Design

The LP Butterworth transfer function with unity d.c. gain and cut off frequency ω_p in

$$T(s) = \frac{\omega_p^2}{s^2 + \sqrt{2}\omega_p s + \omega_p^2} \tag{5.19}$$

The distributed realization is obtained as follows:

Step 1

Use (2.31) to obtain from 5.19

$$G(u) = \frac{u^2}{u^2 + \frac{\sqrt{2}\,u}{R_T C_T \omega_p} + \frac{1}{(\omega_p R_T C_T)^2}} \tag{5.20}$$

Step 2

Equation (5.20) is realized in the u-plane using the network of Figure 4.2. The use of this network, along with the design of section 4.3, leads to:

$$\beta_1 = \beta_2 = -\delta_2 = 1, \quad \gamma_0 = 1 \tag{5.21a}$$

$$\gamma_1 \delta_0 = -2, \quad \gamma_2 = 0 \tag{5.21b}$$

and

$$R_u C_u = \sqrt{2}\,(\omega_p R_T C_T) \tag{5.22}$$

The realization is shown in Figure 5.6.

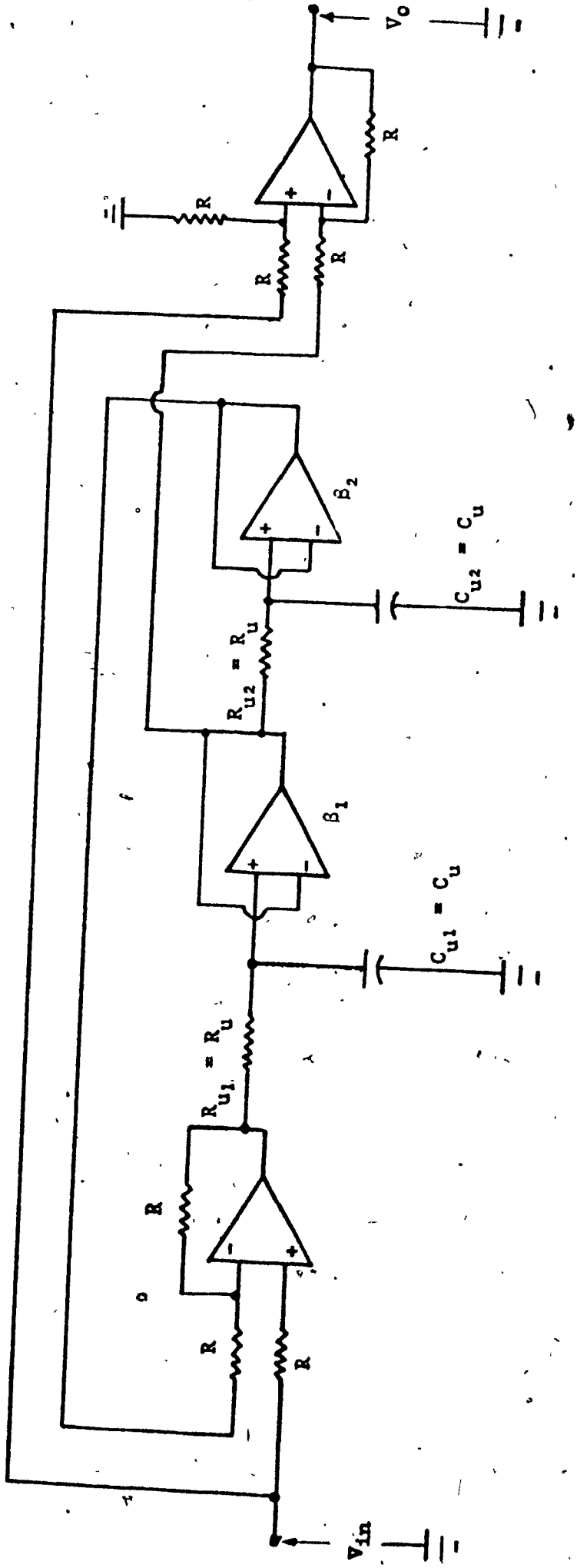

Fig. 5.6: Realization of $\dfrac{u^2}{u^2 + \dfrac{\sqrt{2}\,u}{\omega_p R_T C_T} + \left(\dfrac{1}{\omega_p R_T C_T}\right)^2}$

Step 3

Replace in Figure 5.6 each lumped resistor R_{ui} by the one port of Figure 2.7a and each lumped capacitor C_{ui} by the one port of Figure 2.7b. The distributed realization is shown in Figure 5.7 where

$$R_{1Ti}R_{2Ti} = \sqrt{2}\ (\omega_p RC)\ r_{gi}^2 \quad (i = 1,2) \tag{5.23}$$

It should be noted that $R_{1T1} = R_{1T2}$, $R_{2T1} = R_{2T2}$ and $r_{g_1} = r_{g_2}$ as mentioned in section 5.2.

The values of R_{1Ti}, R_{2Ti} and r_{gi} are now chosen with the following considerations in mind.

1) The non commensurate behaviour of the $\overline{\text{URC's}}$ should not adversely affect the response.
2) The gyrator imperfections and OA poles should have negligible influence on the response.
3) The values of the URC parameters and the gyration resistance r_g should be compatible with thin film technology.

As discussed earlier in this chapter, the first consideration can be satisfied by selecting $\omega_p R_T C_T$ in the region $\omega_p R_T C_T \leq 0.01$. The second one can be met by chosing a suitable value to give large values for R_{1Ti} and (R_{1Ti}/R_{2Ti}), respectively. For the third, the constraints on the ranges of element values in thin film fabrication have to be satisfied.

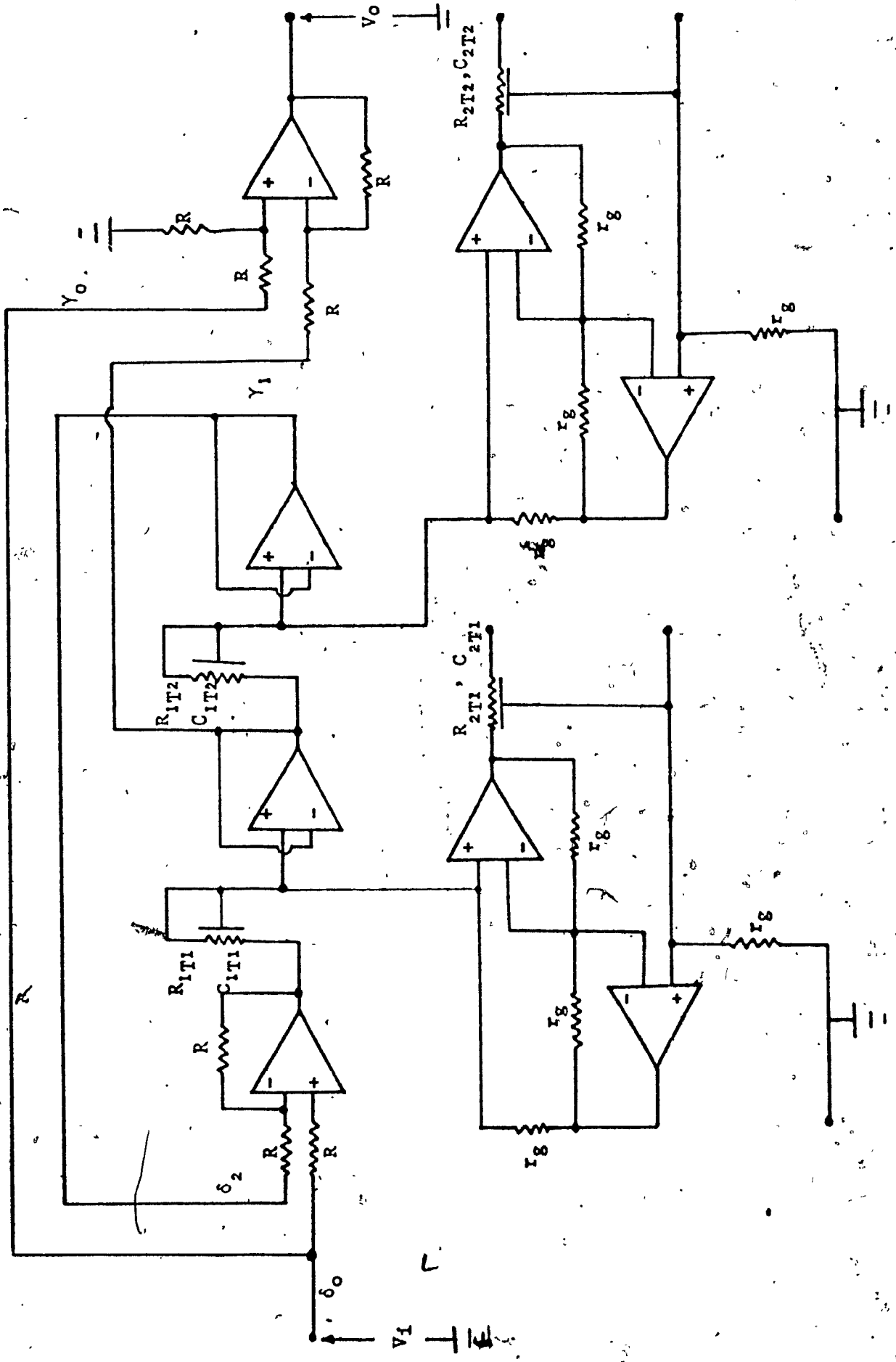

Fig. 5.7: Distributed LP Butterworth Filter

For this purpose the following design values are chosen.

$$\omega_p R_T C_T = 10^{-6} \ , \ r_{g1} = r_{g2} = 30 \ K\Omega \qquad (5.24a)$$

$$R_{1T1} = R_{1T2} = 100\Omega \ , \ R_{2T1} = R_{2T2} = 12.3\Omega \qquad (5.24b)$$

Hence, for $\omega_p = 10$

$$C_{1T1} = C_{1T2} = 10^{-9}f, \ C_{2T1} = C_{2T2} = 8.13 \times 10^{-9}f \qquad (5.24c)$$

It is obvious from the discussion in section (1.5) that the $\overline{\text{URC}}$ parameters are within thin film range. In fact, the values of the total capacitance and the total resistance of all the four $\overline{\text{URC}}$'s taken together are within the capacity of a single thin film chip [27]. The gyration resistance, and hence the resistances of the gyrators, are within thin film element range. The gain determining resistors can easily be chosen to be within the same range. Thus, the entire filter can be fabricated by hybrid IC technology.

Using a computer program (Appendix C.4), the above design and typical data values for μA 741 OA's, the effects of the gyrator imperfections as well as the finite bandwidth of the OA's determining the various finite gains, on the magnitude and phase responses of the designed filter were studied, respectively. The study revealed maximum errors of 0.067 db and 0.16% in the magnitude and phase responses, respectively.

5.7 CONCLUSIONS

The configuration of Figure 4.2 along with the optimum design procedure of section 4.3 has been utilized to demonstrate, by designing second order band pass responses, the $\overline{\text{URC}}$ synthesis procedure presented

in Chapter 2. It is shown that the effect of the lines not being exactly commensurate is negligible on the filter response provided that the RC product of the $\overline{URC}$'s is chosen to lie in the region $\omega_p RC \leq 0.01$ or in the region $\omega_p RC \geq 30$. This establishes the validity of the results derived for $u(j\omega)$ in Chapter 2. The effect of gyrator imperfection on the transformation u is studied and shown to be negligible, if r_g, the gyration resistance, is suitably chosen such that the values of both (R_{1T}/R_{2T}) and R_{1T} are large. The effect of the finite bandwidth of the OA's that realize the finite gains on Q_p and ω_p is examined and it is found that the effect on ω_p is negligible while that on Q_p is a de-enhancement. This Q_p de-enhancement guarantees that the filter will remain stable, which is in contrast with other distributed realizations [34 - 37]. These realizations suffer from Q_p-enhancement that may lead to instability. Finally, a design is presented of a second order LP Butterworth section with a cut off frequency ω_p of 10. The design values of all the components are shown to be such that the entire filter is hybrid integrable. One possible way of fabricating this filter is to have all the OA's on a silicon monolithic chip and to have all the resistors and $\overline{URC}$'s on a thin film chip. It may be desirable, however, to put the resistors and $\overline{URC}$'s on separate thin film chips. The chips then may be secured by gold bonds. The effect of the imperfections of the gyrators as well as those of the OA's that realize the finite gains, on the magnitude and phase responses of the filter is also studied and shown to be

negligible. The success of this design demonstrates that the URC synthesis procedure proposed in this thesis is a feasible technique in practice from the point of view of hybrid IC technology. In fact, it may be difficult to fabricate in hybrid IC technology the above filter, if it is designed using the conventional lumped RC active filter techniques.

CHAPTER VI

SUMMARY AND SUGGESTIONS FOR FURTHER WORK

A synthesis procedure has been developed, for realizing any open circuit rational voltage transfer function, using as basic building blocks, any tapered RC line, its dual, an ideal gyrator and, in general, finite gain amplifiers. The special case of low sensitivity $\overline{\text{URC}}$ realizations, attractive from the point of hybrid IC technology, is then studied in detail.

For this purpose, a new transformation u(s) of the complex frequency variable s is first developed. The transformed variable u(s) has then been employed to derive a technique that can realize any rational transfer functions in s, using any tapered RC line, its dual, an ideal gyrator, and in general, active elements with real gain parameters. As the success of the synthesis procedure depends on the duality of the tapered lines, which ensures the fact that u(s) is rational in s, the effect of the non-duality between the lines on the transformation is also examined. It is shown that the effect of the lines not being duals of each other, on $u(j\omega)$, is negligible in two frequency regions, between which $u(j\omega)$ does not remain rational. It is further found that not much is gained by using tapered lines instead of commensurate $\overline{\text{URC}}$'s in the realization and hence, in subsequent studies only $\overline{\text{URC}}$'s are used.

A systematic realization procedure of rational transfer functions using commensurate $\overline{\text{URC}}$'s has been developed. These $\overline{\text{URC}}$ realizations are

attractive from the point of view of hybrid IC implementation particularly suitable for very low frequency applications, where other distributed realizations usually fail. The synthesis procedure described is simple compared to any of the other known distributed realizations of rational transfer functions. The effect, on the realized response, of the $\overline{\text{URC}}$'s being not exactly commensurate is relatively negligible provided the RC product of the $\overline{\text{URC}}$'s is chosen such that the main part of the desired response lies either in the region $\omega RC \leq 0.01$ or in the region $\omega RC \geq 30$. It is found that, in order to implement efficiently the synthesis procedure, a lumped RC active low sensitivity network is required, in the u-plane, as an intermediate step. In this network, it is desirable to have minimum number of resistors and capacitors with all the capacitors grounded. The number of $\overline{\text{URC}}$'s as well as gyrators will then be minimum. In addition, all the gyrators will be able to share a common power supply.

One such grounded capacitor RC active network capable of realizing any transfer function is then presented. A design procedure that simultaneously minimizes the worst case deviations in Q_p and ω_p has also been derived. The design can be used to obtain low, band and high pass responses. This design is then utilized to obtain notch and all pass filters. The effect of the design on ω_N (ω_z and Q_z) for notch (all pass) sections is investigated and it is found that the worst case deviations for these quantities are also low.

A modification of the above grounded capacitor network is next presented. The modification results in a significantly improved design which yields a lower value for the worst case deviations of Q_p and ω_p, and a lower value for the amplifier gains $[(2\ Q_p)^{2/3}]$. The sensitivity of the realizations to the d.c. gains of the OA's realizing the finite gains has been found to be low. The modified filter is shown to be stable during activation, that is, just after switching on the power supply, when the amplifier gains are rising from zero. The effect of the finite bandwidth of the OA on ω_p has been shown to be negligible while that on Q_p is an enhancement. It is shown that the choice of gains, that minimizes the worst case deviations in Q_p and ω_p, also minimizes the Q_p-enhancement.

A simple scheme has been proposed to compensate for the effect of the bandwidth of the OA on Q_p without affecting ω_p, thus improving the useful frequency range of operation of the circuit. The effect of compensation on the zeros of the notch and all pass sections has been studied. It is found that ω_N and ω_z are negligibly affected, while compensating for Q_p automatically compensates for Q_z. The parasitic effect of the input and output impedances of the OA on the compensated filter has been examined for a band pass section of $Q_p = 10$ and $f_p = 1.01$ KHZ and found to be negligible for μA741 OA. A simple three step tuning procedure, by trimming resistors only, is also given for the compensated network. The effectiveness of the compensation scheme

is demonstrated experimentally for a Q_p of 10. Second order low pass and band pass responses were tested experimentally using the compensated network. Further, a sixth order band pass filter with stringent specifications was built and tested. The experimental results agree closely with the theory.

The modified network is then utilized to illustrate, by designing second order band pass responses, the synthesis procedure developed in the thesis. It is found that the filter response is negligibly affected even if the $\overline{URC}$'s are not exactly commensurate provided that the RC product of the $\overline{URC}$'s is made to lie in the region $\omega_p RC \leq 0.01$ or $\omega_p RC \geq 30$. This establishes the validity of the results obtained earlier with respect to $u(j\omega)$. It has been shown that the effect of gyrator imperfections on the transformation u may be ignored, if r_g, the gyration resistance, is chosen such that the values of both (R_{1T}/R_{2T}) and R_{1T} are large, where R_{1T} and R_{2T} are, respectively, the total resistances of the short and open circuited $\overline{URC}$'s. The effect of the finite bandwidth of the OA's, that determine the finite gains, on Q_p and ω_p has been examined. It is found that ω_p is relatively unaffected, while Q_p suffers from a de-enhancement. This de-enhancement, however, ensures that the filter will remain stable, a fact that is in contrast with other distributed realizations [34 - 37]. These realizations all exhibit Q_p-enhancement that may cause instability. The investigation is concluded by designing a second order LP Butterworth section with a cut off frequency ω_p of 10. It is shown that the designed filter can be easily fabricated by hybrid IC technology.

The effect of the imperfections of the gyrators and those of the gain determining OA's on the magnitude and phase responses of the filter is found to be negligible. This design serves to establish the practical feasibility, of hybrid IC implementation, of the filters realized by the synthesis procedure proposed in the thesis. It is also worthwhile noting that it may be difficult to fabricate the above filter in hybrid IC technology, if it is designed by the conventional lumped RC active filter techniques.

The distributed synthesis procedure presented in this thesis is not, by itself, restricted to any frequency range. However, the fact that a grounded capacitor RC active network is required as an intermediate step in implementing the procedure and the fact that the finite gains in this network are realized by using OA's, all of which have a finite gain bandwidth product, limit the usefulness of the synthesis procedure to low frequency applications. The author, therefore, feels that it is worthwhile investigating techniques of extending the operating frequency range of the distributed network. This requires compensation for the de-enhancement of Q_p. One way of doing this is perhaps by introducing an appropriate lag network in the configuration.

It is also desirable, in the author's opinion, to undertake a comprehensive study of the cost of the realizations resulting from the proposed technique in comparison with other filters suitable for low frequency applications.

The possibility for simultaneous minimization of the chip area as well as the effect, on the realized response, of the imperfections

of the gyrator and OA's, should also be investigated.

The useful frequency range of the grounded capacitor network of Chapter 4 may be possibly extended by designing R_c to vary with temperature in such a way as to compensate for temperature variations of the gain bandwidth product B. This will render the Q_p-levelling technique effective at high frequencies over a wide temeprature range. This seems feasible as B varies almost linearly from 0°C to 70°C and the variation is about 15% for commercially available OA's such as μA 741.

The noise, distortion and dynamic range properties of the realizations should also be studied. However, it was found during experimental tests that the sixth order band pass filter of Chapter 4 could handle a wide range of input signal levels (0.2 to 2 volts) without any apparent distortion.

In conclusion, the author hopes that in view of the rapid advances and considerable interest in hybrid IC technology and the advent of many new areas, such as biomedical engineering, which require very low frequency filters, the results obtained in this thesis should prove useful.

REFERENCES

REFERENCES

[1] L. Weinberg, Network Analysis and Synthesis, N.Y.: McGraw-Hill, 1962.

[2] J.K. Skwirzynski, Design Theory and Data for Electrical Filters, N.Y.: Van Nostrand, 1965.

[3] White Electromagnetics, Inc., A Handbook on Electrical Filters, Maryland: WEI, 1963.

[4] L.P. Huelsman, Ed., Active Filters: Lumped, Distributed, Integrated, Digital and Parametric, New York: McGraw-Hill, 1970.

[5] R.W. Newcomb, Active Integrated Circuit Synthesis, Englewood Cliffs, N.J.: Prentice-Hall, 1968.

[6] S.K. Mitra, Analysis and Synthesis of Linear Active Networks, New York: Wiley, 1969.

[7] A. Antoniou, "New Gyrator Circuits Obtained by Using Nullors", Electron. Lett., Vol. 4, pp.87-89, March 1968.

[8] Private communication with Dr. A. Antoniou, Elec. Eng. Dept., Sir George Williams University, Montreal, Canada.

[9] A. Antoniou and K.S. Naidu, "Modelling of a Gyrator Circuit", IEEE Trans. CT, Vol. CT-20, pp.533-540, Sept. 1973.

[10] S.K. Mitra, Ed., Active Inductorless Filters, IEEE Press, 1971.

[11] W.B. Mikhael and B.B. Bhattacharyya, "New-Minimal Capacitor Low Sensitivity RC Active Synthesis Procedure", Electron. Lett., Vol. 7, pp.694-696, Nov. 1971.

[12] A. Antoniou, "Novel RC-Active Network Synthesis Using Generalized Immittance Converters", IEEE Trans. on Circuit Theory, Vol. CT-17, pp.212-217, May 1970.

[13] A. Antoniou, "Realization of Gyrators Using Operational Amplifiers and their Use in RC-Active Network Synthesis", Proc. IEEE, Vol. 116, pp.1838-1850, Nov. 1969.

[14] W.J. Kerwin, L.P. Huelsman and R.W. Newcomb, "State Variable Synthesis for Insensitive Integrated Circuit Transfer Functions", IEEE J. Solid-State Circuits, Vol. SC-2, pp.87-92, Sept. 1967.

[15] R. Tarmi and M.S. Ghausi, "Very High-Q Insensitive Active RC Networks", IEEE Trans-Circuit Theory, Vol. CT-17, pp.358-366, Aug. 1970.

[16] L.C. Thomas, "The Biquad: Part II-A Multipurpose Active Filtering System", IEEE Trans-Circuit Theory, Vol. CT-18, pp.358-361, May, 1971.

[17] T.A. Hamilton and A.S. Sedra, "Some New Configurations for Active Filters", IEEE Trans. Circuit Theory, Vol. CT-19, pp. 25-33, Jan. 1972.

[18] B.B. Bhattacharyya, W.B. Mikhael and A. Antoniou, "Design of RC-Active Networks Using Generalized-Immittance Converters", Journal of the Franklin Institute, Vol.297, No.1, January 1974.

[19] W.B. Mikhael, "Design of High Performance RC Active Filters", Doctoral Thesis, Sir George Williams University, Montreal, 1973.

[20] P.O. Brackett, "A New Single OP-Amp Active RC Network", Proc. 16th Midwest Symposium on Circuit Theory, April, 1973.

[21] G.S. Moschytz and W. Thelen, "Design of Hybrid Integrated-Filter Building Blocks", IEEE Journal of Solid-State Circuits, Vol. SC-5, pp. 99-107, June, 1970.

[22] G.S. Moschytz, "Gain-Sensitivity Product - A Figure of Merit for Hybrid-Integrated Filters Using Single Operational Amplifiers", IEEE Journal of Solid-State Circuits, Vol. SC-6, pp. 103-110, June 1971.

[23] J. Dupeak, Western Electric, "Manufacture of Thin Film Filters", Workshop on Active Networks, organized by IEEE Circuits and Systems Society, Nov., 1973.

[24] M. Fogiel, Microelectronics, N.Y.: Research and Education Association, 1969.

[25] A. Lessor, L. Maissel and R. Thun, "Part-I Thin Film RC Networks", IEEE Spectrum, Vol. 1, pp. 72-80, April 1964.

[26] Private communication with Dr. B. Lombos: Microelectronics Labs, Sir George Williams University, Montreal, Canada.

[27] W. Happ and G. Riddle, "Limitations of Film-Type Circuits Consisting of Resistive and Capacitive Layers", IRE International Convention Record, Vol. 9, Part 6, pp. 141-165, 1961.

[28] B.B. Bhattacharyya, M.S. Abougabal and M.N.S. Swamy, "On an Integrable Active RC Filter", Proc. of IEEE ISCT, pp. 256-259, April, 1973.

[29] R.W. Berry, P.M. Hall and M.T. Harris, Thin Film Technology, N.Y.: Van Nostrand, 1968.

[30] M. El-Diwany and C. Giguere, "Area Minimization of Distributed RC Networks", Proc. of IEEE International Symposium on CT, pp. 338-340.

[31] R.W. Wyndrum, Jr., "The Exact Synthesis of RC Distributed Networks", New York University Tech. Rep. 400-76, May 1963.

[32] R.P. O'Shea, "Synthesis Using Distributed RC Networks", IEEE Convention Record, Vol. 13, Part 7, pp. 18-29, 1965.

[33] J.C. Giguere, M.N.S. Swamy and B.B. Bhattacharyya, "Driving-Point-Function Synthesis Using Nonuniform Lines", Proc. IEE, Vol. 116, No. 1, pp. 65-70, Jan. 1969.

[34] M.S. Ghausi and V.C. Bello, "Design of Linear Phase Active Distributed RC Networks", IEEE Trans. on Circuit Theory, Vol. CT-16, pp. 526-520, November 1969.

[35] W.J. Kerwin, "Synthesis of Active RC Networks Containing Lumped and Distributed Elements", Proc. 1st Asilomar Conf. on Circuits and Systems, pp. 288-298, November 1967.

[36] J. Walsh, J.C. Giguere and M.N.S.Swamy, "Active Filter Design Using Exponentially Tapered RC-Lines", IEEE Trans. on Circuit Theory, Vol. CT-17, pp.645-648, Nov. 1970.

[37] D.A. Spaulding, "Synthesis of Rational Transfer Functions Approximations Using a Tapped Distributed RC Line with Feedback", The Bell System Tech. J., Vol. 47, pp. 2051-2071, Nov. 1968.

[38] S.P. Johnson and L.P. Huelsman, "High-pass and Band Pass Filters With Distributed-Lumped Active Networks", Proc. IEEE, Vol. 59, pp. 328-331, Feb. 1971.

[39] K.W. Heizer, "Distributed RC Networks with Rational Transfer Functions", IRE Trans. on Circuit Theory, Vol. CT-9, pp. 356-362, December 1962.

[40] D.G. Barker, "Synthesis of Active Filters Employing Thin Film Distributed Parameter Networks", IEEE Int. Convention Record, Vol. 13, Part 7, pp. 119-126, 1965.

[41] Y. Fu and J.S. Fu, "Synthesis of Active Distributed RC Networks", IEEE Trans. on Circuit Theory, Vol. CT-13, pp. 259-264, September 1966.

[42] S.Y. Hwang and W.C. Duesterhoeft, Jr., "Distributed RC Networks with Rational y Parameters Having Prescribed Poles", IEEE Trans. on Circuit Theory, Vol. CT-16, pp. 423-429, November 1969.

[43] E.D. Walsh and C.M. Close, "On the Synthesis of Any RC Realizable Rational Transfer Function Using a Nonuniform RC Distributed Circuit", IEEE Trans. on Circuit Theory, Vol. CT-17, pp. 217-223, May, 1970.

[44] M. Clynes and J. Milsum, Biomedical Engineering Systems, N.Y.: McGraw-Hill, 1970.

[45] Private communication with Dr. Outerbridge, M.D., Dept. of Otolaryngeology, McGill University, Montreal, Canada.

[46] E. Kimura et al., "Automatic ECG and Arrhythmia Interpreter - An Almost Analog Device", Journal of Electrocardiology, pp.137-145, No.6, 1973.

[47] J. Silva and M. Intaglieta, "Measurement of Pulsatile Blood Flow Velocity in Microvessels from Single Photometric Detector", IEEE Trans. on Biomedical Engineering, Vol. BME-20, pp. 310-312, July 1973.

[48] W. Cooley and K. Moser, "A Simple Signal Processor for a Respiratory Rate Monitor", IEEE Trans. on Biomed. Eng., Vol. BME-20, pp.309-310, July 1973.

[49] W. Holsinger and K. Kempner, "Portable ECG Telephone Transmitter", IEEE Trans. on Biomed. Eng., Vol. BME-19, pp.321-323, July 1972.

[50] J. Cox et al., "Digital Analysis of the Electroencephalogram, the Blood Pressure Wave, and the Electrocardiogram", Proc. of IEEE, Vol. 60, pp. 1137-1164, October 1972.

[51] Private communication with Dr. C.J. Giguere, Elec. Eng. Dept., Sir George Williams University, Montreal, Canada.

[52] A.M. Khalil and P. Fazio, "Moiré-Fringe Measurement", Experimental Mechanics, Vol. 13, No. 6, pp. 253-254, June 1973.

[53] Private communication with Dr. T.S. Sankar, Mechanical Engineering Department, Sir George Williams University, Montreal, Canada.

[54] B.B. Bhattacharyya and M.N.S. Swamy, "Dual Distributions of Solvable Nonuniform Lines", Proc. of IEEE, Vol. 54, pp. 1979-1980, December 1966.

[55] M.N.S. Swamy and B.B. Bhattacharyya, "Generalized Nonuniform Lines and Their Equivalent Circuits", Conf. Record, 10th Midwest Symposium on Circuit Theory, Purdue Univ., Lafayette, Paper No. II-4, pp. 1-10, May 1967.

[56] J.C. Giguere, "The Synthesis of Network Functions Using Nonuniform Lines", Ph.D. Thesis, Nova Scotia Technical College, Halifax, 1968.

[57] J.C. Giguere, "The Approximation of a Nonuniform Transmission Line by a Cascade of Uniform Lines", Electron. Lett., Vol. 7, pp.511-152, September 1971.

[58] J.C. Giguere, M.N.S. Swamy and B.B. Bhattacharyya, "Driving Point Function Synthesis Using Tapered Lines and Their Duals", IEEE Trans. on Circuit Theory, Vol. CT-16, pp. 93-94, February 1969.

[59] M.S. Abougabal, B.B. Bhattacharyya and M.N.S. Swamy, "A Low Sensitivity Active Distributed Realization of Rational Transfer Functions", Proc. of IEEE ISCT, pp. 328-332, April 1972 (Accepted as paper for the IEEE Trans. on Circuit Theory).

[60] M.N.S. Swamy and B.B. Bhattacharyya, "A Study of Recurrent Ladders Using the Polynomials Defined by Morgan-Voyce", IEEE Trans. on CT, Vol. CT-17, pp. 217-223, May 1970.

[61] M.S. Abougabal and B.B. Bhattacharyya, "Easily Integrable Very Low Sensitivity Active RC Filter", Electron. Lett., Vol. 8, pp. 303-304, May 1972.

[62] W.B. Mikhael and B.B. Bhattacharyya, "Stability Properties of Some Active RC Realizations", Electron. Lett., Vol. 8, No. 11, June 1972.

[63] A. Antoniou, "Realization of Gyrators Using Operational Amplifiers and Their use in RC-Active Network Synthesis", Proc. IEE, Vol. 116, pp. 1838-1850, Nov. 1969.

[64] L.C. Thomas, "The Biquad, Part I - Some Practical Design Considerations", IEEE Trans. Circuit Theory, Vol. CT-18, pp. 350-357, May 1971.

[65] A. Budak and D.M. Petrela, "Frequency Limitations of Active Filters Using Operational Amplifiers", IEEE Trans. Circuit Theory, Vol. CT-19, pp. 322-328, July 1972.

```
      PROGRAM NANCY(INPUT,OUTPUT)
C     ***************************************
C     EFFECT OF FIRST POLE APPROX. ONLY
C     ***************************************
      DIMENSION XCOF(16),COF(6),ROOTR(6),ROOTI(6)
      M=6
      DO 100 K=1,3
      READ 3,GD
    3 FORMAT(E13.6)
      GD=3D
    4 FORMAT(1H1,10(1H*),5HGD=,E13.6,10(1H*))
      DO 100 A=1,10
      C=A*10
      B=3*(2*C)**(4./3.)
      A=3**(2*C)**(2./3.)
      PRINT 4,GD
      PRINT 1
    1 FORMAT(1H0,2HWC,8X,3HWPO,8X,3HPER)
      WC=1
      SIGMA=-WC/(C*2)  SQMEGA=WC*SQRT(1-1/(4*C**2))
      QD=SQRT(WC**2+SIGMA**2)/(2*ABS(SIGMA))
      C*B=3*GD/(GD-A*WC)
      X=A/GD  SY=0.
      WAD=WC/(1+WC*X/2)**0.5
      X=0.
      T=2*C/WC
      T1=T**3+X*Y+T*Y+T*X
      T2=3*T+X+Y
      XCOF(1)=4*C**3*GD**3
      XCOF(2)=T2*GD**3+3*(2*C)**(2./3.)*GD**2+4*C**2*GD**3*(X+Y)
      XCOF(3)=T1*GD**3+C**2*T2 *A+B*C+4*C**2*GD**3*X*Y
      XCOF(4)=T1 *GD**2*A+T2 *B*GD+4*C**2
      XCOF(5)=T1 *GD*A+T2*4*C**2
      XCOF(6)=4*C**2*T1
C     COMPUTING THE ROOTS USING THE LIB. SUBROUT. POLRT.
      CALL POLRT (XCOF, COF,M,ROOTR,ROOTI,ILR)
      WA=ROOTI(1)
      XMAX=ROOTR(1)
      DO 50 L=1,5
C     TESTING FOR RHS PLANE POLES
      IF (ROOTR(L).GE.0.0) GO TO 51
      IF (ROOTR(L).GE.XMAX.AND.ROOTI(L).NE.0.) GO TO 52
      GO TO 50
   52 XMAX=ROOTR(L)
      WA=ROOTI(L)
      QA=SQRT(XMAX**2+WA**2)/(2*ABS(XMAX))
      PER=(QA-QD)/QD*100
      WPOLE=SQRT(XMAX**2+WA**2)
      GO TO 50
   51 QA=11111.1111
      WPOLE=11111.1111
      WA=11111.1111
      PER=11111.1111
      GO TO 101
   50 CONTINUE
```

[66] A. Budak and E.R.Zeller, "Practical Design Considerations for a Variable Center Frequency, Constant Bandwidth and Constant Peak-Value Filter", IEEE Journal of Solid-State Circuits, Vol. SC-7, pp. 308-311, August 1972.

[67] D.J. Millar, "An Algorithm for the Rapid Analysis of Sparse Electrical Networks", M. Eng. Thesis, McGill University, Montreal, Canada, March 1970.

APPENDIX A

APPENDIX A.1

THE INFLUENCE OF THE AMPLIFIER POLE ON Q_p AND ω_p

Assuming ideal OA's, Q_p and ω_p of any RC-active network will be functions of the different resistors and capacitors only. Hence,

$$Q_p = f_1(R,C) \tag{A.1}$$

$$\omega_p = g_1(R,C) \tag{A.2}$$

where R and C denote the resistive and capacitive parameters. From physical considerations, f_1 and g_1 are continuous functions of these elements.

If the network employs either positive gain and/or negative gain amplifiers only and if these amplifiers are realized using OA's (Fig. A.1) and assuming the OA's to be identical and having the one pole model given by (1.1), then the gains are function of s and B, provided $K_o < \mu_o$, as shown in Figure A.1. Similarly, if the summers are also realized using OA's the gains again will be functions of s and B only. Therefore, for such a network, if the one pole model of the OA's used is taken into consideration, then the Q-factor Q_{PB} and pole frequency ω_{PB} actually realized may be expressed in the form

$$\frac{Q_p}{Q_{PB}} = f_2(R, C, B) \tag{A.3}$$

$$\frac{\omega_{PB}}{\omega_p} = g_2(R, C, B) \tag{A.4}$$

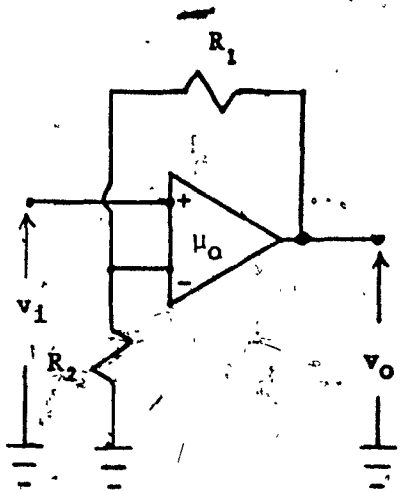

$$\frac{v_o}{v_i} = K(s, B) = \frac{K_o B}{K_o s + B}$$

$$K_o = 1 + \frac{R_1}{R_2}$$

(a)

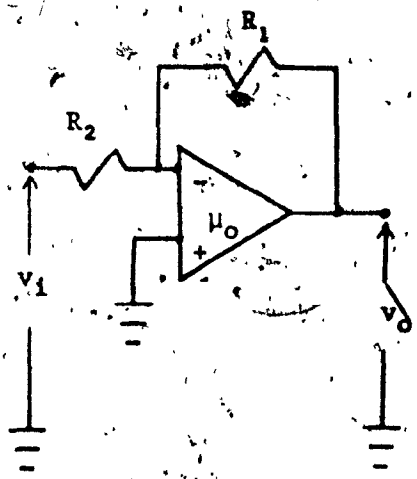

$$\frac{v_o}{v_i} = -K(s, B) = -\frac{K_o B}{(1 + K_o)s + B}$$

$$K_o = \frac{R_1}{R_2}$$

(b)

Fig. A.1: (a) Realization of a Positive Gain Amplifier Using OA.

(b) Realization of a Negative Gain Amplifier Using OA.

For ideal OA's $Q_{PB} = Q_P$ and $\omega_{PB} = \omega_P$ or

$$\lim_{B \to \infty} \frac{Q_P}{Q_{PB}} = 1^* \tag{A.5}$$

and

$$\lim_{B \to \infty} \frac{\omega_{PB}}{\omega_P} = 1 \tag{A.6}$$

For any given design, R's and C's may be regarded as constants of the design in evaluating the effect of B on pole-Q and pole frequency. Therefore, expanding $\frac{Q_P}{Q_{PB}}$ as well as $\frac{\omega_{PB}}{\omega_P}$ in a Taylor's series around the point $B \to \infty$ or around the point $\frac{1}{B} = 0$, and retaining up to second order terms, we have

$$\frac{Q_P}{Q_{PB}} = 1 + \frac{\alpha_1}{B} + \frac{\alpha_2}{B^2} \tag{A.7a}$$

and

$$\frac{\omega_{PB}}{\omega_P} = 1 + \frac{\gamma_1}{B} + \frac{\gamma_2}{B^2} \tag{A.7b}$$

where the α's and γ's are constants related to the derivatives of $(\frac{Q_P}{Q_{PB}})$ and $(\frac{\omega_{PB}}{\omega_P})$ with respect to $(\frac{1}{B})$ evaluated at $\frac{1}{B} = 0$ and where use has been made of (A.5) and (A.6).

The three feedback gains β_1, β_2 and δ_2 in the network of Figure 4.2 determine the poles of its transfer function. For such a network, if the three OA's determining these feedback gains have gain bandwidth products B_1, B_2 and B_3, then format (A.7) becomes

---

* $B \to \infty$ implies $\mu_o \to \infty$ or $\omega_c \to \infty$

$$\frac{Q_P}{Q_{PB}} = 1 + \frac{\alpha_{11}}{B_1} + \frac{\alpha_{12}}{B_2} + \frac{\alpha_{13}}{B_3} + \frac{\alpha_{21}}{B_1 B_2} + \frac{\alpha_{22}}{B_1 B_3} + \frac{\alpha_{23}}{B_2 B_3} + \frac{\alpha_{31}}{B_1^2} + \frac{\alpha_{32}}{B_2^2} + \frac{\alpha_{33}}{B_3^2} \qquad \text{(A.8a)}$$

and

$$\frac{\omega_{PB}}{\omega_P} = 1 + \frac{\gamma_{11}}{B_1} + \frac{\gamma_{12}}{B_2} + \frac{\gamma_{13}}{B_3} + \frac{\gamma_{21}}{B_1 B_2} + \frac{\gamma_{22}}{B_1 B_3} + \frac{\gamma_{23}}{B_2 B_3} + \frac{\gamma_{31}}{B_1^2} + \frac{\gamma_{32}}{B_2^2} + \frac{\gamma_{33}}{B_3^2} \qquad \text{(A.8b)}$$

The formats (A.8a) and (A.8b) are used in subsequent analysis.

Equations (4.36) and (4.37) can be rearranged as:

$$\frac{1}{\omega_{PB}^2} = b_2 - \left(\frac{\omega_{PB}}{\omega_P}\right)\left(\frac{Q_P}{Q_{PB}}\right)\frac{\omega_P}{Q_P} b_3 - \left(\frac{\omega_{PB}}{\omega_P}\right)^2 \omega_P^2 b_4 \left[1 - \left(\frac{Q_P}{Q_{PB}}\right)^2 \frac{1}{Q_P^2}\right] + \left(\frac{\omega_{PB}}{\omega_P}\right)^3 \left(\frac{Q_P}{Q_{PB}}\right)\frac{\omega_P^3}{Q_P} b_5 \left[2 - \left(\frac{Q_P}{Q_{PB}}\right)^2 \frac{1}{Q_P^2}\right] \qquad \text{(A.9a)}$$

and

$$\frac{1}{\omega_{PB} Q_{PB}} = b_1 - \left(\frac{\omega_{PB}}{\omega_P}\right)^2 \omega_P^2 b_3 + \left(\frac{\omega_{PB}}{\omega_P}\right)^3 \left(\frac{Q_P}{Q_{PB}}\right)\frac{\omega_P^3}{Q_P} b_4 + \left(\frac{\omega_{PB}}{\omega_P}\right)^4 \omega_P^4 b_5 \left[1 - \left(\frac{Q_P}{Q_{PB}}\right)^2 \frac{1}{Q_P^2}\right] \qquad \text{(A.9b)}$$

where

$$b_1 = \frac{1}{4Q_p^2}\left(\frac{\beta_1}{B_2} + \frac{\beta_2}{B_3} - \frac{\delta_2}{B_1}\right) + \frac{1}{Q_p\omega_p}$$

$$b_2 = \frac{1}{4Q_p^2}\left(\frac{\beta_1\beta_2}{B_2B_3} - \frac{\beta_1\delta_2}{B_1B_2} - \frac{\beta_2\delta_2}{B_1B_3}\right) + \frac{1}{\omega_pQ_p}\left(\frac{\beta_1}{B_2} + \frac{\beta_2}{B_3} - \frac{\delta_2}{B_1}\right) + \frac{1}{\omega_p^2}$$

$$b_3 = \frac{1}{B_1B_2B_3} + \frac{1}{Q_p\omega_p}\left(\frac{\beta_1\beta_2}{B_2B_3} - \frac{\beta_1\delta_2}{B_1B_2} - \frac{\beta_2\delta_2}{B_1B_3}\right)$$

$$+ \frac{1}{\omega_p^2}\left(\frac{\beta_1}{B_2} + \frac{\beta_2}{B_3} - \frac{\delta_2}{B_1}\right) \qquad \text{(A.10)}$$

$$b_4 = \frac{4Q_p}{\omega_pB_1B_2B_3} + \frac{1}{\omega_p^2}\left(\frac{\beta_1\beta_2}{B_2B_3} - \frac{\beta_1\delta_2}{B_1B_2} - \frac{\beta_2\delta_2}{B_1B_3}\right)$$

$$b_5 = \frac{4Q_p^2}{\omega_p^2B_1B_2B_3}$$

Substituting (A.10) in (A.9), using formats (A.8), and neglecting terms which will introduce only second and higher order terms of (1/B) in the final expression, we have, for $Q_p \gg 1$

$$\frac{1}{\omega_{PB}^2} = \frac{1}{\omega_p^2} \qquad \text{(A.11)}$$

and

$$\frac{1}{Q_{PB}} = \frac{1}{Q_p} - \omega_p x \qquad \text{(A.12)}$$

where

$$x = \frac{\beta_1}{B_2} + \frac{\beta_2}{B_3} + \frac{1 - \delta_2}{B_1} \qquad \text{(A.13)}$$

If it is required to study the second order effects of (1/B) on the pole Q and pole frequency, the following may be obtained, using (A.8), (A.9) and (A.10) neglecting terms that contribute only to third and

higher order terms of (1/B), for $Q_p >> 1$

$$\frac{1}{\omega_{p_B}^2} = \frac{1}{\omega_p^2} + (2Q_p)^{4/3} \left(\frac{1}{B_1} + \frac{1}{B_2} + \frac{1}{B_3}\right)^2 \qquad \text{(A.14)}$$

and

$$\frac{1}{Q_{p_B}} = \frac{1}{Q_p} - \omega_p x - \omega_p^2 (2Q_p)^{1/3} \left(\frac{1}{B_1} + \frac{1}{B_2} + \frac{1}{B_3}\right)^2 \qquad \text{(A.15)}$$

where x is given by (A.13)

```
      PROGRAM NANCY(INPUT,OUTPUT)
C ***********************************
C EFFECT OF FIRST POLE APPROX. ONO
C ***********************************
      DIMENSION XCOF(16),COF(6),ROOTR(6),ROOTI(6)
      M=5
      DO 100 K=1,3
      READ 3,GP
    3 FORMAT(E13.6)
      GPO=GP
    4 FORMAT(1H1,10(1H*),3GP=,E13.6,10(1H*))
      DO 100 N=1,10
      G=N*10
      B=3*(2*G)**(4./3.)
      A=3*(2*G)**(2./3.)
      PRINT 4,GP
      PRINT 1
      DO 100 I=1000,10000,1000
      WO=I
      SIGMA=-WO/(G*2)  OMEGA=WO*SQRT(1-1/(4*G**2))
      QO=SQRT(WO**2+SIGMA**2)/(2*ABS(SIGMA))
      GAP=2*GP/(GP-A*WO**2)
      X=A/GP  Y=0.
      WLP=WO/(1+WO*X/G)**0.5
      X=0.0
      T=2*G/WO
      T1=T**2+X*X+T*Y+T*X
      T2=2*T+X+Y
      XCOF(1)=4*G**2*GP**3
      XCOF(2)=T2*GP**3+3*(2*G)**(2./3.)*GP**2+4*G**2*GP**2*(X+Y)
      XCOF(3)=T1*GP**3+G**2*T2*X+G*GP+4*G**2*GP**2*X*Y
      XCOF(4)=T1*GP**2*A+T2*B*GP+4*G**2
      XCOF(5)=T1*GP*B+T2*4*G**2
      XCOF(6)=4*B**2*T1
C     COMPUTING THE ROOTS USING THE LIB. SUBROUT. POLRT.
      CALL POLRT (XCOF, COF,M,ROOTR,ROOTI,IER)
      WA=ROOTI(1)
      XMAX=ROOTR(1)
      DO 50 L=1,5
C     TESTING FOR RHS PLANE POLES
      IF (RCOTR(L).GL.0.0) GO TO 51
      IF (RCOTR(L).GE.XMAX.AND.ROOTI(L).NE.0.) GO TO 52
      GO TO 50
   52 XMAX=ROOTR(L)
      WA=RCOTI(L)
      QA=SQRT(XMAX**2+WA**2)/(2*ABS(XMAX))
      PER=(QA-QD)/QD*100
      WPOLE=SQRT(XMAX**2+WA**2)
      GO TO 50
   51 QA=11111.1111
      WPOLE=11111.1111
      WA=11111.1111
      PER=11111.1111
      GO TO 101
   50 CONTINUE
```

APPENDIX A.2

COMPUTER PROGRAM FOR CALCULATING THE EXACT VALUES OF Q_{PB} AND ω_{PB}

```
101 PRINT 2,WC,OD,OA,OAP,PER,WA,WPOLE,WAP,IER
  2 FORMAT(2X,8F15.4,I3)
  1 FORMAT(///,5X,*WC*,10X,*OD*,10X,*OA*,10X,*OAP*,10X,*PER*,10X,
   1*WA*,10X,*WPOLE*,10X,*WAP*)
100 CONTINUE
    STOP
    END
```

APPENDIK B

APPENDIX B

DERIVATION OF Q_{PB} FROM PHASE CONSIDERATIONS

The poles of the various transfer functions generated by the network of Figure 4.2 are all identical to those of a "basic" low pass section contained in this network. This section is shown in Figure B.1. The transmission poles of the LP section are, in turn, determined by the feedback loop containing the gains β_1, β_2 and δ_2.

For real gains δ_2, β_1 and β_2, the phase shift ϕ around the feedback loop at ω_p is

$$\phi = \pi - 2 \tan^{-1} (\omega_p RC) \qquad (B.1)$$

Therefore,

$$\tan (\pi/2 - \phi/2) = \omega_p RC \qquad (B.2a)$$

or

$$\cos (\phi/2) = \omega_p RC \qquad (B.2b)$$

From (4.2) and (4.12) it may be shown that

$$\omega_p RC = 2Q_p \qquad (B.3)$$

Hence

$$\tan (\phi/2) = \frac{1}{2Q_p} \qquad (B.4)$$

Thus, for $Q_p >> 1$,

$$\phi \approx \frac{1}{Q_p} \qquad (B.5)$$

The above equation shows that for highly selective responses, the total phase change around the feedback loop is equal to the reciprocal of the pole-Q.

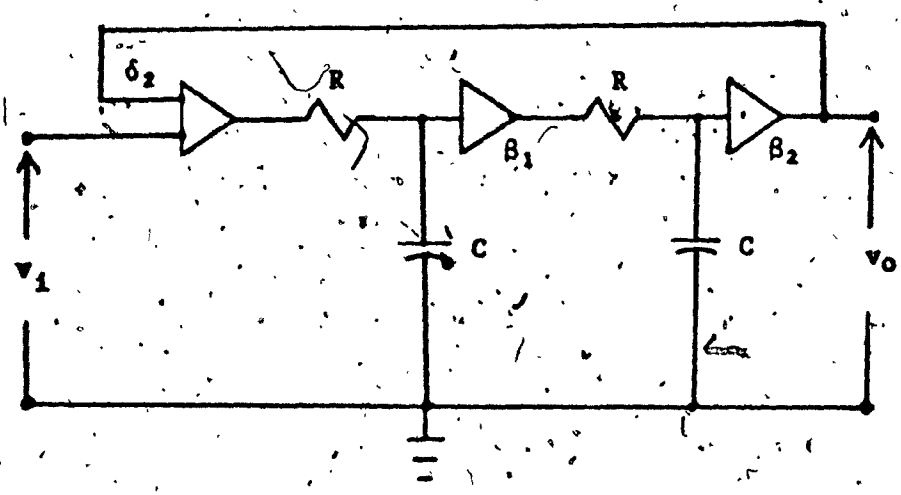

Fig. B.1: Basic Low Pass Section

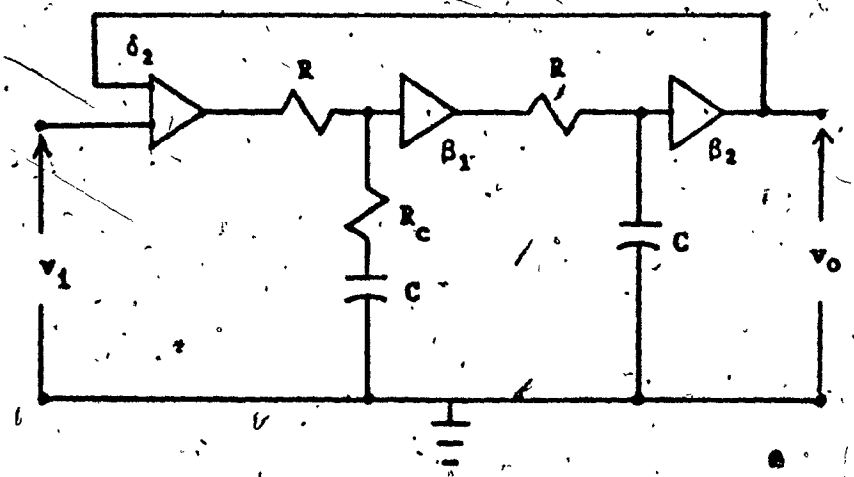

Fig. B.2: Compensated Network

When the amplifier gains β_1, β_2 and δ_2 are frequency dependent, then additional phase changes are introduced by them in the feedback loop. Assuming again the OA's realizing the gains to be identical and with a gain bandwidth product B and also that the gains are given by

$$\beta_1 = \beta_2 = -\delta_2 = (2Q_p)^{2/3} \tag{B.6}$$

as in the optimum design of section (4.3), then under one pole model of the OA's, the expressions for these gains reduce to

$$\beta_{1B} = \beta_{2B} = -\delta_{2B} = \frac{(2Q_p)^{2/3}}{1 + s\,\dfrac{(2Q_p)^{2/3}}{B}} \tag{B.7}$$

We now assume that, with the different gains as given by (B.7), the total phase change ϕ_B at ω_p around the feedback loop is still very closely given by the reciprocal of Q_{PB}, the Q-factor actually realized, that is,

$$\phi_B \simeq \frac{1}{Q_{PB}} \tag{B.8}$$

Under this assumption, we have

$$\phi_B = \frac{1}{Q_{PB}} = \pi - 2\tan^{-1}(\omega_p RC) - 3\tan^{-1}\left\{\frac{(2Q_p)^{2/3}\,\omega_p}{B}\right\}$$

$$\simeq \frac{1}{Q_p} - 3\tan^{-1}\left\{\frac{(2Q_p)^{2/3}\,\omega_p}{B}\right\} \tag{B.9}$$

That is,

$$\tan\left(\frac{1}{3Q_p} - \frac{1}{3Q_{PB}}\right) = \frac{2(Q_p)^{2/3}\,\omega_p}{B} \tag{B.10}$$

Since Q_p has to be very close to Q_{PB}, for the network to be useful, we have

$$\frac{1}{Q_{PB}} = \phi_B = \frac{1}{Q_p} - \frac{3(2Q_p)^{2/3}\,\omega_p}{B} \qquad (B.11)$$

It is to be noted that equation (B.11) is the same as (4.38b), thereby justifying the validity of the assumption (B.8).

The effect of the frequency dependence of the gains is seen to introduce a phase lag in the total phase change in the feedback loop. Thus, in order to compensate for this phase lag, a phase lead should be introduced in the feedback loop.

If the basic LP section is now modified by introducing a Resistor RC as shown in Figure B.2, the phase shift around the loop may be shown, by a similar analysis, to be

$$\phi_c = \frac{1}{Q_p} + R_c C\omega_p - \frac{3(2Q_p)^{2/3}\,\omega_p}{B} \qquad (B.12)$$

Thus, compensation, or Q_p-levelling, may be achieved by choosing the resistor R_c such that

$$R_c = \frac{3(2Q_p)^{2/3}}{C\,B} \qquad (B.13)$$

APPENDIX C.1

COMPUTER PROGRAM FOR CALCULATING Q_R AND ω_R

```
      PROGRAM NANCY(INPUT,OUTPUT)
C ***************************************************************
C OR AND WR FOR -5PER. CHANGE IN C'S.
C ***************************************************************
      DIMENSION TA(6),AMAX(6),WX(6),OC(6),W1(3)
       DIMENSION WO1(18),MM(18),NN(18),YY(18)
      REAL INCR
      READ 5,(WO1(J),J=1,18)
    5 FORMAT(9F6.2)
      READ 6,((MM(J),NN(J),YY(J)),J=1,18)
    6 FORMAT(4(2I5,F8.0))
      DO 100 KK=10,100,40
      Q=KK
      DO 100 I=1,4
      PRINT 701
  701 FORMAT(1H1)
      DO 100 L=1,18
      AMAX(I)=-100000.
      LL=L
      WO=WO1(LL)
      M=MM(LL)
      N=NN(LL)
      XX=YY(LL)
      PRINT 700,WO,Q
  700 FORMAT(/,2(3X,F10.4))
  120 DO 50 J=M,N
      W=J/XX
      CALL TF(Q,WO,W,TA,I)
      IF(AMAX(I).LT.TA(  I)) GO TO 61
      GO TO 60
   61 AMAX(I)=TA(  I)
      WX(I)=W
   60 CONTINUE
   50 CONTINUE
      DO 2000 J=1,7,2
      K=J-2
      INCR=0.01
      IF(WO.EQ.0.01)INCR=0.001
      IF(WO.GT.10.0) INCR=1.0
      INCR=K*INCR
      TL=0.000001
      W1(J)=WX(I)
   11 W1(J)=W1(J)+INCR
      W=W1(J)
      CALL TF(Q,WO,W,TA,I)
      DR=ABS(AMAX(I)-3.0-TA(  I))
      IF(DR.LE.TL) GOTO 2000
      IF(TA(I).LE.AMAX(I)-3) GOTO 3
      GOTO11
    3 W1(J)=W1(J)-INCR
```

```
      INCR=INCR/10.
      GO TO 11
 2000 CONTINUE
    4 QC(I)=WX(I)/(W1(3)-W1(1))
      WR=WX(I)/WC
      QR=   QC(I)/Q
      PRINT 3000,WX(I),W1(1),W1(3),QC(I),QR,WR
 3000 FORMAT(   6(3X,F10.5))
  100 CONTINUE
      STOP
      END
      SUBROUTINE TF(Q,WO,W,TA,I)
      DIMENSION TA(6),T(6)
      COMPLEX S,Z,A,B,C,D,E,T,U1,U2,G
      A1=0.95
      F=SQRT(A1)
      S=(1.0E-30,1.0)*W
      Z=CSQRT(S)
      A=CEXP(Z*(1+F))
      B=CEXP(Z*(1-F))
      C=1/B
      D=1/A
      E=(A-B+C-D)/(A+B-C-D)
      GO TO (1,2,3,4), I
    1 C1=2*WO*Q
      C2 = 2*WO*Q
      U1 = E/(F*S)
      U2 = 1/S
      GO TO 5
    2 C1=2*WO*Q
      C2 = 2*WO*Q
      U1=1/(F*E*S)
      U2=1/S
      GO TO 5
    3 C1=2*WO*Q
      C2=2*WO*Q
      U1=1/S
      U2= E/(F*S)
      GO TO 5
    4 C1 = 2*WO*Q
      C2=2*WO*Q
      U1=1/S
      U2 = 1/(E*F*S)
    5 T(I)=2*C2*U2/(C1*C2*U1*U2+C1*U1+C2*U2+4*Q**2)
      G = T(I)
      TA(I)=20*ALOG10(CABS(G))
      RETURN
      END
```

APPENDIX C.2

COMPUTER PROGRAM FOR STUDYING THE EFFECT OF GYRATOR IMPERFECTIONS ON u(s)

```
      PROGRAM NANCY(INPUT,OUTPUT)
C***** EFFECT OF GYRATOR IMPERFECTIONS ON U(S)*****
      COMPLEX S, X, Y, TANH, Q, YL, Z2, Y11, Y12,Y21,Y22,YI,ZI,P,Z1,U1,U
     12
      GB=2.*22./7*1000000.  $A0=200000.
      READ 30,RI,RO
      R1=1000.
      DO 10 ION=1,4
      READ 30,QN
   30 FORMAT(2F15.3)
      DO 10 IWO=1,3
      READ 30,WO
      DO 10 J=1,2
      IF(J.EQ.1) R2C2=RC=0.001/WO
      IF(J.EQ.2) R2C2=RC=0.01/WO
      WORC=WO*RC
      DO 10 N=1,2
      IF(N.EQ.1) R=10000
      IF(N.EQ.2)R=5000.
      IF(N.EQ.3) R=5000
      R2=2.0*QN*WO*RC*R**2/R1
      PRINT 2,QN,WO,WORC,R,R1
    2 FORMAT(1H1,5X,*QN=*,F10.4,*WO=*,F10.4,*WORC=*,F10.4,*R=*,F10.4,*R1
     1=*,F10.4)
      PRINT 1
    1 FORMAT (8X,*W*,15X,*EMAG*,15X,*EPHASE*)
      DO 10 I=2,1200,10
      W= I
      S=(1.0E-60,1.0)*W
      X=CSQRT(S*R2C2)
      Y=CEXP(X)
      TANH = (Y-1/Y)/(Y+1/Y)
      Q=1/(X*TANH)
      YL= 1/(R2*C)
      GA=(2+RO/R)/(AO*R)
      GC=2*W**2*(1+4*R1/R)/(GB**2*R)
      Y11=GA+GC+S*(2+R1/R)/(GB*R)
      Y21=-1/R-2*W**2*(R-RO)/((GB**2*RO**2)+S*(RO*RI-RO**2)/(GB*R**2*RI)
      Y12=1/R +2*W**2*(1-RO/R)/((GB**2*RO**2)-S*RO/(GB*R**2)
      Y22=2/(AO*R)+3*RC/(AO*R**2)+2*W**2*(R+5*RC)/(GB**2*R**2)+S*(2*R+3*
     1RO)/(GB*R**2)
      YI= Y11- (Y12*Y21)/(Y22+YL)
      ZI= 1/YI
      P=TANH/X
      Z1=R1*P
      U1=(R1*R2)/(R**2*RC*S)
      U2=Z1/ZI
      A1=CABS(U2)  $ A2=CABS(U1)
      P1= REAL(U2)/A1  $ P2=REAL(U1)/A2
      EMAG= 1-A1/A2 $ EPHASE=1- ACOS(P1)/ACOS(P2)
      PRINT 20, W, EMAG, EPHASE
   20 FORMAT (3 E15.6)
   10 CONTINUE
      STOP $ END
```

APPENDIX C.3

COMPUTER PROGRAM FOR CALCULATING THE EXACT VALUES OF $\hat{Q}_{pd}$ AND $\hat{\omega}_{pd}$

```
      PROGRAM NANCY (INPUT,OUTPUT)
      COMMON GB,A0,RI,RO,R1,R2,R2C2,RC,R,ON,W0,G
C****EFFECT OF GYRATOR'S AND OP. AMP. IMPER. ON A B.P. REALIZATION****
C
C***DATA FOR 741 OP. AMPS.****
      GB=2.*22./7*1000000.  $A0=200000.
      RI = 2000000. $ RO= 75
      ON=50.
      G=(4*ON**2-1)**(1./3)
      PRINT 1,ON
    1 FORMAT(1H1,5X,*ON=*,F4.0,//,8X,*W0*,9X,*W0A*,8X,*Q*8X,*R*,8X,*R1*,
     18X,*R2*)
      I=100
      R1=100000.
      WP=I
      W0=I
      R=31000.
      R2C2=RC=0.00001/W0
      R2=2.0*ON*W0*RC*R**2/R1
      CALL W0C(W0,Q,W0A)
   10 PRINT 100,WP,W0A,Q,P,R1,R2
  100 FORMAT(6F12.4)
      STOP $END
      SUBROUTINE VAL(W,T1)
      COMMON GB,A0,RI,RO,R1,R2,R2C2,RC,R,ON,W0,G
      COMPLEX S, X, Y, TANH, Q, YL, Z2, Y11, Y12,Y21,Y22,YI,ZI,P,Z1,U1,U
     12,T,G0,G1,G2,G3,E1,B2
      S=(1.0E-60,1.0)*W
      X=CSQRT(S*R2C2)
      Y=CEXP(X)
      TANH = (Y-1/Y)/(Y+1/Y)
      Q=1/(X*TANH)
      YL= 1/(R2*Q)
      GA=(2+RC/R)/(A0*R)
      GC=2*W**2*(1+4*RC/R)/(GB**2*R)
      Y11=GA+GC+S*(2+RC/R)/(GB*R)
      Y21=-1/R-2*W**2*(R-RO)/(GB**2*R**2)+S*(RO*RI-R**2)/(GB*R**2*RI)
      Y12=1/R +2*W**2*(1-RO/R)/(GB**2*R**2)-S*RO/(GB*R**2)
      Y22=2/(A0*R)+3*RC/(A0*R**2)+2*W**2*(R+6*RO)/(GB**2*R**2)+S*(2*R+3*
     1RO)/(GB*R**2)
      YI= Y11- (Y12*Y21)/(Y22+YL)
      ZI= 1/YI
      P=TANH/X
      Z1=R1*P
      U2=Z1/ZI
      U1=U2
C FOR UNITY MID FREQ. GAIN
      A=1./G
      B1=GB/(S*(1+A)+GB)
      B2=-GB*A/(S*(1+A)+GB)
      G0=GB**2*A/(S*(1+G)+GB)
```

```
      G1=G*GB/(S*G+GB)
      G2=G*GB/(S*G+GB)
      G3=G*GB/(S*(1+G)+GB)
      T=(B1*G1*GB*(U2+1)+B2*GB*G1*G2)/(U1*U2+U1+U2+1+G1*G2*G3)
      T1=CABS(T)
      RETURN $END
      SUBROUTINE WOQ(WC,C,WOA)
       DIMENSION XW(3)
      CALL VAL(WC,T) $W=WO-.01 $CALL VAL(W,T1) $W=WO $X=T1-T
      D1=SIGN(.1,X)*WO $DO 20 J=1,4 $D=D1/10**J $DO 10 I=1,20 $W=W-D
  100  FORMAT(5E14.7)
      CALL VAL(W,T1) $ IF(T1.GT.T)GO TO 10 $D1=-D1 $GO TO 20
   10 T=T1 $IF(I.GE.20)GO TO 50
   20 T=T1 $XW(2)=WO=W $ TM=T/1.414 $DO 40 K=1,3,2 $W1=W
      W2=(1+(K-2)*0.3)*W $DO 30 I=1,20 $W3=0.5*(W1+W2) $CALLVAL(W3,T1)
      IF(T1.LT.TM)W2=W3 $IF(T1.GT.TM)W1=W3
   30 CONTINUE
   40 XW(K)=W3 $C=XW(2)/(XW(3)-XW(1)) $WOA=XW(2) $RETURN
   50 PRINT 60
   60 FORMAT(*CANNOT FIND WO*)
      RETURN $END
```

APPENDIX C.4

COMPUTER PROGRAM FOR STUDYING THE EFFECT OF IMPERFECTIONS OF GYRATORS AND OPERATIONAL AMPLIFIERS ON THE LOW PASS BUTTERWORTH RESPONSE

```
      PROGRAM NANCY (INPUT,OUTPUT)
C****EFFECT OF GYP. AND CP. AMP. IMP. ON A LP. FILTER W0=10****
      COMPLEX S, X, Y, TANH, Q, YL, Z2, Y11, Y12,Y21,Y22,YI,ZI,P,Z1,U1,U
     12,T1,T2,B,B0,B1,B2,G1,G2,G3,G0,N,D
C***DATA FOR 741 OP. AMP.****
C
      GB=2.*22./7*1000000.  $A0=200000.
      RI = 2000000. $ R0= 75
      QN=1./2**0.5
      W0=10.
      G=(4*QN**2-1)**(1./3)
      A=1/G  $C=(-4*QN**2+2)*A/2.
      R2C2=RC=0.000001/W0
      W0RC=W0*RC
      R=30000.  $R1=100.
      R2=2.0*QN*W0*RC*R**2/R1
      PRINT 2,QN,W0,W0RC,R,R1
    2 FORMAT(1H1,5X,*QN=*,F10.4,*W0=*,F10.4,*W0RC=*,F10.4,*R=*,F10.4,*R1
     1=*,F10.4)
      PRINT 1
    1 FORMAT (8X,*W*,15X,*EMAG*,10X,*EPHASE*,10X,*EMAGT*,10X,*EPHASE
     1T*)
      DO 10 I=1,2000,10
      W=I/100.
      S=(1.0E-60,1.0)*W
      X=CSQRT(S*R2C2)
      Y=CEXP(X)
      TANH = (Y-1/Y)/(Y+1/Y)
      Q=1/(X*TANH)
      YL= 1/(R2*Q)
      GA=(2+R0/R)/(A0*R)
      GC=2*W**2*(1+4*R0/R)/(GB**2*R)
      Y11=GA+GC+S*(2+R0/R)/(GB*R)
      Y21=-1/R-2*W**2*(R-R0)/(GB**2*R**2)+S*(R0*RI-R**2)/(GB*R**2*RI)
      Y12=1/R +2*W**2*(1-R0/R)/(GB**2*R**2)-S*R0/(GB*R**2)
      Y22=2/(A0*R)+3*RC/(A0*R**2)+2*W**2*(R+6*R0)/(GB**2*R**2)+S*(2*R+3*
     1R0)/(GB*R**2)
      YI= Y11- (Y12*Y21)/(Y22+YL)
      ZI= 1/YI
      P=TANH/X
      Z1=R1*P
      U1=(R1*R2)/(R**2*RC*S)
      U2=Z1/ZI
      A1=CABS(U2)  $ A2=CABS(U1)
      P1= REAL(U2)/A1  $ P2=REAL(U1)/A2
      EMAG= 1-A1/A2 $ EPHASE=1- ACOS(P1)/ACOS(P2)
      B=S*(1+1+C)+GB
      B0=GB/B
      B1=-GB/B
      B2=-GB*C/B
      G0=GB*2*A/(S*(1+G)+GB)
```

```
      G1=G*GB/(S*G+GB)
      G2=G*GP/(S*G+GP)
      G3=G*GB/(S*(1+G)+GP)
      N=B0*U2**2+U2*(2*B0+B1*G1*G0)+B0*(1+G1*G2*G3)+B1*G1*G0+B2*G1*G2
     1*G0
      D=U2**2+2*U2+1+G1*G2*G3
      T2=N/D
      T1=W0**2/(S**2+WC/QN*S+W0**2)
      AT1=CABS(T1)   $AT2=CABS(T2)
      PT1=REAL(T1)/AT1     $PT2=REAL(T2)/AT2
      EMAGT=1-AT2/AT1     $EPHASET=1-ACOS(PT2)/ACOS(PT1)
      DB1=20*ALOG10(AT1)   $DB2=20*ALOG10(AT2)
      PRINT 20, W, EMAG, EPHASE,EMAGT,EPHASET,DB1,DB2
   20 FORMAT(8E15.6)
   10 CONTINUE
      STOP $ END
```